AARHUS UNIVERSITY
DEPARTMENT OF GEOSCIENCE

Master of Science Thesis (60 ECTS)

Identification of saltwater intrusion based on Danish databases

A case-study of saltwater intrusion in Djursland, eastern Jutland

Tania Beate Thomsen

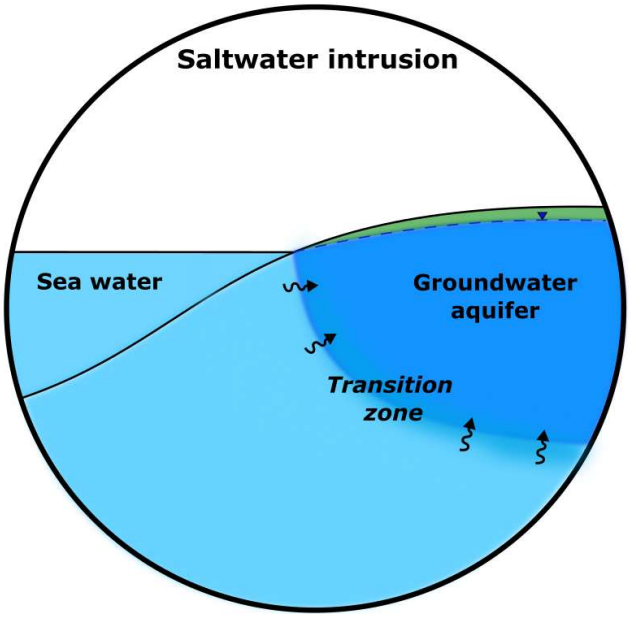

Supervisor: Carlos Duque Calvache
Co-supervisor: Torben O. Sonnenborg (University of Copenhagen)

Date: 10-06-2021

Department of Geoscience
Faculty of Natural Science

University of Aarhus

JUNE 2021

Abstract

Coastal areas are vulnerable to saltwater intrusion and overexploitation of groundwater resources can increase this threat. With rising sea level, the natural balance between fresh- and saltwater is affected, and the result is a landward displacement of the transition zone, for which especially low-lying areas are vulnerable. Denmark is a flat area with coastal areas representing a large part of the total extent. Djursland in eastern Jutland has been chosen for investigation of saltwater intrusion, as the area comprises low-lying and coastal areas and excessive drainage pumping in Kolindsund. This paper will identify saltwater intrusion based on Danish databases by using a multi-method approach, that combines an analytical solution, a multi-geochemical analysis, a geophysical AEM method and numerical modelling in SEAWAT. Results show saltwater intrusion is impacting the pre-Quaternary aquifer in the northeastern Djursland. Origin of saltwater is assigned to the Kattegat seawater where fossil and connate water contribute. In the Quaternary aquifer raised chloride content is observed in the upper layers of the aquifer. As Djursland mainly comprises croplands, the salinity source possibly originates from fertilization and anthropogenic effects. By applying the four methods with data from Danish databases, saltwater intrusion is recognized, and possible causes identified. Therefore, this multi-method can be suggested to be applied to other coastal sites in Denmark to study saltwater intrusion, but data must be used with caution, and this paper provides suggestions for other alternatives if some data are lacking.

Acknowledgement

First, I would like to thank my supervisor Carlos Duque for this great opportunity to write about a subject I find highly interesting. I will also thank him for challenging me to do many oral presentations and believing in me for fulfilling the modelling part. Next, I will thank Torben Sonnenborg and the team from GEUS, for listening to my presentations and providing me with valuable feedback. Then I would like to thank Per V.M. from Norddjurs municipality for showing me around in Kolindsund and answering all my many questions about the area. I will also thank my study group Nikolaj G. and Hasfa M. for making this special Corona year better with good laugh and educational conversations. Finally, I will thank my dad Peter S.T. for reading and reviewing the entire thesis.

Table of Contents

1. Introduction

Sea level is predicted to rise 0.84 meter by the end of the 21st century, which increases the risk of saltwater intruding coastal aquifers (Oppenheimer *et al.*, 2019). The world population living in coastal regions is increasing which intensify a growing demand for drinking-water supply and domestic and agricultural consumption (Anders *et al.*, 2013; Najib *et al.*, 2017). This leads to overexploitation of groundwater resources in coastal aquifers and increases the pressure on the groundwater system which in addition can lead to saltwater intrusion (Safi *et al.*, 2018; Bachtouli and Comte, 2019). When excessive pumping occurs, it lowers the water table and the hydraulic gradient in the freshwater, which changes the direction of flow of freshwater towards inland. This change in flow impacts the saltwater too as seawater will be drawn toward the pumping well from below and contaminate the fresh groundwater (Bear *et al.*, 1999; Werner *et al.*, 2013). Seawater has a high concentration of total dissolved solids (TDS), where especially the major ions sodium (Na^+) and chloride (Cl^-) predominates the composition. In that way, fresh drinking-water becomes contaminated by TDS and especially chloride (Bear *et al.*, 1999; Barlow, 2003). If the fresh groundwater quality deteriorates and exceeds the acceptable drinking-water standard of 250 mg L^{-1} of chloride, groundwater cannot be used for consumption or irrigation, and abstraction wells must be abandoned. This induce a worldwide problem for coastal communities (Cai *et al*., 2015; Bachtouli and Comte, 2019).

Some of the earliest recognitions of saltwater intrusion, was on Long Island in New York in 1854, but within the coastal aquifers of Israel, the southern Floridian aquifer (U.S), in the province of Noord-Holland in the Netherlands, and within the Nile Delta in Egypt as examples, impacts of saltwater intrusion have been observed (Vengosh and Rosenthal, 1994; Essink, 2001; Barlow, 2003; Mabrouk *et al.*, 2013).

To investigate saltwater intrusion, different approaches can be applied. In the study of Jørgensen (2002) hydrochemistry of saline groundwater from Læsø, Denmark, has been used to identify different salinity sources and describe mixing process based on major ion chemistry and environmental isotopes. Meyer et al. (2019) describes how the use of numerical modelling in combination with geophysical and geochemical data can be applied to understand the historical development of a large-scale groundwater system affected by saltwater intrusion and to use the model to simulate the effect of rising sea level. In

northern Salinas Valley, California, airborne electromagnetic (AEM) method has been used to map the extent of saltwater intrusion (Gottschalk *et al.*, 2020). These are beneficial methods to investigate saltwater intrusion.

In Denmark few studies have been conducted concerning groundwater salinization. Of those, should be mentioned a comprehensive study in the northeastern Zealand that lasted from 2002 to 2005 *(Klitten et al*., 2006). The purpose of the study was to determine the depth to, and characteristics of the saltwater-freshwater transition zone within pre-Quaternary aquifers. Geophysical methods as TEM and borehole logging were applied, and additionally, geochemical data from the Danish national database, Jupiter, was applied to determine different water types with the geochemical program PHREEQC. Another large project investigated the vulnerability of Danish groundwater aquifers to road de-icing salt (Kristiansen *et al*., 2009). The research was based on geochemical data from the Jupiter database and numerical modelling with MIKE SHE. But as Denmark is a flat country with maximum heights of a few hundred meters (~170 m MSL) and is comprised by almost 400 islands which represents about 20 percentage of the total areal extent and contributes to the coastline of 8,750 kilometers (Danmarks Statistik, 2019), investigating saltwater intrusion could be very important. Especially with the effect of increasing sea level due to climate changes.

During the 1930's Andersen and Ødum (1936) were among the first to identify areas in Denmark affected by saltwater intrusion. A few years later, salt domes of Zechstein depositions were identified as the salinity source. The water type was characterized as mineral water, and the characteristics was an extremely high chloride content exceeding chloride concentrations within seawater (Dinesen, 1961). In 1989, a Danish groundwater monitoring programme by the Geological Survey of Denmark and Greenland (GEUS) was initiated. The purpose was to provide quality and quantitative knowledge of groundwater, and to fulfill obligations to relevant legislation and international conventions of the EU (Jørgensen and Stockmarr, 2009). In 1995, a groundwater report was published including status and results obtained from the monitoring programme. Based on the national results from the monitoring programme and local results from counties across Denmark, a saltwater map was established to emphasize areas impacted by saltwater intrusion (***Figure 1***). Most areas were located in coastal areas with the exception of Djursland, eastern Jutland (GEUS, 1995).

Figure 1. Identified areas influenced by saltwater related issues in Denmark by the Geological Survey of Greenland and Denmark (GEUS, 1995).

The entire central to northern part of Djursland were identified as an area having issues with saltwater. But as the only location, is was emphasized that empirical data was lacking (GEUS, 1995).

As most parts of Denmark, Djursland was influenced by advancing ice sheets during the last glaciation, the Weichselian Glaciation lasting from ~110 ka B.P to 11.7 ka B.P. (Pedersen and Petersen, 2000). Glacial and post-glacial effects formed the landscape and eroded a deep major valley system into the pre-Quaternary sediment across the central part of Djursland. During the following interglacial period, as result of retreating ice, sea level rose four meters above present-day sea level. The low-lying formed strait was completely flooded by the past Littorina sea during the end of the Stone Age (4,000 yrs. B.P.). But with time, due to isostatic rebound and aeolian sand depositions, the strait became enclosed and isolated from the seawater. This changed the environment from saline to fresher conditions. By the end of the last century, the strait was turned into a large freshwater lake, the second largest lake in Denmark. In the 1870's the lake, named Kolindsund, was reclaimed and a pumping system was established to drain the lake (Pedersen and Petersen, 2000; Hansen, 2011).

Today the drainage system is still active, but due to soil subsidence as result of the lowering of the groundwater table, the pumping depth has increased to -5 m below sea level and this has questioned

continuation of the drainage of Kolindsund. Another side effect, that has been questioned the last couple of years, is the effect of saltwater intrusion due to excessive pumping of the area. Very limited investigations has been conducted in the area regarding saltwater intrusion (Hansen, 2011). In the 80's two independent investigation were conducted within the area, and results showed high chloride content in the eastern part (Korkman, 1980; Nielsen and Rauschenberger, 1982). But as no recent investigations have been conducted, the extend of saltwater intrusion within and in the surrounding area is unknown.

1.1. Objective

This paper aims to investigate saltwater intrusion based on accessible data from Danish databases. In terms to do so, Djursland has been chosen as case-study, because coastal environments, low-lying areas and excessive pumping are present within the area. In the research, hydrological, geochemical, and geophysical data will be applied by the use of a multi-method approach, comprising analytical solution, multi-geochemical analysis, geophysical investigation and numerical modelling to identify saltwater intrusion.

The two main objectives of the study are to identify saltwater intrusion, and to evaluate and validate if the multi-method approach based on data only accessed from public databases, is a solid method to apply in a saltwater intrusion investigation.

To identify saltwater intrusion, the following will be evaluated:

1. Areas at risk of saltwater intrusion in the pre-Quaternary and Quaternary aquifer
2. Associated salinity sources leading to increased salinity levels
3. Key parameters important for the development of saltwater intrusion

The second objective is an assessment of applying data extracted from Danish databases which includes limitations, and dis- and advantages, and it will be discussed if this approach will be applicable for an arbitrary site in Denmark.

2. Area description

Djursland is located in the central most eastern part of Jutland (***Figure 2***). The areal extent is ~1122 km^2 and in the western boundary it is constrained from Hevring in the north to Rønde in the south. The rest of Djursland, is constrained by the sea Kattegat. Djursland was heavily influenced by glacial dynamics during the latest glaciation and post-glacial processes have affected the area too. This is reflected in the topography of the landscape due to the higher relief. Meltwater runoff from the last glaciation, eroded into the pre-Quaternary sediment and formed a major valley system across the central Djursland from west to east. The lowest elevations are within Kolindsund where topography is below sea level (***Figure 2***). On both sides of the strait, elevations increase rapidly to 20-40 meters above sea level. The southern part of Djursland is especially characterized by wavy topography and many hills as Mols Bjerge, where average elevations reaches up to 100 m above sea level. The highest elevation is 137 m (MSL) and located within Mols Bjerge in the southwestern part (Pedersen & Petersen, 2000).

The climate is a mix of coastal and valley climate. Because of the proximity to the ocean, the temperature variations are minor. In the northern part of Djursland the ocean lowers the average temperatures while in the southern part, the temperatures follow the average temperature of Denmark. In sandy areas temperatures are often a little higher which can result in precipitation. Within the valley system, there is often foggy and lower temperatures. The average temperature of Djursland is 8.85 °C. The Jutland Ridge (Jyske Højderyg) crossing central Jutland from north to south, has a major effect on the climate in Djursland. Winds travelling eastward meets the ridge and air are forced to rise up and as a result of compaction, they precipitate leaving clouds empty and dry when they reach Djursland. In the southern part of Djursland where hills predominate, orographic precipitation occurs too. The driest months are November and December. The average annual precipitation is 677 mm. The result of a dry climate increases the hours of sunshine. The Norwegian mountains also have an impact on the higher number of sunshine hours. When northwestern winds affect the area, the mountains shield and decrease the number of clouds reaching Djursland from the north. The proximity to the sea also has an effect, as oceans decrease cloud formation during summer time (Theilgaard, 2017b, 2017a).

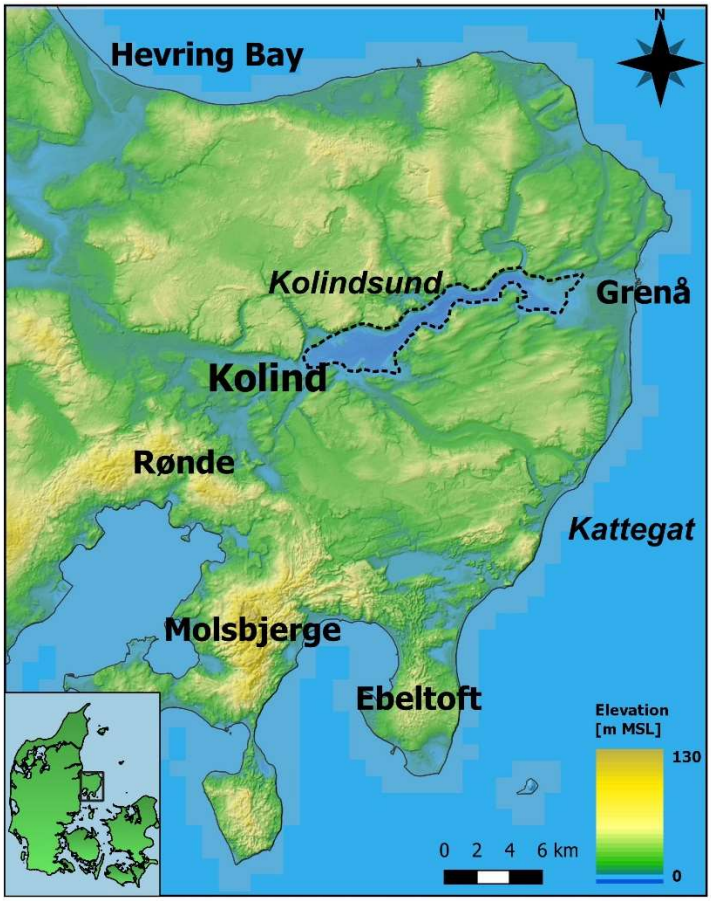

Figure 2. Location of the study area Djursland and Kolindsund.

In Djursland, croplands represent the largest part of land-use with 66% and forests represent 22%. Natural areas as meadows, marshes, grasslands, lakes and wetlands represent 7.5%. Grenå in the eastern Djursland and Ebeltoft in the southeastern Djursland represent the majority of urban areas (Pedersen and Petersen, 2000; Miljøministeriet By- og Landskabsstyrelsen, 2009).

2.1. Hydrogeological evolution

The strait crossing the central Djursland from east to west was formed during the end of the Quaternary Period, in the Late Pleistocene. The Pleistocene Epoch was a geologically period dominated by shifting glacial and interglacial periods. The most recent glacial period was the Weichselian Glaciation from ~115 ka B.P. to 11.7 ka B.P. (Larsen and Sand-Jensen, 2017). At the end of the glaciation (26.5 - 19.0 ka B.P.), global ice sheets reached their maximum extend, a period called the LGM - Last Glacial Maximum (Clark *et al.*, 2009). Due to the colder conditions during the Early and Middle Weichsel, sea level had decreased

and towards the initiation of the LGM (28 - 26 ka B.P.), the northern Denmark experienced the first ice advance by the Kattegat Ice Stream which was part of the major ice sheet impacting Scandinavia, the Scandinavian Ice Sheet (SIS). The ice sheet retreated for a short period of time and subsequently, it had a second advance where it reached its maximum volume during the peak of the LGM (~21 ka B.P.). During its second advance, coming from the northeastern direction, it covered major parts of Denmark (Larsen and Sand-Jensen, 2017; Pedersen, 2017). As it retreated again, a third readvance occurred around 19 - 18 ka B.P. from the Gulf of Bothnia through the Baltic Sea. The third advance was by the Young Baltic Ice Stream and reached the southeast to central part of Jutland during its maximum extent (***Figure 3***) (Pedersen and Petersen, 2000; Larsen and Sand-Jensen, 2017).

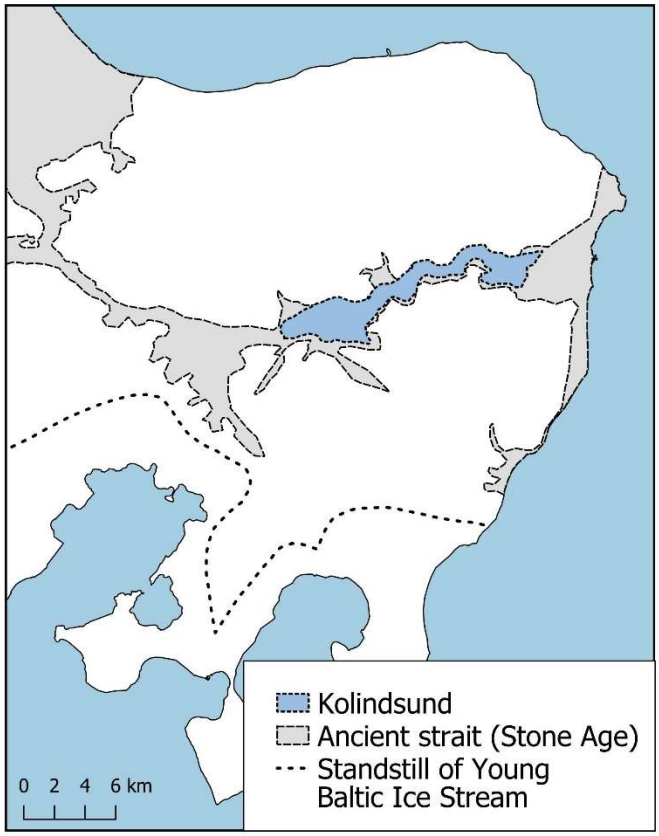

Figure 3. Standstill of the Young Baltic Ice Stream (19-18 ka B.P.), the ancient strait when it was filled in the end of the Stone Age (4,000 yrs. B.P., and Kolindsund when it was a freshwater lake prior to 1874 (Inspired by GEUS, 2021).

While Djursland was ice covered, meltwater and morainal material were deposited beneath and in front of the ice in the northern Djursland. The following millennials the ice sheet slowly retreated northeastward and as a post-glacial result, the areas which once had been ice covered isostatically

rebounded. Additionally, meltwater runoff from dead ice eroded the Pre-Quaternary sediment (chalk and limestone) and formed a strait crossing central Djursland from east in Grenå, westward through Auning and northward to Hevring Bay. In the eastern part of the strait, a valley system was formed which today is known as Kolindsund. From 9,000 to 8,800 yrs. B.P global sea level rose and in the Littorina Sea - the ancient sea surrounding Djursland during this time, increased to four meters above sea level of today, turning Kolindsund into a fjord system. Subsequently, during the Stone Age period (~7,000 - 4,000 yrs. B.P.) the rest of the strait was filled with seawater from the Littorina Sea (***Figure 3***) which resulted in an isolation of the northern Djursland (Kolindsundnatur.dk, no date; Krøyer and Jensen, 2013; Pedersen, 2017).

At the end of the Stone Age the northwestern part of the strait closed due to isostatic rebound and the connection to the sea was cut off. Towards the Viking Age (800 - 1050 C.E.), the eastern part of the strait closed too, due to aerial sand deposits forming sand dunes closing the final connection to the surrounding sea. With the closure of the eastern part conditions changed and Kolindsund became one of the largest freshwater lakes in Denmark (Kolindsundnatur.dk, no date; Århus Amts, 2000; Pedersen and Petersen, 2000).

2.2. Geology

Older pre-Quaternary geology is only known from one well located in Rønde (southwestern Djursland). The well has a depth of 5,300 meters and ends in a depth of -5,244 m (MSL). The oldest layer is of Upper Silurian Period with age of ~350 Myr. and the following layers are of Permian, Triassic, Jurassic, Cretaceous periods. The upper layers are from the Cenozoic Era - the most recent era in geologically history which include the Paleogene, Neogene and Quaternary Period (Pedersen and Petersen, 2000) The most well-known Pre-Quaternary sediment in Djursland are from the oldest period of Cenozoic, in the Paleogene Period (***Figure 4***). The sediment types comprise Danian Limestone, Paleocene Clay and Eocene Clay. Danian sediment covers the northern to central part of Djursland whereas Paleocene and Eocene clay covers the southern part. On top Late Quaternary sediment covers the entire Djursland (***Figure 5***). Only one location in the eastern part of Djursland, the older Quaternary sediment has been correlated to the penultimate interglacial period, the Holstein, based on the content of foraminifera. The

rest of Quaternary sediment is related to the latest glaciation (Weichselian) and subsequently interglacial period, the Holocene Epoch (Pedersen and Petersen, 2000).

2.2.1. Pre-Quaternary sediment

Danian Limestone is the oldest sediment, deposited in the Danian stage, the oldest stage of the Paleocene Epoch (Pedersen and Petersen, 2000). It covers of the largest part of Djursland (***Figure 4***) and has a slope increasing from southwest towards northeast. The limestone comprises the upper limestone 'kalksandskalk', the 'slamkalk' and the lower bryozoan limestone. The 'kalksandskalk' is fine-grained with light gray to yellow-ish color and varying hardness. The main components are coccoliths, foraminifera and skeleton fragments, including flint. The 'slamkalk' is characterized by a white to light gray color. It is fine-grained with fifty percentage of sediment smaller than 5 µm composed of coccoliths and nannofossils. It is often non-hardened because it is not affected by diagenetic processes. The bryozoan limestone is bedded and gray-white-ish with dark flint layers. It is characterized by a high content of bryozoan fragments (20-45%). Macrofossils as brachiopods, mussels and sea urchins can be found within the limestone. The sea urchin Tylocidaris Abildgaardi fossil determine this sediment as related to Lower Danien (Pedersen and Petersen, 2000; Vangkilde-Pedersen *et al.*, 2011).

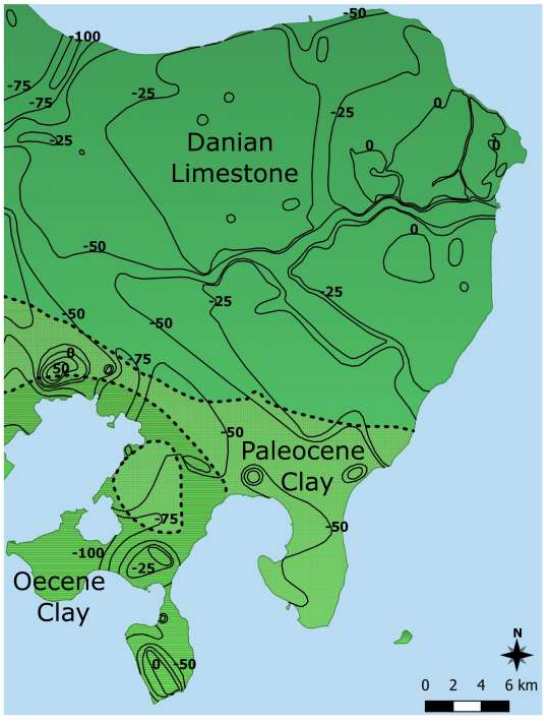

Figure 4. The pre-Quaternary surface and sediment types in Djursland in m [MSL] (Inspired by (Pedersen and Petersen, 2000).

Below the Danian Limestone, Maastrichtian Chalk (skrivekridt) can be found in some wells across Djursland. The Maastrichtian stage is from the Upper Cretaceous Period. The Maastrichtian and Danian stages are on each side of the K-T boundary (66 Myr. B.P.) which reflects the mass extinction event where dinosaurs became extinct. The Maastrichtian Chalk is characterized as homogenous, fine-grained and composed of coccoliths which contributes with 90% of the calcium carbonate within the chalk. It has a low hardness and contains 5 to 10% flint (Vangkilde-Pedersen *et al.*, 2011).

Paleocene Clay occupies the southern part of Djursland and is younger than Danian Limestone. It mainly occurs as marl or gray clay and can therefore act as a hydraulic barrier. Most commonly, it is restricted to depths of 25-50 m below sea level (Pedersen and Petersen, 2000; Vangkilde-Pedersen *et al.*, 2011).

Eocene Clay is the youngest of pre-Quaternary sediment and extends in the southwestern Djursland and can be found in depths approximately equivalent to mean sea level. The clay is characterized with layers of volcanic ashes whereas, the ash layers are connected to the opening of the North Atlantic 50 Myr. B.P. The clay was deposited in marine environments when the Eocene ocean covered Djursland (Pedersen and Petersen, 2000).

2.2.2. Quaternary sediment

Quaternary sediment is a result of glacial and post-glacial processes from the last glaciation (***Figure 5***). The most extended Quaternary sediment is limey, sandy and gravelly till, and mixed meltwater deposits in the northern part, and mixed meltwater deposits, and limey clayey till in the southern part. Chalk and limestone are often found within Quaternary sediment as result of glaciotectonics from Quaternary glaciers. In the central part of Djursland, an outwash plain dominates with outwash sand and gravel (Pedersen and Petersen, 2000; Nilsson and Gravesen, 2018). In Kolindsund, marine and freshwater deposits dominate. The lower marine depositions are characterized with clay to silty clay-gyttja and reflects the result of the Atlantic transgression. The upper freshwater depositions are composed of calcareous silty clay-gyttja. The sediments reflect the change in conditions from saline to fresher. Quaternary sediment varies in thickness. Thinnest layers of Quaternary sediment (< 20 m) are in the northeastern part of Djursland and towards southwest the thickness increases. Within Kolindsund, Quaternary sediment exist in the upper 50 meters. Thickest Quaternary depositions (> 150 meter) are in Mols Bjerge (Pedersen and Petersen, 2000).

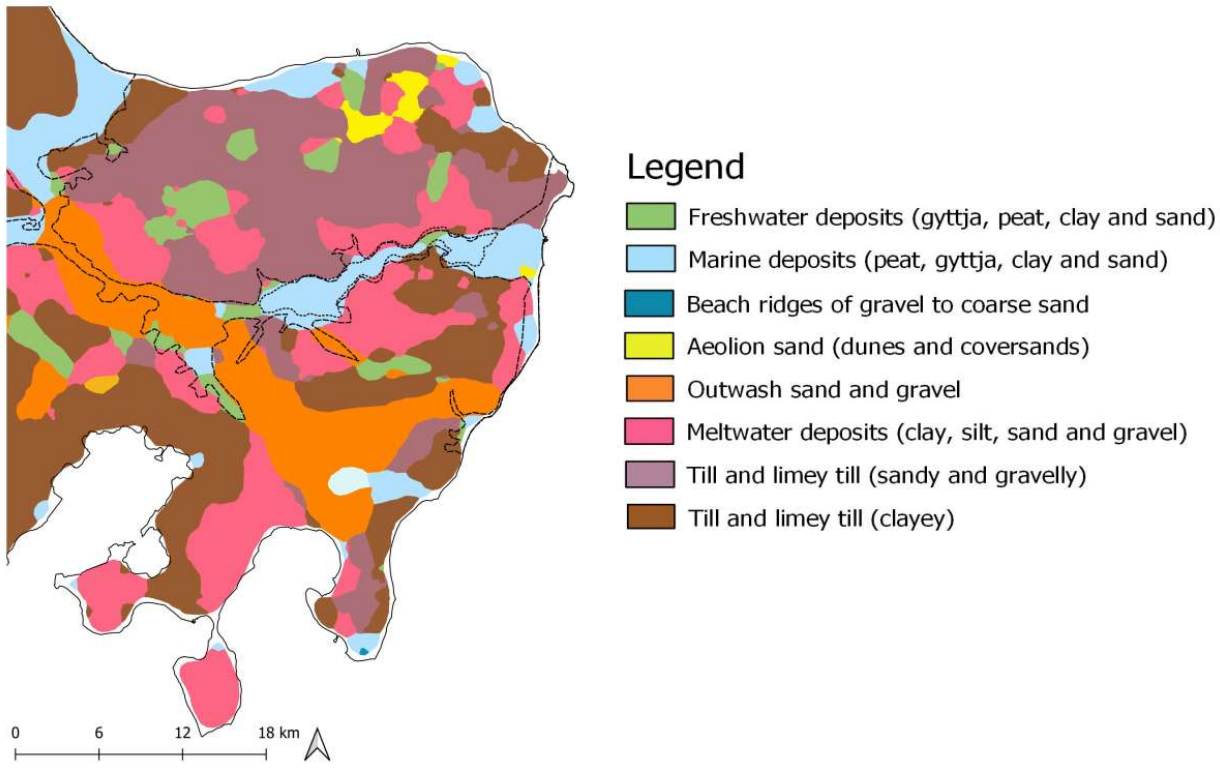

Figure 5. Quaternary geology in Djursland (GEUS, 2021).

2.3. Hydrogeology, hydrology, and hydrochemistry

2.3.1. Hydrogeology

As geology in Djursland is dominated by chalk, limestone and tilly sand, two types of groundwater reservoirs are predominant. Quaternary sand aquifers mostly artesian, and pre-Quaternary aquifers as unconfined in the northeastern part of Djursland, and as artesian in the rest of Djursland (Larsen & Sand-Jensen, 2017). In Djursland groundwater exploitation is mainly derived from pre-Quaternary aquifers located close to the surface. The aquifers are primarily covered by sand and characterized by fractures which make them vulnerable to spreading of contamination as percolating nitrate. Karst features in the northeastern part of Djursland have been observed, which also can have a major impact on water exchange within the aquifers (Århus Amt, 1995; Thomsen *et al.*, 2005; Nilsson and Gravesen, 2018).

Over half of all abstracted water in Djursland is for drinking-water supply (***Figure 6-left***), but as croplands represent a major part of the areal extend, abstracted water for irrigation contributes with the

second largest part (32.4 %). The largest water works, abstracting more than 200,000 m^3 per year, are mainly located in the eastern part of Djursland (GEUS, 2021).

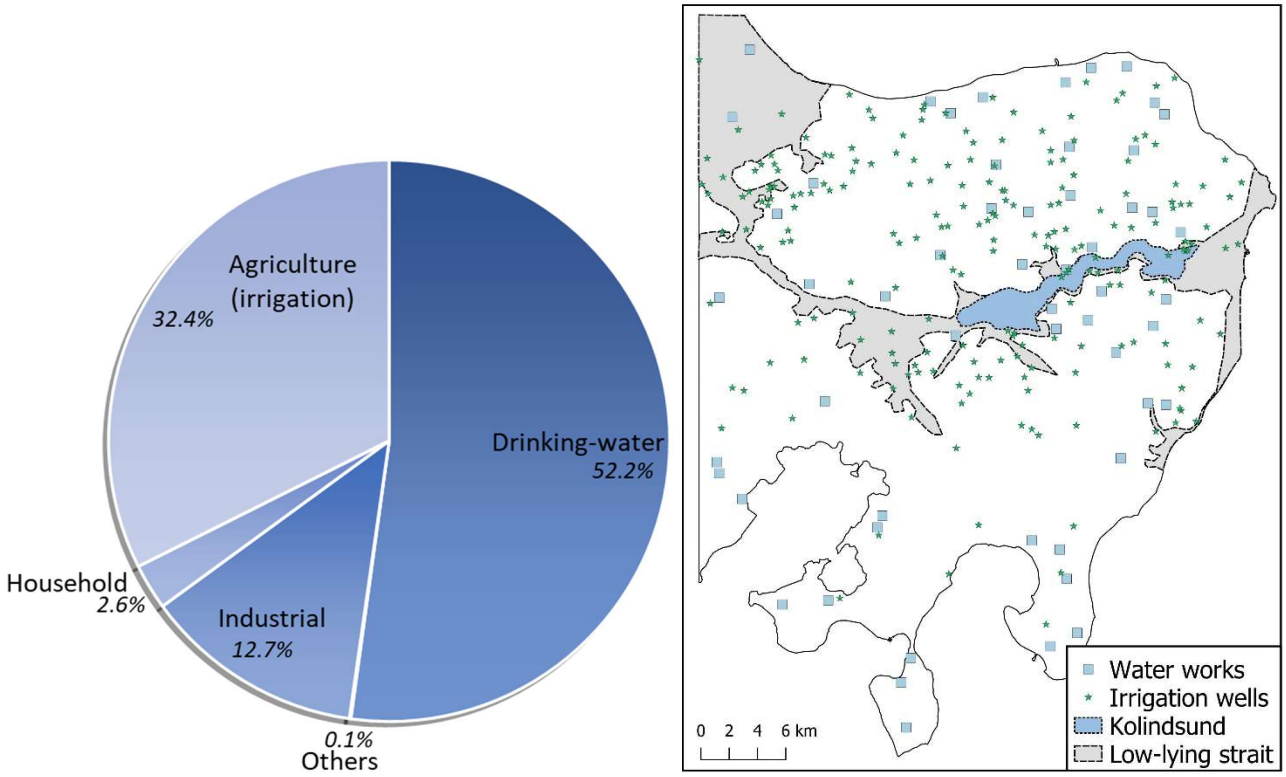

Figure 6. Left: Distribution of water abstraction (GEUS, 2021). Right: Distribution of water works and irrigation wells in Djursland (GEUS, 2021).

2.3.2. Hydrology

Because of the proximity to the sea and the presence of Jutland Ridge west of Djursland, climate is characterized as dry and averagely sunnier during summertime which decreases the annual precipitation. According to DMI annual precipitation for the period 2006-2015 was 679 mm for the southern part and 675 mm for the northern part where July and August are the wettest months (DMI, 2021b). The difference in precipitation patterns is due to orographic precipitation in the southern part because elevated hills predominates the area (Theilgaard, 2017b). According to a groundwater report of Århus County in 2005, the evaporation is 500 mm yr^{-1}, runoff is 175 mm yr^{-1} and annual groundwater recharge is 75 mm and ranges between 50-100 mm yr^{-1} for eastern Jutland (Århus Amt, 1995).

In Kolindsund, before the area was reclaimed it was the major lake where creeks and streams from the northern and southern side discharged into the lake and from there the water flowed to the sea through

the Grenå stream. But in the 1872 a pumping system was established to drain Kolindsund. The drainage system was initiated in 1874 and the groundwater table was lowered from +1 m to -3 m (MSL). The system comprises three canals, two encircling the area and one within the area crossing from west to east. Before the 1930's the drainage system comprised two pumping stations, but renewal of the pumping system provided better pumps and today, three pumping stations are in charge of the drainage. The pumping stations connects the outer canals with the central canal. The pumping stations, Enslev and Fannerup pump water into the northern canal and Allelevsund pumping station is pumping to the southern canal. The outer canals are also fed by water from streams and creeks from the catchment zone of Kolindsund (Korkman, 1979; Århus Amts, 2000). Korkman (1980) calculated the annual discharged water into the canal system to 60 mm and the total discharge by the pumping system to 4-5 m^3 s^{-1} (Korkman, 1980). The initial pumping depth was -2.6 m below sea level but in 1930's the pumping was adjusted from -3 to -4 m below sea level and today the pumping depth is -5 m (MSL). Due to the higher content of organic material in the soil the result of pumping induces compaction of the soil and a subsidence of the ground surface occurs. Therefore, the pumping depth needs to be adjusted (Århus Amts, 2000; Hansen, 2011).

2.3.3. Hydrochemistry

The background chemical composition of fresh groundwater depends on the chemical composition of precipitation that recharges to the aquifer. The concentration of salts in the average precipitation in Djursland is determined to 10-45 mg L^{-1} for sodium (Na^+) and 15-70 mg L^{-1} for chloride (Cl^-) (Århus Amt, 1995; GEUS, 1995). In the northern to central part of Djursland saltier water has been observed in deeper parts (100-150 m below terrain) of pre-Quaternary aquifers. It has been claimed the origin of saltwater was residual water from when the strait was flooded. In a well in Kirial, northeast of the eastern Kolindsund the depth to the saltwater-freshwater interface has been determined to be -50 m (MSL) and in a well further north in Skindbjerg, the depth to the interface is determined to be -70 m (MSL) (Århus Amt, 1995; Hansen, 2011).

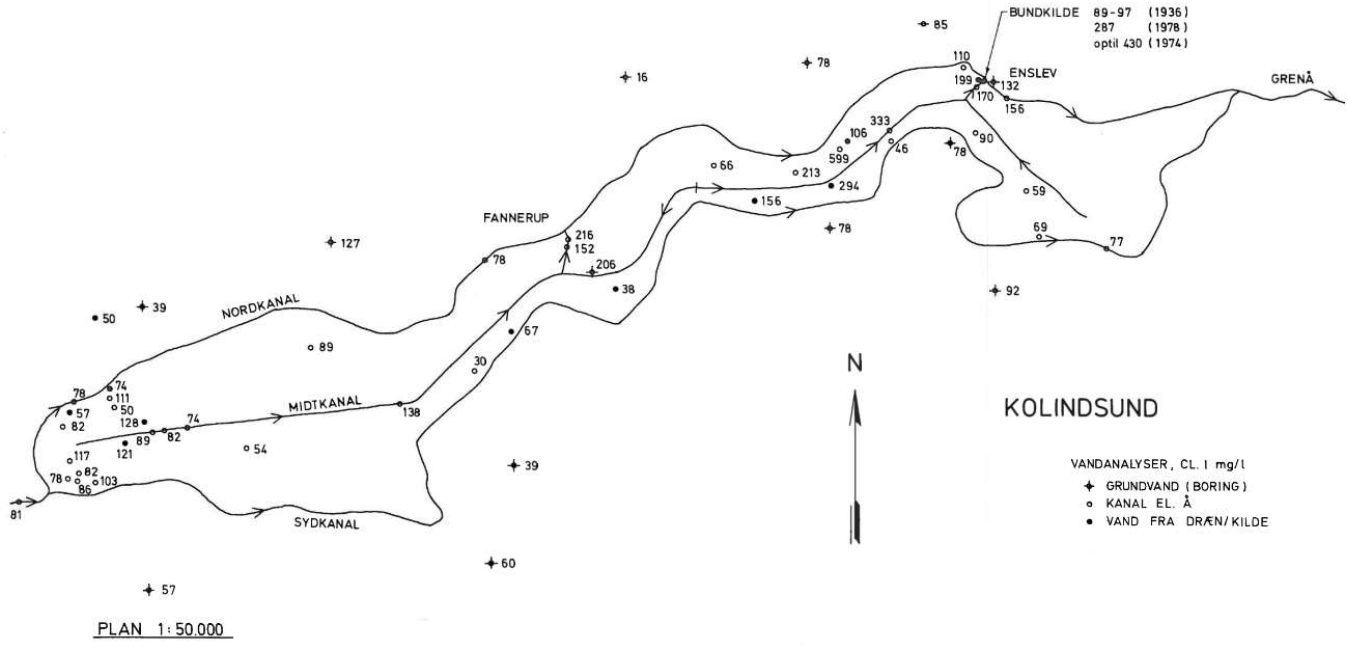

Figure 7. Chloride measurements within Kolindsund measured in the beginning of the 1980's (Nielsen & Rauschenberger, 1982).

At Enslev pumping station, pre-Quaternary sediment is exposed at the surface and during the establishment of the pumping station in 1936-1937, chloride concentrations were measured to 89-97 mg L^{-1}. Later, measurements measured from the municipality of Grenå showed chloride content of 287 mg L^{-1} and up to 430 mg L^{-1} in the same area (Korkman, 1981). A study by Korkman (1981) showed the identification of two springs at the inlet to the station which could cause the increased chloride content. The same degradation of water quality was registered in the village of Enslev. In the 1930's at the depth of 11 meters, chloride content was measured to 35 mg L^{-1} and thirty years later in a well at depth of twenty-eight meters nearby within the village, chloride concentration was measured to 132 mg L^{-1} (Korkman, 1981). In 1982 another geochemical investigation was conducted in the entire Kolindsund to determine if the springs identified earlier by Korkman, could be used as a groundwater resource for water supply and irrigation. The investigation showed that the chloride concentration was too high for groundwater exploitation (**Figure** *7*). This was particularly observed in the eastern end of Kolindsund near Enslev (Nielsen and Rauschenberger, 1982).

2.4. Oceanography of Kattegat

Djusland borders the Kattegat sea. Kattegat extends along the eastern coastline of Jutland. In the north it borders the waters of Skagerrak, in the east the Sweden's west coast and in the south the islands Zealand and Funen, and the Baltic Sea. The average depth of the sea is ~30 m. The waters of Kattegat is a transition zone between the highly salinized water of the North Sea and the brackish water of the Baltic Sea (Lund-Hansen *et al.*, 1994; Hansen *et al.*, 2012). In a study of the island Læsø, in the northern Kattegat, seawater salinity and composition has been measured (***Table 2.1***) showing the variation in salinity reflected in the hydrochemical composition (Jørgensen, 2002).

Table 2.1. Seawater composition of water samples of Kattegat (Jørgensen, 2002).

	Salinity ‰	**Ca**	**Mg**	**Na**	**K**	**HCO_3**	**SO_4**	**Cl**
Sample 1	21	260	775	6500	265	157	1610	11,900
Sample 2	27	300	1040	8200	310	175	2000	14,900

The salinity of the surface water of the North Sea is about 34‰ while Baltic Sea has a salinity of 8 - 10‰ due to the influx of freshwater from the surrounding rivers. The two waters stratify the water column in Kattegat. Outflow from the Baltic Sea decreases the salinity in the upper part of the water column, while inflow of the North Sea through Skagerrak increases the salinity in the lower parts. The effect of the Baltic Sea intensifies the stratification while the inflow of the North Sea decreases it (Lund-Hansen *et al.*, 1994). There are two main causes to the in- and outflows: water density difference creates a barocline flow, and the difference in head creates a barotropic flow. During an inflow of the North Sea, the westerly wind pushes water from the southern Baltic Sea towards the Gulf of Bothnia and water from the North Sea to Skagerrak and Kattegat. This creates a difference in head and therefore, a barotropic flow of the surface water from the North Sea to the Baltic Sea (Lund-Hansen *et al.*, 1994). If the effect of westerly wind cause a barotropic flow from the Baltic Sea to the North Sea, it can initiate a barocline flow of the bottom water in the opposite direction while the barotropic flow from the North Sea to the Baltic Sea does not initiate a barocline flow. Easterly winds dominates in periods of high pressure while westerly winds dominates in periods of low pressure (Lund-Hansen *et al.*, 1994).

3. Theory

3.1. Saltwater intrusion

About 71 % of the Earth surface is covered by water. Fresh groundwater accounts for 0.6% of the total amount of water, while seawater in oceans and inland seas account for 97% (Bear *et al.*, 1999). In coastal regions, fresh groundwater in coastal aquifers is in contact with saline water at the seaward margin of the aquifer. As water always flows toward lower elevations, freshwater flows toward coastal areas where the water table is lowest. A natural boundary exists between the freshwater from the aquifer and the saline, denser seawater. This boundary is a mixing zone reflecting the change of salinity where molecular diffusion and mechanical dispersion are the dominant processes. As freshwater has a lower density than seawater, saltwater infiltrates from below by the generation of a saltwater wedge. In an equilibrium state of the system (***Figure 8***), the hydraulic gradient and the density difference, forces seawater to move upwards and causes a natural infiltration into the coastal aquifer (Bear *et al.*, 1999; Barlow, 2003; Prince Edward Island Department of Environment, 2011).

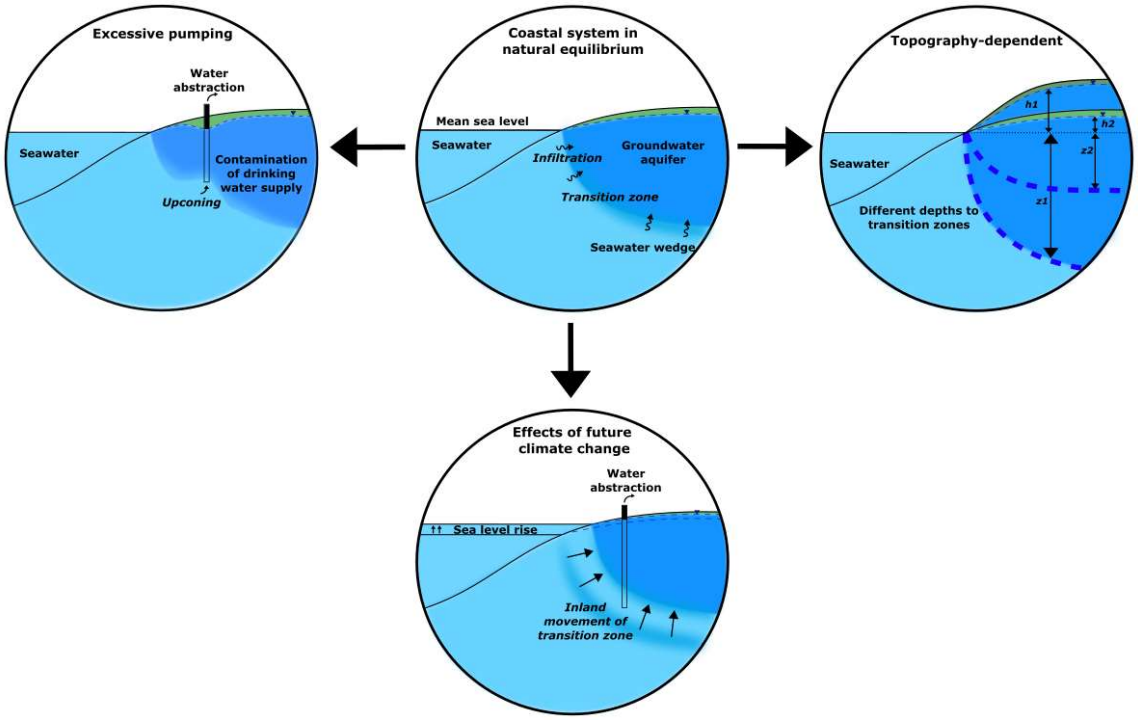

Figure 8. Saltwater intrusion and processes that can intensify or control saltwater intrusion.

Heterogeneities of hydraulic properties and the geological structure of aquifers are important factors to the transition or mixing zone. In addition, dynamic forces which include seasonal and annual variations in recharging water to the aquifer, tidal effects and long-term changes in sea level are processes affecting saltwater intrusion (Barlow, 2003; Werner *et al.*, 2013).

Within the last half century, exploitation of groundwater resources has steadily increased. The result is an increasing risk of saltwater contaminating coastal groundwater aquifers and deteriorating groundwater supply for human consumption and irrigation. As water abstraction lowers the water table and changes the direction of groundwater flow towards the pumping well (***Figure 8***), this interrupt the natural equilibrium state of the system and a vertical movement of saltwater upwells, creating an upconing and vertical saltwater intrusion (Bear *et al.*, 1999; Barlow, 2003).

Rising sea level also affect saltwater intrusion. As the seawater head increases, a lateral inland movement of seawater shifts the transition zone landward with the risk of jeopardizing abstraction wells located near the coastline (***Figure 8***). Depending on the geohydrological characteristics of the coastal aquifer time lag of the salinization can vary (Barlow, 2003; Prince Edward Island Department of Environment, 2011; Werner *et al.*, 2013).

3.2. Ghyben-Herzberg Approximation

At the end of the 19th century, two scientists Badon-Ghyben (1888) and Herzberg (1901) independently of each other, developed an analytical solution describing the relationship between the groundwater level and the depth to saltwater under steady conditions of flow. This relationship is described by the Ghyben-Herzberg approximation (FAO, 1997; Bear *et al.*, 1999).

The solution is a simple and widely used equation describing the pressure equilibrium balance of the saltwater-freshwater interface (***Figure 9***). It is based on the following assumptions:

- The system has hydrostatic conditions - with no vertical flow in the salt- and freshwater
- It is a homogenous, unconfined coastal aquifer
- The waters have constant densities
- The saltwater-freshwater interface is abrupt and sharp, and no mixing is occurring
- At the shoreline, freshwater head and sea level elevation are equal.

Due to the assumptions about a sharp interface between fresh- and saltwater, the approximation is also known as the sharp-interface approach (Custodio, 2005; Hendriks, 2010; Dokou and Karatzas, 2012; Fitts, 2013).

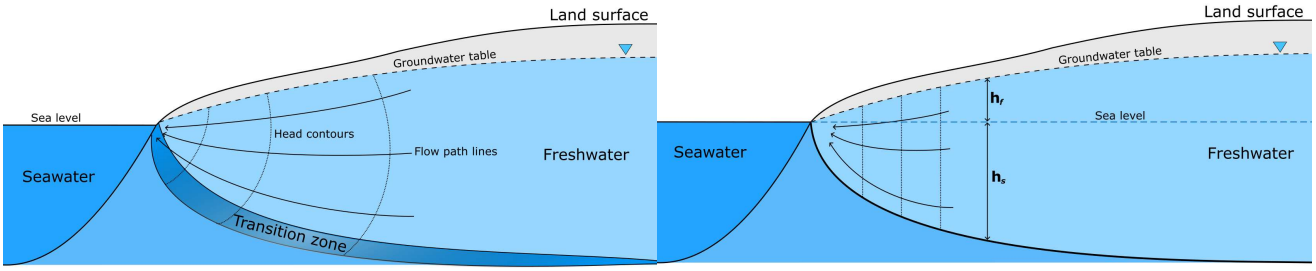

Figure 9. A coastal aquifer system a) In natural conditions. b) A system according to Ghyben-Herzberg approximation under hydrostatic conditions.

Under hydrostatic conditions where the interface is stationary, the weight of freshwater extending from the water table to a point on the interface equals the weight of a saltwater column extending from sea level to the same point on the interface (Schwartz and Zhang, 2003). The hydraulic head h is the sum of the elevation head z and the pressure head $\frac{P}{\rho_w g}$, where ρ is the density of water, and g is gravitational acceleration. The hydraulic head of freshwater h_f, and saltwater h_s within a given system, are defined as

$$h_f + h_s = z + \frac{p_f}{\rho_f g} \tag{3.1}$$

$$h_s = z + \frac{p_s}{\rho_s g} \tag{3.2}$$

In this case, the freshwater head is called the differential head, because it represents the distance from the water table to the sea level. If the elevation head z equals the reference level, then $z = 0$ anywhere along the interface and becomes eliminated. For each point in a fluid, there can only be one hydrostatic pressure, therefore must $p_f = p_s$ and Eq. 3.1 and 3.2 can be combined

$$h_s(\rho_s g) = h_f + h_s(\rho_f g) \tag{3.3}$$

Solving for h_s yields the Ghyben-Herzberg relationship between fresh- and saltwater

$$h_s = \frac{\rho_f}{\rho_s - \rho_f} h_f = \alpha\, h_f \tag{3.4}$$

ρ_f is the density of freshwater, ρ_s is of saltwater and α is the density difference between the two fluids. If standard density values are applied for freshwater and seawater, 1.000 g cm^{-3} and 1.025 g cm^{-3}, respectively, the depth to the interface will be 40 meters below sea level with a groundwater table one meter above sea level. This means, groundwater above sea level will push down the interface 40 times the height of the water table (Bear *et al.*, 1999; Schwartz and Zhang, 2003; Custodio, 2005).

Applying this method, the reader should have following considerations in mind. At or near the coastline the solution predicts the interface to be a depth zero, at the same level as sea level but in natural conditions, the interface can be found below sea level (***Figure 9-a***). The reason for this can be found in the assumption taken about the hydrostatic conditions. In groundwater flow the vertical component is not negligible (Fitts, 2013). Near the shoreline, freshwater has an upward vertical flow which causes the freshwater head to be above sea level instead of being equal to the elevation of the sea level. This entails the actual interface to be located deeper than at zero at the shoreline (Fitts, 2013).

3.3. In coastal settings: interactions between groundwater and saltwater

In coastal environments, the difference in density of fresh- and saltwater is reflected in their chemical composition and the total amount of total dissolved solids (TDS). TDS comprises dissolved organic and inorganic solutes and gasses, whereas inorganic ions make up the majority of the solutes (Fitts, 2013). Average TDS content in seawater is 30,000 - 35,000 mg L^{-1} while freshwater generally contains less than 1,000 mg L^{-1}. The water in between fresh- and saltwater is called brackish water and contains 10,000 - 30,000 mg L^{-1} of TDS (Fitts, 2013a). Total dissolved solids (TDS) is closely related to electrical conductivity (EC) and reflect the ability of water to conduct electricity. Freshwater is defined by a conductivity below 1,000 µS cm^{-1} (Hendriks, 2010).

3.3.1. Composition of seawater and groundwater

The elements sodium (Na) and chlorine (Cl) predominate seawater composition in the form of a dissolved cation Na^+ and anion Cl^-. A water molecule (H_2O) is composed of two hydrogen atoms and one oxygen atom. The polarity of a water molecule is asymmetric because it is bounded by two positively charged atoms and one negative charged atom. From its polarity, water molecules attract other polar charged molecules by electrostatic forces. Sodium and chlorine as elements, have a positively and negatively

charge, respectively. When surrounded by polar water molecules, they dissolve within the water and become dissolve ions (Schwartz and Zhang, 2003; Fitts, 2013).

The high concentration of Na^+ and Cl^- is a result of halite (NaCl) dissolution. Halite is the most abundant salt (Wright and Colling, 1995). Evaporites are salt rocks formed from evaporation and reflect warm periods within Earth geological time. Most evaporites are composed of halite (NaCl) therefore, ocean waters are dominated by these ions (Sørensen, 2012).

Other constituents in seawater composition are calcium (Ca^{2+}), magnesium (Mg^{2+}), potassium (K^+), sulphate (SO_4^{2-}), bicarbonate (HCO_3^-) and bromide (Br^-) (***Table 3.1***). The concentration of ions in seawater depend on the solubility of the elements. The solubility reflects how easily an element can be dissolved in the water. Halite (NaCl) and the elements calcium, sodium and potassium are very soluble. Whereas, weathered product as silicon, aluminum and iron is not as soluble (Bear, 1999; Schwartz & Zhang, 2003; Wright and Colling, 1995).

Table 3.1. Average composition of seawater (Barlow, 2003).

Constituents	Seawater (mg L^{-1})
Cl^-	19,000
Na^+	10,500
SO_4^{2-}	2,700
Mg^{2+}	1,350
Ca^{2+}	410
K^+	390
HCO_3^-	142
Br^-	67

Groundwater composition depends on the aquifer sediment and the time in contact with sediment. The composition of recharging water infiltrating to the aquifer also contributes to the groundwater composition. In coastal regions rainfall has a higher concentration of salts due to the proximity to the ocean. Especially during storms (Bear *et al.*, 1999; Kristiansen, 2012; Fitts, 2013). Calcite dissolution is an important process as the ions calcium and bicarbonate predominates the groundwater composition

$$CaCO_3 + H^+ = Ca^{2+} + HCO_3^- \quad (3.5)$$

Additional ions as magnesium, sulphate and chloride have relatively high concentrations in groundwater too but in a different scale than in seawater (Bear *et al.*, 1999; Appelo and Postma, 2005).

3.3.2. Cation exchange in the saltwater-freshwater interface

The process cation exchange has been pointed out by Appelo and Postma (1993) as an important process in relation to saltwater intrusion. Seawater contains high concentrations of sodium whereas groundwater contains large amounts of calcium. In marine sediment the cation Na^+ is the most prevalent and sorbed ion as the sodium represents a large part within the seawater composition. In coastal aquifers the cation Ca^{2+} is the cation exchanger within aquifers containing clay minerals, organic matter, oxyhydroxide or fine-grained rock material (Bear *et al.*, 1999; Appelo and Postma, 2005). In the transition zone during a seawater intrusion, Na^+ replaces part of the Ca^+ on the sediment surface, and calcium becomes released from the sediment, described by the following reaction

$$Na^+ + \frac{1}{2}CaEx \rightarrow NaEx + \frac{1}{2}Ca^{2+} \tag{3.6}$$

Ex represents the natural exchanger. When seawater encroaches coastal aquifers, Na^+ is adsorbed to the sediment while Ca^+ is released. This reaction changes the composition of water from NaCl to $CaCl_2$ water type. The reverse process, refreshening, occur when freshwater intrudes a saline aquifer. During the cation exchange (independent of the process direction) the chloride (Cl^-) concentration remains unchanged due to the fact that chloride is an conservatively anion (Bear *et al.*, 1999; Appelo and Postma, 2005).

3.3.3. Salinization and salinity sources

Average salinity based on TDS in oceans is 35‰ but can vary due to local conditions as observed for the sea of Kattegat. Salinity (S) and temperature (T) are controlling factors for density of seawater. The relation between those factors is described in the International Equation of State of Seawater from 1980

$$\rho(S,T,P) = \frac{\rho(S,T,0)}{1-\frac{P}{K(S,T,P)}} \tag{3.7}$$

Where ρ is the density of seawater [kg m^{-3}], S is the salinity [‰], T is the temperature [°C] and P is the applied pressure [bars] where the standard atmospheric pressure is used. The term $\rho(S,T,0)$ is the one-

atmosphere International Equation of State of Seawater (1980) and the term $K(S,T,P)$ is the secant bulk modulus (Unesco, 1981).

In average seawater composition, chloride represents ~19,000 mg L^{-1}. As chloride contributes with the largest ion concentration to the seawater composition it is widely used as a proxy for salinity in relation to seawater intrusion (Wright and Colling, 1995; Bear *et al.*, 1999). A simple, empirical equation describes the relationship between salinity and chlorinity of a sample - where chlorinity is defined as the concentration of chloride. The equation is based on the assumption of bromide and iodide have been replaced by chloride (Wright and Colling, 1995)

$$S = 1.80655Cl \tag{3.8}$$

The effect of one percentage of seawater into a coastal aquifer increases the chloride content about three times. If the aquifer mixes with 5 percentage of seawater, chloride concentrations will increase ten times (Bear *et al.*, 1999). But intrusion of modern seawater is not the only source of salinization in coastal aquifers. Other sources of salinity include:

- Seawater spray, especially during strong winds
- Intense evapo-concentration of surface- and phreatic water in dry climates
- Tides and storm surges of seawater into low-lying coastal areas
- Dissolution of evaporites from geological formations
- Old marine fossil water trapped in unflushed slow-flowing aquifers or aquitards during past invasion of sea level rise
- Displacement of saline groundwater and brines in deep formations as results of natural advection or leaking through fault systems
- Agriculture return flow of irrigation water

Anthropogenic pollution by saline waters and waste from mine water drainage, industrial effluent from softening, de-ionization and desalinization industrial plants, dissolution from de-icing road salt and leakage from industrial processes and cooling facilities using brackish to saline water, are also sources of salinization of groundwater (FAO, 1997; Bear *et al.*, 1999; Custodio, 2005).

3.3.4. Determination of salinity sources

Seawater encroachment is not the only source to saltwater intrusion, as salt can have other origins. Identification of salinity sources is important in relation to groundwater exploitation to obtain a better knowledge of the system (Custodio, 2005). To distinguish salinity sources, ratios of different ions are widely used. Of those, can be mentioned Cl/Br (***Table 3.2***) and Na/Cl (FAO, 1997; Bear *et al.*, 1999; Werner *et al.*, 2013). The concentration of fluoride in chalk and limestone aquifers has also been used to determine saltwater origin (Århus Amt, 1995; Fyens Amt, 2001; Mielby and Sandersen, 2005; Kristiansen *et al*., 2009).

Chloride to bromide (Cl/Br) mass ratio

In the ratio Cl/Br, Br^- represents the anion bromide. Bromide contributes to the seawater composition too. As chloride, bromide is a conservative ion due to its small ionic size and its hydrophilic character (Bear *et al.*, 1999; Alcalá and Custodio, 2008). Both ions are not included in the ion exchange processes and neither are they adsorbed to the aquifer sediment. Average concentrations of Cl^- and Br^- in the composition of seawater are 19,000 mg L^{-1} and 67 mg L^{-1}, respectively.

Due to the minor fraction of bromide in seawater, its ionic concentration is hard to measure. Measured concentrations below 0.2 Br mg L^{-1} are mostly inaccurate. This limits the application of the Cl/Br ratio to waters containing chloride concentrations exceeding 60-100 mg L^{-1} (FAO, 1997; Alcalá and Custodio, 2008). Some sources of Cl^- and Br^- are atmospheric fallen material, evaporite dissolution, brine extrusion from clay layers and seawater intrusion into coastal aquifers (Davis *et al*, 1998).

The Cl/Br mass ratio of seawater is between 288 to 297. The Cl/Br ratio of seawater is used as a reference point to compare ratios of other types of waters. The Cl/Br ratio of precipitation varies from coastal to continental environment depending on the distance to the ocean. Coastal precipitation affected by evaporation of seawater ranges from 130-180 Cl/Br. Further inland (up to few hundreds of kilometers) ratios vary from 75 to 120. For several of hundreds of kilometers inland ratios can be as low as 50 (Davis *et al*., 1998). In shallow aquifers with fresh to brackish water, Cl/Br ratios are below 112. If water evaporates, the salt halite (NaCl) is the first to be precipitated leaving the residual brine enriched in bromide. Cl/Br ratios of brines is generally below the ratio of seawater ranging from 112-296. Freshwater streams with low chloride content (< 100 mg L^{-1}) and no interference with human activity as the ones

discharging to Lake Superior, have mean ratios of 107. Water affected by halite dissolution have Cl/Br ratios above >1300 (Davis *et al*., 1998).

Anthropogenic sources of bromine are pesticides, medicines, industrial solvents, water purification compounds and gasoline additives. Human activity can affect the Cl/Br ratio (Davis *et al*., 1998; Alcalá and Custodio, 2008; Han *et al.*, 2011). Alcalá and Custodio (2008) listed few anthropogenic sources as wastewater with NaCl or leaching of solid waste give ratios above 666, whereas the use of Br-based pesticides or leaching of farm animal and septic waste decreases the ratio to < 133. Leaching of industrial NaCl increases ratios to >444 (Alcalá and Custodio, 2008). Winter runoff impacted by de-icing salt from roads is described to contain Cl/Br ratio up to 1,176. Studies from England and the United States show ratios vary from 300 to 600 for urban sewage (Davis, Whittemore and Fabryka-Martin, 1998).

Table 3.2. Cl/Br ratio values and associated salinity sources from Alcalá and Custodio (2008), Davis *et al*. (1998) and Han *et al*. (2011).

Salinization source	Cl/Br ratio
Seawater	288 - 297
Brines	112 ≤ 282
Coastal precipitation	130 - 180
Continental precipitation	50 - 150
Connate water (incl. oil field water)	200 - 400
Domestic sewage effluents	300 - 600
Freshwater to brackish water	< 112
Shallow groundwater (< 5 Cl mg L^{-1})	80 - 160
Urban street runoff (summer)	10 - 100
Urban street runoff (winter)	~1167
Water affected by halite dissolution	1,000 - 10,000
Wastewater or leaching solid waste with NaCl	> 666
With pesticides or farm animal and septic waste	> 133

Sodium to chloride (Na/Cl) molar ratio

As the cation Na^+ is one of the major components in the ion exchange process and is one of the largest contributors to seawater composition, it is an important tracer of salinity. In combination with the conservatively anion chloride (Cl^-) the molar ratio of sodium to chloride Na/Cl can be used as an indicator

of seawater intrusion. As modern seawater intrudes a coastal freshwater aquifer, Na^+ from seawater adsorbs onto the aquifer sediment decreasing the content of sodium in the water. At the same time chloride concentrations remain unchanged as Cl^- does not take part in the exchange process (Bear *et al.*, 1999; Appelo and Postma, 2005). The molar Na/Cl ratio of seawater is 0.86 and therefore, ratios of saltwater intrusion in coastal aquifers will be lower (< 0.86). Higher Na/Cl ratios (> 1 Na/Cl) can be of anthropogenic sources like domestic waste waters or from connate water as the reverse process of ion exchange (refreshening) increases the content of sodium (Bear *et al.*, 1999; Appelo and Postma, 2005).

Fluoride concentration

In Danish studies, the concentration of fluoride in combination with high chloride concentrations, has been used as an indicator of fossil, stagnant water in chalk- and limestone aquifers (Århus Amt, 1995; Mielby and Sandersen, 2005; Kristiansen *et al*., 2009). The fluoride content depends on the time water has been in contact with the calcareous minerals as fluorite (CaF_2) (and/or phosphorite [$Ca_5(PO_4,CO_3,OH)_3F$]). Dissolution of fluorite follows (Larsen and Berger, 2006)

$$CaF_2 = Ca^{2+} + 2F^- \tag{3.9}$$

3.3.5. Regulations and monitoring of water quality

Legislations of drinking water quality are determined by the Danish directive of drinking-water. The directive is based on the European Drinking Water Directive. The ions sodium (Na^+) and chloride (Cl^-), and the electrical conductivity (EC) are all indicative parameters of saltwater intrusion and are used within regulations and monitoring of water quality (***Table 3.3***). In corporation with the Geological Survey of Denmark and Greenland (GEUS), monitored water quality (water chemistry) data is stored in a database administered by GEUS. (Miljøstyrelsen, no date; Miljø- og Fødevareministeriet, 2019).

Table 3.3. Selected indicator parameters used to access quality of drinking water for human consumption according to the Danish Directive of Drinking Water (Miljø- og Fødevareministeriet, 2019).

Parameter	Parametric maximum value
Conductivity [µS cm^{-1}]	2,500 at 20 °C
Chloride [mg L^{-1}]	250
Sodium [mg L^{-1}]	175

GEUS is an independent research- and advisory institution in the Danish Ministry of Climate, Energy and Utilities (GEUS, 2021). In terms of groundwater, GEUS is part of the National Groundwater Mapping by the Environmental Protection Agency where the purpose is to ensure clean water in the future. GEUS contributes to groundwater mapping by making several public databases with relevant data available. This includes the Jupiter database, the GERDA database, the Report database and the Model database (GEUS, 2021).

The Jupiter database is the national well database, comprising multi-screened redox wells, piezometric wells, abstraction wells and monitoring wells in order to supply data of groundwater. Data is compiled from more than 280,000 wells across Denmark. Technical structure and location of the wells, geological information, water level measurements and groundwater chemistry, are some of the information that can be found for each well (GEUS, 2021). The Danish monitoring programme (GRUMO) is part of the National Monitoring and Assessment Programme for the Aquatic and Terrestrial Environment (NOVANA) by the Environmental Protection Agency. The purpose of the programme, is to provide accessible data for groundwater modeling, and for identifying contamination and pollution sources. GRUMO comprises over 1,000 monitoring wells (Jørgensen and Stockmarr, 2009).

Besides monitoring sodium and chloride, main components as potassium (K), magnesium (Mg), sulphate (SO_4) and calcium (Ca) etc. are monitored. In addition, inorganic trace elements, organic micro pollutants, pesticides and metabolites are monitored too. Within agricultural catchments main components are monitored six times per year while for drinking-water supply abstractions wells, main components are monitored every third to fifth year (Jørgensen and Stockmarr, 2009).

The GERDA database contains geophysical data of surface-near geophysics and have special focus on areas of drinking-water interest. Geophysical data includes log, Wenner, seismic, TEM, skyTEM, paces, pacep, MEP, MRS and Schlumberger (GEUS, 2021).

3.3.6. The effect of future climate change on coastal aquifers

From the beginning of the pre-industrial period (~1850), the average global surface temperature has shown an increasing trend (Masson-Delmotte *et al.*, 2018). The main effect of rising temperatures is the melting of ice sheets, caps and glaciers which contributes to global sea level rise. Within the last century, sea level rise has increased from 1.4 mm yr^{-1} (1901-1990) to 3.2 mm yr^{-1} (1993-2015) to 3.6 mm yr^{-1}

(2006-2015), where anthropogenic forces (since 1970's) has been the dominant causes (Oppenheimer *et al.*, 2019).

On global scale, ice melting, land-water storage changes and thermal expansion of the ocean due to increasing surface temperatures are identified as the cause of sea level rise. Thermal expansion of the oceans depends on salinity and water temperature. Especially surface water in the upper few hundred meters can be affected by thermal expansion as heating of bottom water may take up to centuries (FAO, 1997; Oppenheimer *et al.*, 2019). At the end of this century, global sea level rise is predicted to 0.43 meters (ranging from 0.29-0.59 m) according to the 'very stringent' scenario Representative Concentration Pathway RCP2.6, and rise to 0.84 meters (ranging from 0.61-1.10 m) for the very high GHG (Green House Gas) emissions scenario RCP8.5 (***Figure 10***) (IPCC, 2014).

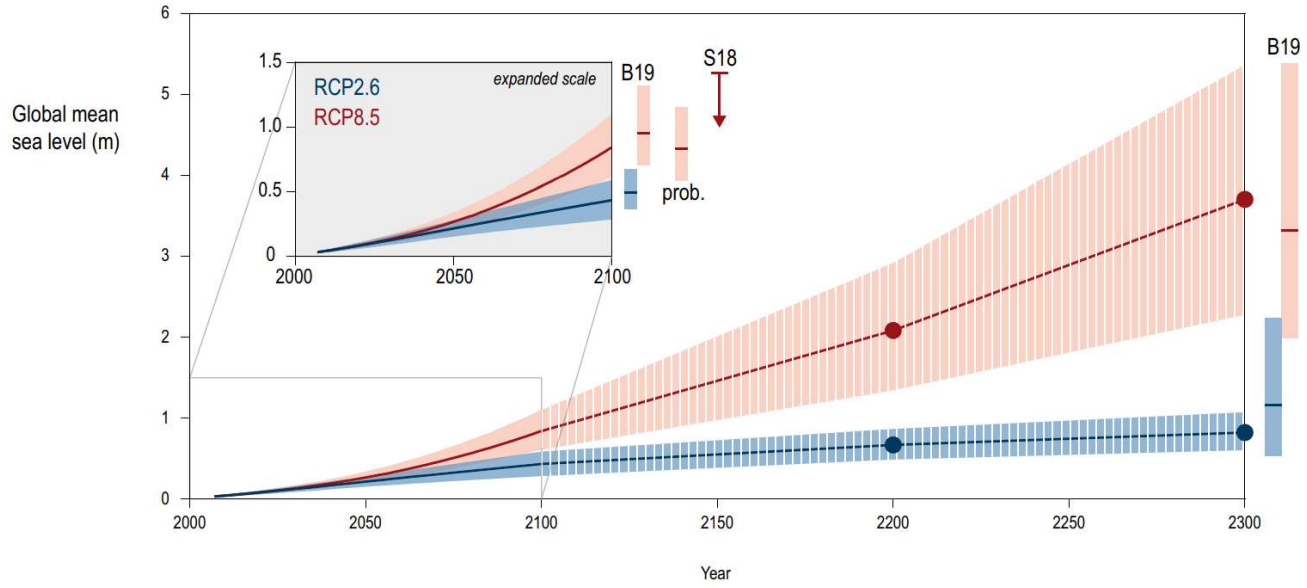

Figure 10. Predicted sea level rise according to the IPCC climate scenarios RCP2.6 and RCP8.5 (Oppenheimer *et al.*, 2019).

On regional scale, subsidence, ocean dynamics, climate variability and geodynamics (changing of water mass distribution between land, ice and ocean reservoirs) are driving mechanisms impacting regional mean sea level changes and extreme sea level events. Low-lying areas and coastal regions are the first to be impacted by the effect of sea level rise. Coastal hazards as permanent submergence, coastal flooding, enhanced coastal erosion, loss and changes of coastal ecosystems, salinization of soil, surface- and groundwater, and impeded drainage can be the consequence of sea level rise (Oppenheimer *et al.*, 2019).

Saline water intrusion of coastal aquifers and surface waters and soils is according to the 'IPCC Special Report on the Ocean and Cryosphere in a Changing Climate' expected to become more frequent and occur further inland (Oppenheimer *et al.*, 2019). Land-based drought events, decreasing river discharge, water extraction and sea level rise, are all expected mechanisms of future climate changes and driving forces of increasing salinization in coastal low-lying regions. Coastal erosion is also a resulting hazard of sea level rise and can impact a landward shift in the transition zone in coastal systems. Variations in precipitation patterns are expected to increase which impact the groundwater level and volume of groundwater aquifers. Marine flooding events affecting the water table heigh can intensify salinization. At many locations, direct human activity as groundwater exploitation already impact salinization stronger than expected from the effect of sea level rise in the 21st century. Groundwater depletion from exploitation, can contribute to land subsidence and increase the risk of coastal flooding. As a consequence of increasing surface temperatures, an enhanced demand of freshwater supply can occur (Prince Edward Island Department of Environment, 2011; Oppenheimer *et al.*, 2019). From long-term records of salinity and statistical models, a significant upward trend in salinity and a positive correlation between increasing salinity and sea levels have been shown (Oppenheimer *et al.*, 2019).

3.3.5.1. Climate change in Denmark

Since 1870, mean temperature has increased 1.5°C and precipitation has increased approximately 100 mm in Denmark. Both increasing numbers and intensity of heavy precipitation events have been observed (Task Force for Klimatilpasning, 2012). The government in Denmark has implemented initiatives for climate adaptations. This include municipalities to have specific strategies to mitigate and adapt to future climate changes. As part of a national mitigation strategy, a national database of climate change named Klimaatlas (DMI, 2021a) has been established by DMI and is based on the IPCC reports and climate scenarios. The database comprises data for the climate scenarios RCP4.5 and RCP8.5. It includes data about temperature, precipitation, sea level rise and storm surges for each municipality in Denmark in order for the municipalities to mitigate and adapt (DMI, 2021a).

For the municipality of Norddjurs and Syddjurs, the largest climate changes are increasing precipitation and heavy rain events (***Table 3.4***).

Table 3.4. Predicted parameters according to scenario RCP4.5 and RCP8.5 by the end of the 21st century (Klimaatlas, 2020).

	Norddjurs		Syddjurs	
Scenarios (by end of 21st century)	**RCP4.5**	**RCP8.5**	**RCP4.5**	**RCP8.5**
Average precipitation	+7.48 %	+13.23 %	+7.33 %	+13.05 %
Heavy rain events	+49.78 %	+79.03 %	+50.66 %	+76.80 %
Average temperature	+1.92°C	+3.42°C	+1.92 °C	+3.41°C
Potential evaporation	+2.23 %	+4.61 %	+2.14 %	+4.53 %
Extreme winds	-0.01 %	+0.01 %	0.00 %	+0.01 %

Coastal areas	**Ålborg Bugt**		**East coast of Djursland**		**Århus Bugt**	
Scenarios (by end of 21st century)	**RCP4.5**	**RCP8.5**	**RCP4.5**	**RCP8.5**	**RCP4.5**	**RCP8.5**
Mean sea level rise [m]	0.31	0.48	0.27	0.49	0.29	0.51

Djursland has three coastal areas, from the north Ålborg Bugt, the east coast of Djursland, and Århus Bugt in the south. Sea level rise along the entire coast of Djursland is approximately 0.29 meters for the RCP4.5 scenario and 0.49 meters for the RCP8.5 scenario (Klimaatlas, 2020).

3.4. Airborne Electromagnetic (AEM) method

Geophysical methodology can be applied in groundwater investigations to identify the location of the saltwater-freshwater interface (Bear *et al.*, 1999; Werner *et al.*, 2013). The airborne electromagnetic (AEM) method is a time-domain geophysical method and investigates the electrical properties of subsurface sediment. The electrical properties of the sediment or water depend on the properties of rock and sediment and the mineral content in porewater. Clay sediment and saline groundwater decreases the resistivity (Bear *et al.*, 1999; Werner *et al.*, 2013). AEM methods are beneficial in geological and hydrogeological surveys when mapping geological structures and sediment types as well as identifying groundwater reservoirs for drinking-water supply. This is because they are relatively in-expensive, fast in surveying and can therefore cover large areas (Jørgensen *et al.*, 2012; Werner *et al.*, 2013).

SkyTEM is a AEM method and is new tool to investigate aquifers electronically. The skyTEM system was developed by Sørensen and Auken (2004) and it comprises a large wire loop transmitter and a small receiver loop, both connected to an airborne helicopter. The transmitter loop can vary in size depending on the depth needed for the investigation (Sørensen and Auken, 2004; Jørgensen *et al.*, 2012). The system consists of a transmitter loop, a receiver coil, a laser altimeter and inclinometer. The transmitter loop is driven by a high current pulsed direct current (DC), creating a primary magnetic field which, when

switched off, an eddy current is induced in the ground. As response, a secondary magnetic field is created and the time-derivative is measured by the receiver coil (Høyer *et al.*, 2011). This response of the ground material makes skyTEM suitable for detecting conductive layers where eddy currents are stronger as in groundwater aquifers but also for sediment saturated with saline water. With depth, diffusion within the ground decreases the resolution of the electromagnetic field, which makes it difficult to obtain detailed structures only applying skyTEM. Therefore, it is recommended to use the method in combination with other methods (Høyer *et al.*, 2011; Jørgensen *et al.*, 2012). SkyTEM often operates with two transmitter modes to achieve higher resolution. One mode providing high resolution of the upper subsurface geology by a lower current fast pulse, and another focusing on the deeper geology down to depths of 200-300 meters by a high current longer pulse. The transmitter modes are joined together and combined to a single location measurement. The height of the frame is measured by the altimeter and the inclinometer make up the correction of the movement of the frame (Høyer *et al.*, 2011; Jørgensen *et al.*, 2012).

The time responded data is processed and inversed to resistivity data and in Denmark, stored in the geophysical GERDA database by the Geological Survey of Denmark and Greenland (GEUS, 2021).

3.5. SEAWAT model

Numerical modelling is a computable method to simulate seawater intrusion with a density-dependent transport and flow model. There exist a variety of public domain computer codes where some are based on finite-elements and others on finite-differences method (Guo and Langevin, 2002). One very used code is the SEAWAT computer program (e.g. Vijay and Monapatra, 2016; Janardhana and Khairy, 2019; Rasmussen *et al*., 2013; Meyer *et al*., 2019; Batchtouli and Comte, 2019).

SEAWAT is based on the finite-difference method and was developed by US. Geological Survey (USGS) to simulate 3D, variable-density, transient groundwater flow and transport in a porous medium. The code is based on a combination of MODFLOW and MT3DMS into a system that solves governing equations describing couple flow and solute transport problems (Guo and Langevin, 2002; Langevin *et al.*, 2007).

To solve the governing equations, some basic assumptions have been made; validation of the Darcy's Law, standard expression for specific storage in a confined aquifer, the diffusive approach to dispersive transport is based on Fick's Law, and lastly, the isothermal conditions are prevailed. In addition, the porous medium of the aquifer is fully saturated with water (Guo and Langevin, 2002).

The governing equation of groundwater flow based on the principle of conservation of mass is

$$-\nabla(\rho\vec{q}) + \bar{\rho}q_s = \frac{\partial(\rho\theta)}{\partial t} \tag{3.10}$$

Where ∇ is gradient operator $\frac{\partial}{\partial x} + \frac{\partial}{\partial y} + \frac{\partial}{\partial z}$, ρ is the density of the fluid, $\vec{q}$ is the specific discharge vector, $\bar{\rho}$ is the water density either as a source/sink, q_s is the volumetric flow rate per unit volume of an aquifer representing source/sink, θ is the dimensionless porosity and t is the time (Guo and Langevin, 2002; Vijay and Mohapatra, 2016). Equation 3.10 can be extended to a partial differential equation for variable-density groundwater flow in a porous media

$$-\nabla(\rho\vec{q}) + \bar{\rho}q_s = \rho S_p \frac{\partial P}{\partial t} + \theta \frac{\partial \rho}{\partial C}\frac{\partial C}{\partial t} \tag{3.11}$$

Where S_p is the specific storage in terms of pressure, P is fluid pore pressure and C is the solute concentration. If the density is constant the term $\frac{\partial \rho}{\partial C} = 0$ and the remaining term equals zero too. For a variable-density system only fluid volume is conserved whereas for a constant density-system both fluid volume and fluid mass is conserved (Guo and Langevin, 2002).

As groundwater flow redistribute solute concentration and the redistribution of solute concentration changes the density field this will affect the groundwater movement. Therefore, groundwater movement and the transport of solutes in an aquifer are a coupled process and SEAWAT solve the two equations jointly. Main mechanisms in solute transport is groundwater advective flow, molecular diffusion and mechanical dispersion. The partial differential equation describes solute mass transport

$$\frac{\partial C}{\partial t} = \nabla\,(D\,\nabla C) - \nabla(\vec{v}C) - \frac{q_s}{\theta}C_s + \sum_{k=1}^{N} R_k \tag{3.12}$$

Where D is the hydrodynamic dispersion coefficient, $\vec{v}$ is the fluid velocity, C_s is the solute concentration of water from source/sinks, and R_k where $k = 1,...N$, is the rate of solute production or decay in a reaction k of N different reactions (Guo and Langevin, 2002).

4. Methodology

To identify saltwater intrusion in Djursland, a combination of four methods will be applied. Ghyben-Herzberg analytical solution will be used to determine the spatial location of the saltwater-freshwater interface. A multi-geochemical analysis will identify areas vulnerable to saltwater intrusion and determine associated salinity sources based on ionic ratios and main components of groundwater and seawater. Geophysical airborne electromagnetic (AEM) method will be used to discriminate fresh groundwater from saline groundwater based on resistivity skyTEM data. Finally, a 2D numerical SEAWAT model will be constructed to identify key parameters through a sensitivity analysis. Further the model will be used to simulate past, present and future scenarios of the drained Kolindsund to achieve a better understanding of the dynamics of the system and the response of the system to drainage and effects of future climate changes. Only available data from public Danish databases will be applied in the multi-method approach (***Figure 11***).

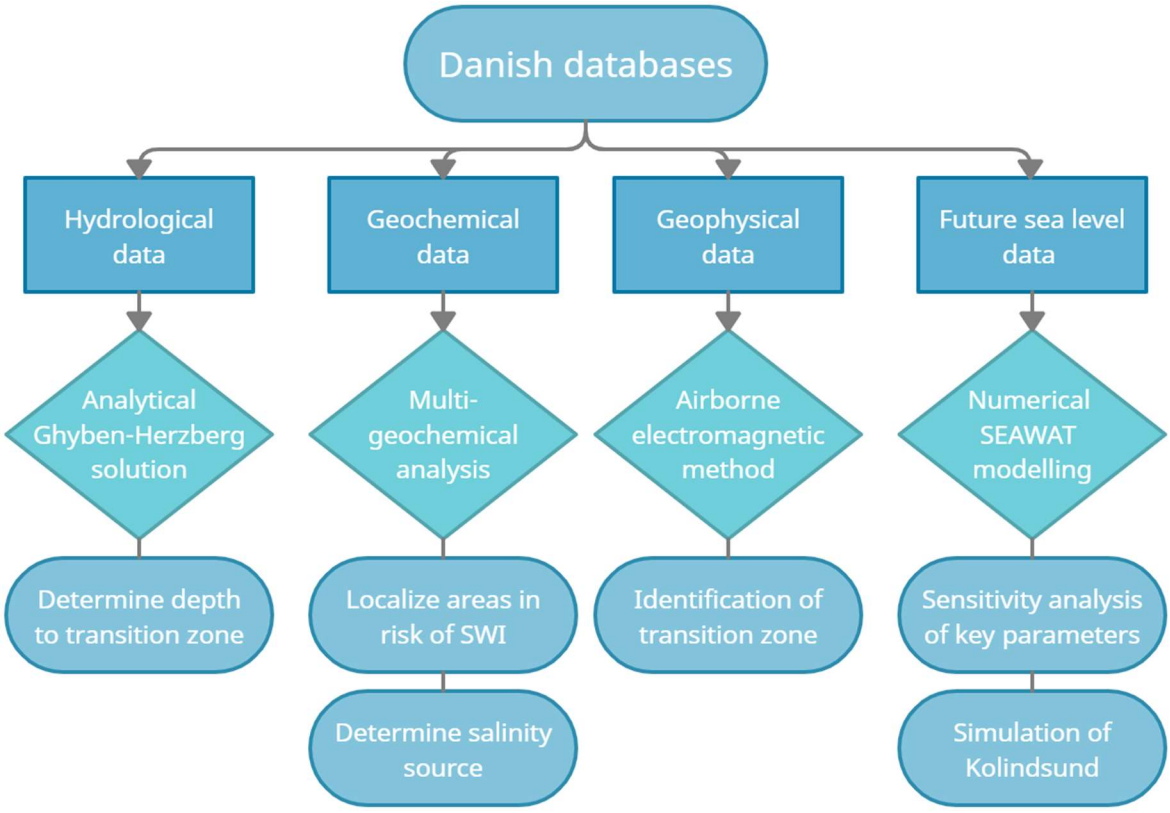

Figure 11. Multi-method approach used to identify saltwater intrusion based on data from public Danish databases.

4.1. Data from Danish databases

Hydrological and geochemical data used in this study are compiled from the national Jupiter database (JUPITER, https://jupiter.geus.dk/), and geophysical data is extracted from the GERDA database, (GERDA, https://gerda.geus.dk/). Relevant climate data for simulated future scenarios, is extracted from the Klimaatlas database (Klimaatlas, https://www.dmi.dk/klimaatlas/).

Hydrological data within the study area comprises 3,255 groundwater head measurements measured in DVR90 (extracted date 11-01-2021). Data includes measurements of minimum, maximum, median and latest measured groundwater head. Head measurements have been measured from 1903 till 2020. Due to fluctuations of the water table, median groundwater head measurements are applied in the data processing. Of all samples, 205 head measurements have head values below mean sea level. Those samples are found within the Kolindsund strait, in coastal areas and within Kolindsund.

Extracted geochemical data contains main components measurements and electrical conductivity (EC) measurements. Relevant main components include sodium, chloride, sulphate, calcium, potassium, bicarbonate, magnesium, and fluoride. Data of the trace element bromide has additionally been extracted. Two datasets were extracted (extracted date 01-03-2021) from the database. Dataset 1 contained all temporal data measured and reported to the database of main components and EC, and dataset 2 contained maximum, minimum, median and latest measured data of the main components and the trace element, including EC. In addition, relevant information includes sampling depth relative to terrain surface (meter below terrain in DVR90) and a geological description of the well (aquifer sediment). Information about geochemical data can be found in ***Appendix A1***.

Aquifer sediments include pre-Quaternary and Quaternary sediments. Within approximately 1/10 of all geochemical samples no aquifer sediment was identified and are classified as unidentified sediment. Pre-Quaternary sediment includes Danian Limestone, Maastrichtian Chalk, unidentified chalk and 'not Quaternary aquifer'. Quaternary sediment comprises Quaternary sand and clay, unidentified sand and clay, Quartz sand and gravel, organic sediment, and diverse sediment.

The GERDA database provided log, seismic, paces, pacep, tTEM, TEM and MEP geophysical data within the study area. But those data are restricted to limited areas within Djursland. SkyTEM data is the only datatype covering the largest part of the study area. The data was extracted by applying the software

GeoScene3D which includes GERDA and Jupiter databases. Information about the skyTEM data can be found in ***Appendix A2***.

Estimated sea level rise data from the Klimaatlas database has been extracted (extracted date 13-05-2021) for Ålborg Bugt, the east coast of Djursland, and Århus Bugt which together comprises the coastline of Djursland.

4.2. Analytical solution

The Ghyben-Herzberg equation (Eq. 3.4) has been used to calculate the depth to the saltwater-freshwater interface based on groundwater head data extracted from the study area. To determine the density ratio α between groundwater and Kattegat seawater, the density of Kattegat water has been calculated (***Table 4.1)*** based on salinity and temperature of the sea (***Figure 12***), with the use International Equation of State of Seawater (Eq. 3.9).

Table 4.1. Calculated densities of stratified waters of Kattegat and associated density ratio factor α.

Salinity [‰]	Temperature (average) [°C]	Water density [kg m^{-3}]	Factor α
16	9.6	1012	81.5
26	9.6	1020	49.9
32	8.4	1025	40.2

According to the study of Hansen *et al*., (2012), the values 16‰ and 26‰ represent minimum and maximum salinity values of the surface water in Kattegat. 32‰ represents salinity of the bottom water. Associated temperatures of surface and bottom water of Kattegat (**Figure *12***) were applied to calculate the density (Hansen *et al.*, 2012).

The software GMS (Groundwater Modelling System) was used in processing and interpolation of calculated depths to the interface. Natural Neighbor - Gradient was used as interpolation method as it smoothens the surface due to the concept of local coordinates (AQUAVEO, 2017). The purpose of applying GMS was to create a surface map that represented the saltwater-freshwater interface in Djursland.

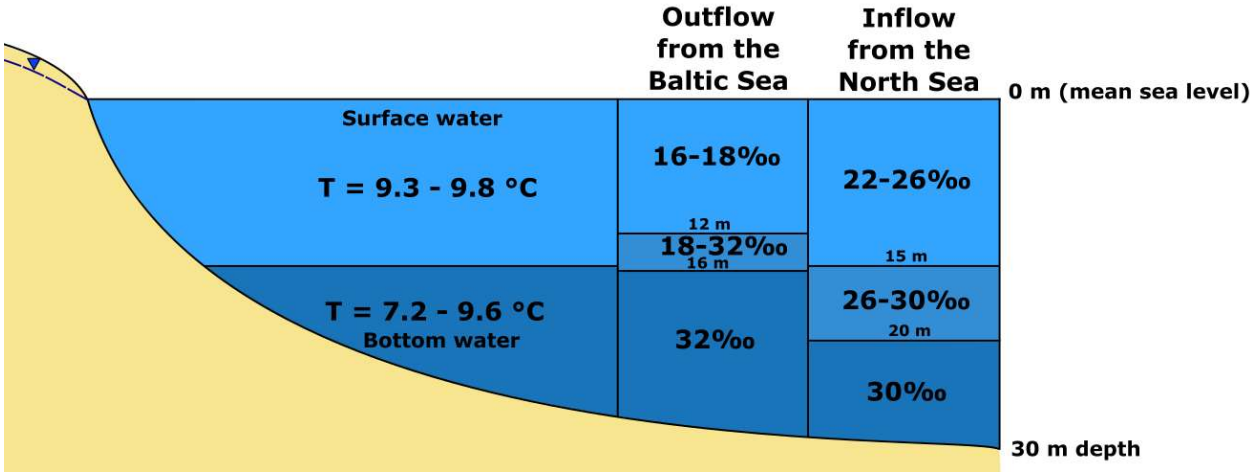

Figure 12. Conceptual stratified column within Kattegat based on Lund-Hansen (1994) and Hansen *et al*., (2012).

4.3. Multi-geochemical analysis

The multi-geochemical analysis comprises seven methods to identify areas in risk of saltwater intrusion and salinity sources. The methods include:

- Chloride and electrical conductivity (EC) used as proxies of salinity
- Identify hydrofacies (water types) with piper diagram
- Illustrate composition of groundwater samples with stiff diagrams
- Use Base-Exchange Index to determine state of water
- Apply geochemistry data to determine salinity sources
    - Molar ratio of Na/Cl
    - Mass ratio of Cl/Br
    - Fluoride content

To identify salinized areas, chloride (Cl^-) and electrical conductivity (EC) will be used as proxies of salinization (FAO, 1997; Bear *et al.*, 1999). Fresh groundwater represents water containing less than 100 mg L^{-1} of chloride and less than 1,000 µS cm^{-1} of electrical conductivity (Lyles, 2000; Barlow, 2003). Groundwater exceeding Danish drinking-water standards, of chloride (> 250 mg L^{-1}) and electrical conductivity (> 2,500 µS cm^{-1}) is defined as saline water (Miljø- og Fødevareministeriet, 2019). Water containing chloride concentration in the range of 100-250 mg L^{-1} and electrical conductivity within 1,000-2,500 µS cm^{-1}, is defined as transition water.

As salinity can vary in Kattegat due to the inflow and outflow of the North Sea and the Baltic Sea (Lund-Hansen *et al.*, 1994; Hansen *et al.*, 2012), respectively, so can chloride concentrations within the composition of seawater. Hypothetical chloride concentrations have been calculated based on Eq. 3.8 (***Table 4.2***) using earlier applied salinity values 16‰, 26‰ and 32‰. The hypothetical will be used to compare measured chloride concentrations obtained from the database,

Table 4.2. Calculated chloride content based on representative salinity values of Kattegat.

Salinization [‰]	Calculated Cl content [mg/L]
16	8,857
26	14,392
32	17,713

To determine the hydrochemical facies of groundwater samples in Djursland, the Piper diagram (1944) has been widely used as a tool in saltwater intrusion studies (e.g. Carol & Kruse, 2012; Jørgensen, 2002; Najib *et al*, 2017; Thorn, 2011). The trilinear (piper) diagram (***Figure 13-left***) graphically illustrates the geochemical abundance of major ions and is a beneficial way to illustrate a large number of samples in a single diagram (Appelo and Postma, 2005). The main components calcium, magnesium, sodium, potassium, bicarbonate, carbonate, chloride, sulphate and total dissolved solids (TDS) are used within the diagram and their concentrations are converted to percentage (%). The diagram is composed of two triangles illustrating proportions of cations and anions, and a diamond shape in between the triangles. Depending on the location of a sample within the diamond shape, a water sample can represent groundwater or seawater composition, mixing, saltwater intrusion or refreshening (Schwartz and Zhang, 2003; Appelo and Postma, 2005). The software Groundwater Chart (GW chart, U.S.G.S) was applied to illustrate the Piper diagram.

To illustrate the geochemical composition of a single sample in a diagram, stiff diagram is applied (***Figure 13-right***). The diagram is composed of three to four horizontal axes of different ionic components. In the left side of the axes, the cations are represented and in the right side, anions are represented, both measured in milliequivalent per liter (meq L^{-1}). The cation Na^+ and anion Cl^- represents the upper axis because they reflect the impact of seawater into groundwater as the main salt (NaCl) contributors in seawater composition.

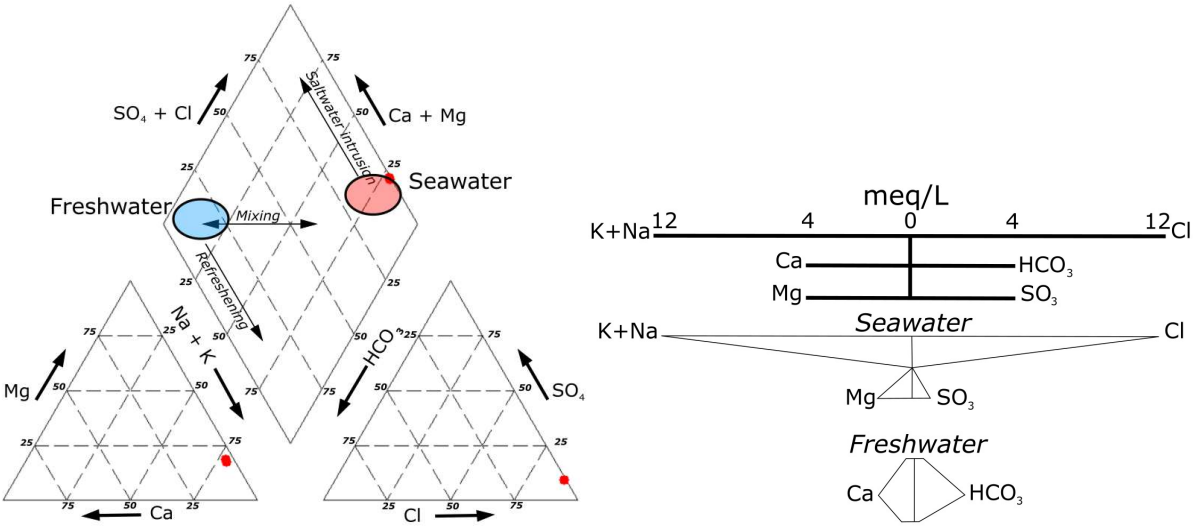

Figure 13. Left: Piper diagram showing average composition of freshwater and seawater (Appelo and Postma, 2005). The seawater samples from Katttegat, from the study of Jørgensen (2002) is plotted (red dot).
Right: Stiff diagrams for average seawater and freshwater composition (inspired by Appelo and Postma, 2005).

The next axis contains Ca^{2+} and HCO_3^- which reflect the calcite ($CaCO_3$) dissolution. The third axis contains Mg^{2+} and SO_4^{2-} which represent the remaining components of water. Based on the composition and concentration of each ion within a sample, a specific shape will be formed reflecting the water type or compositions of the sample (Appelo and Postma, 2005). The software GeoStiff (GeoStiff, Texas Water Development Board) has been used to create stiff diagrams for chosen water samples.

The Base-Exchange Index (BEX-index) proposed by Stuyfzand in 1986 reflects the state of an aquifer if it is subjected to a saltwater intrusion or a refreshening depending on the index. As seawater intrudes a freshwater aquifer an ion exchange process occurs, displacing relative concentrations of sodium (Na^+) and calcium (Ca^{2+}). Ion exchange occurs too when freshwater intrudes a saltwater aquifer and the reverse process takes place between the ions, Na^+ and Ca^{2+}. This ion exchange process is reflected in the BEX-index and depends on the concentration of sodium, potassium, magnesium and chloride (Stuyfzand, 2008)

$$BEX\text{-}index = Na + K + Mg - 1.0716\,Cl \quad (4.1)$$

The factor 1.0716 reflects the total sum of Na, K and Mg over the concentration of chloride expressed in milliequivalent per liter (meq L^{-1}) for mean seawater. A negative BEX-index value indicates a salinization while a positive value indicates a refreshening of the system. If the BEX-index is equal zero, the system is stabilized (Stuyfzand, 2008). Besides indicating the direction of ion exchange, the

magnitude of the exchange process is reflected too within the index value (Stuyfzand, 2008). The BEX-index is applied for groundwater samples within the study area.

The ratios Na/Cl and Cl/Br and the content of fluoride are used to identify salinity sources of groundwater samples in Djursland. Sodium to chloride (Na/Cl) ratio is calculated in molar concentration (mmol L^{-1}). A low ratio < 0.86 Na/Cl reflect modern seawater as salinity source while a high ratio (> 0.86 Na/Cl) represents connate water or anthropogenic effects. Chloride to bromide is calculated in mass per unit volume concentration (mg L^{-1}) and reflects the weight ratio (Bear *et al.*, 1999). Values of Cl/Br ratio with associated salinity source can be found in table 3.2, section 3.3.4. Fluoride is used as an indicator of fossil stagnant water, when fluoride content exceeds 1.5 mg L^{-1} together with high chloride content (Kristiansen *et al*., 2009).

4.4. Geophysical approach

The software program GeoScene3D was applied to process airborne electromagnetic (AEM) data. The geophysical database GERDA is integrated in the GeoScene3D program, therefore AEM skyTEM data was extracted within the program. Two models will be constructed. One showing interpolated resistivity skyTEM data, and another identifying water types (fresh, transition and saline water) and the boundaries between them.

A three-dimensional grid was constructed (191 columns x 152 rows x 121 layers) for processing the data. The Inverse Distance Weighted (IDW) interpolation method was applied as the grid intersect the data points (GeoScene3D, no date).

Furthermore, a voxel model was constructed with same spatial discretization as the 3D grid mentioned above (***Appendix A3***). The voxel model was used to distinguish the water types; freshwater, transition water, and saline water, and identify the location of the boundary between the waters based on the value of resistivity. As resistivity is the reciprocal of conductivity (***Table 4.3***), freshwater is defined as > 10 Ωm, transition was as 10 - 4 Ωm, and saline water is defined as < 4 Ωm according to Danish drinking-water standards of electrical conductivity (2,500 µS cm^{-1}) (Jørgensen *et al.*, 2012; Fødevareministeriet, 2019). Identified boundaries between the waters from the second model, will be plotted on top of the interpolated resistivity data in the first model.

Kolindsund in the eastern Djursland has been chosen as target study area for the geophysical investigation because there is a lack of geochemical data within the area.

Table 4.3. Water types and their associated conductivity and resistivity value.

Water type	Conductivity [µS cm^{-1}]	Resistivity [Ωm]
Freshwater	< 1000	> 10
Transition water	1000 - 2500	10 - 4
Saline water	> 2500	< 4

4.5. Numerical modelling in SEAWAT

A 2D density-dependent flow and transport model was constructed with SEAWAT v4. (incl. MODFLOW and MT3DMS). GMS (Groundwater Modeling System) software version 10.4 was used as the interface. The model represents a cross-section of Kolindsund (***Figure 14***). The model will be used to do a sensitivity analysis and to simulate the hydrogeological development of Kolindsund from the end of the Stone Age (4,000 yrs. B.P.) to present time (2020 C.E.), and future scenarios will be simulated to test the effect of climate change and continuous drainage versus no drainage.

Figure 14. Location of model cross-section in northeastern Djursland.

Model setup

A cross-section from Kolind to the coastline of Grenå with length of 25.5 km and depth of 1.5 km represents the 2D model. Top elevation is 5 m above sea level. The profile is spatially discretized into 51 rows, 1 column and 50 layers with thickness x = 500 m, y = 1 m, and z = 30 m, respectively (***Figure 15***).

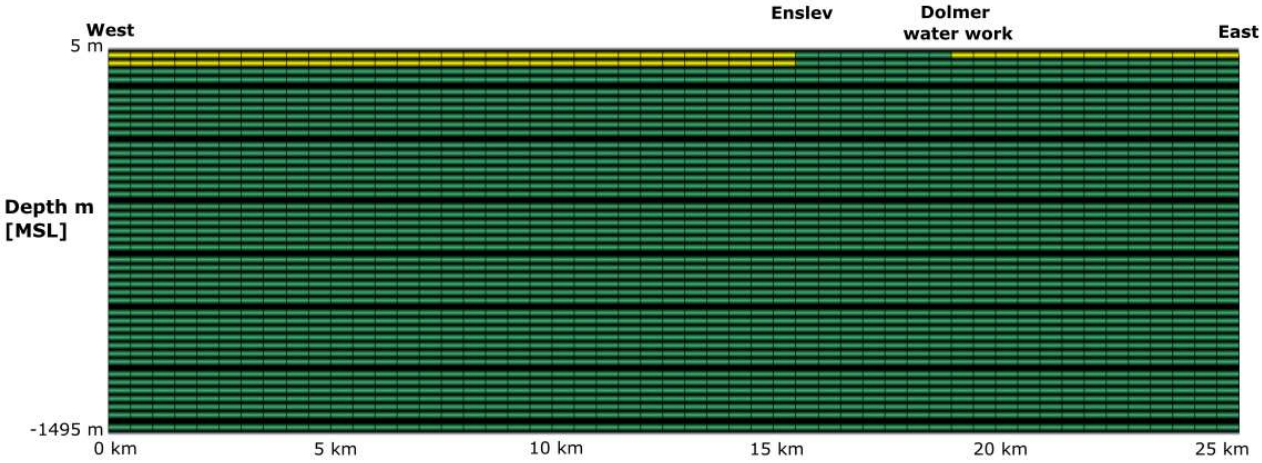

Figure 15. 2D numerical grid of model used in simulations of Kolindsund aquifer.

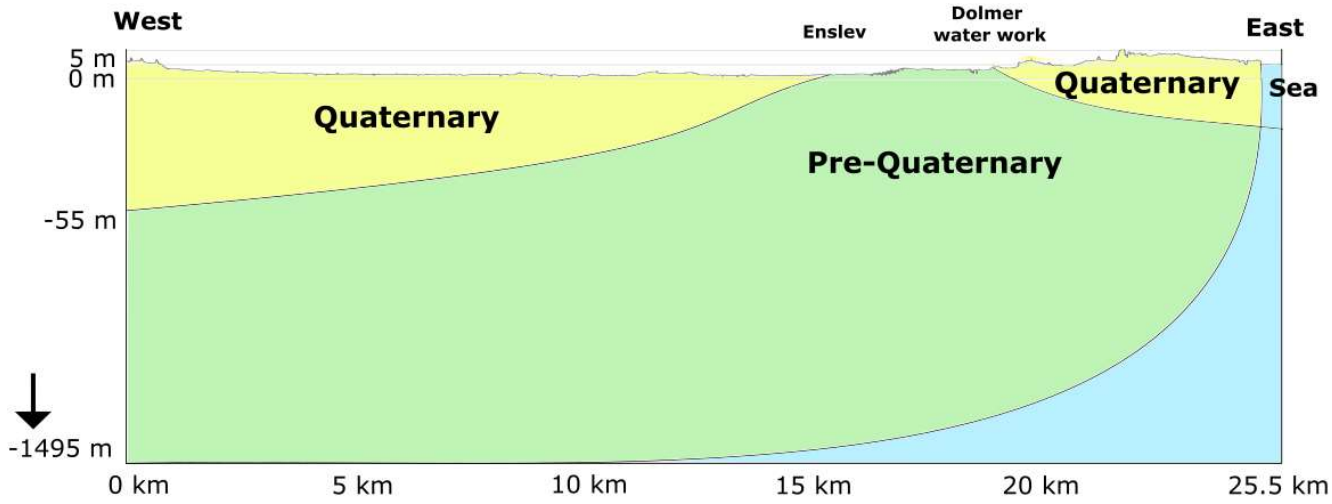

Figure 16. Conceptual geological model of Kolindsund aquifer (inspired by Korkman (1980) and Nielsen & Rauschenberger (1982).

Based on geological interpretations of Kolindsund by Korkman (1980) and Nielsen & Rauschenberger (1982), a conceptual simplified model of the geology in Kolindsund was established (***Figure 16***). The model is composed of two units, a lower pre-Quaternary unit and an upper Quaternary unit.

In the western part of the cross-section, the Quaternary units represent the two upper layers while in the eastern part, only the first upper layer represent Quaternary unit. This is due to the NE-SW sloping of the pre-Quaternary sediment. Between cell $j = 32$ to $j = 38$ in the two upper layers, the cells represent the pre-Quaternary unit. This area represent the area of Enslev where pre-Quaternary sediment is exposed at the surface (Korkman, 1980; Nielsen and Rauschenberger, 1982).

Boundary conditions

Constant recharge flux is used as a specific flux boundary (Neuman boundary condition) assigned to the upper layer of the cross-section. In the right side of the cross-section the cell in the top layer is assigned a specified head (Dirichlet boundary) as it represents the head of the sea. The other cells in all layers to the right in the cross-section have assigned constant concentration boundary (Dirichlet boundary) as they represent the dense, salty seawater, Kattegat. To simulate the drainage system of Kolindsund and the water work Dolmer, drains were added in the upper layer as a drain boundary condition.

4.5.1. Sensitivity analysis

In the base simulation past and present condition of Kolindsund will be simulated. A base model will be constructed to test the effect of different parameters on the saltwater-freshwater system and the results of present conditions will be compared to geophysical AEM data of Kolindsund. This is to determine appropriate values of parameters in a new model that will be used to simulate future scenarios of Kolindsund.

Base model

The base simulation is composed of two phases. Phase one represent a 4,000-year period where a saline aquifer is refreshened. By the end of the Stone Age (4,000 B.P.) the surrounding Littorina Sea has flooded the Kolindsund strait and past sea level was 4 meters above present-day sea level. With time the strait became enclosed and salinity decreased. Before 1874 Kolindsund was a large freshwater lake (Pedersen and Petersen, 2000; Hansen, 2011). Phase one represent the time from the end of the Stone age to the initiation of the pumping of Kolindsund in 1874. As initial conditions, all cells were assigned a starting head of 4 m and starting concentration of 26 TDS g L^{-1} assuming seawater had similar salinity as today. The cells in the outer right column were assigned a constant concentration of 26 g L^{-1} reflecting salinity of Kattegat and in the top layer of the column, the cell was assigned time-variant head boundary (4 m to 0 m) reflecting the retreat of the Littorina Sea with time.

Phase two represents the time from the pumping began (1874) to 2020. In phase two drains were added to the system including a drain that represents the waterwork Dolmer located nearby Kolindsund. The elevation of the drains are -5 m (MSL) as the pumping depth in Kolindsund of today (Hansen, 2011) with a calibrated conductance of 500 m^2 day^{-1}. Drains were added to the upper layer in cells $j = 4$ to $j = 34$ and in cell $j = 39$. During both phases a constant recharge was added to the system with base value of 75 mm

yr^{-1} as the recharge range according to Århus Amt (1995) was between 50-100 mm yr^{-1}. During both phases of the base simulation, longitudinal dispersity base value was chosen. In the study of Rasmussen et al. (2013) the value 8 m of longitudinal dispersity was applied, and due to the similarities of geology with the study, the same value of longitudinal dispersity has been applied for the base model.

Values of hydraulic conductivity *K*, specific storage *Ss* and specific yield *Sy* applied in the base model are from the DK-model of Central Jutland (Højberg *et al.*, 2010). Values for Quaternary sand in the DK-model are $K = 2.0\ 10^{-4}$ m s^{-1}, $Ss = 5.0\ 10^{-5}$ m^{-1} and $Sy = 0.2$ and will be applied for the Quaternary unit in the model. Values for chalk in the DK-model are $K = 7.13\ 10^{-5}$ m s^{-1}, $Ss = 1.00\ 10^{-5}$ m^{-1} and $Sy = 0.15$ and will be applied for the pre-Quaternary unit. In the study of Meyer *et al.,* (2019), the porosity θ of Pleistocene sand is described to vary between 0.13 to 0.26. The average value (θ = 0.195) within the range, has been chosen as base value for porosity of the Quaternary unit as Pleistocene is the first epoch within the Quaternary Period (Cohen *et al.*, 2020). It is described in the study of Vangkilde-Pedersen et al (2011) Bryozoan limestone and Maastrichtian chalk ranges from approximately 0.33 to 0.53. As Bryozoan limestone is a subclass of Danian limestone and Maastrichtian chalk is found in the Djursland too, an average value of porosity (θ = 0.43) is applied for the pre-Quaternary unit. All base values applied in the base model can be found in ***Table 4.4***.

Table 4.4. Parameter values tested in the sensitivity analysis and applied values in the base model.

Parameter	**Values tested**	**Base value**
Hydraulic conductivity K [m s^{-1}] (Quaternary)	$2.00\ 10^{-5}$	$2.00\ 10^{-4}$
Hydraulic conductivity K [m s^{-1}] (pre-Quaternary]	Upper 60 m = $7.13\ 10^{-4}$ Lower layers =$7.13\ 10^{-5}$	$7.13\ 10^{-5}$
Longitudinal dispersity [m]	0 and 50	8
Porosity θ [%] (pre-Quaternary)	33 and 53	43
Recharge [mm yr^{-1}]	50 and 100	75
Salinity [g L^{-1}]	16 and 32	26
Constant parameters	**Pre-Quaternary unit**	**Quaternary unit**
Specific storage *Ss* [m^{-1}]	$1.0\ 10^{-5}$	$5.0\ 10^{-5}$
Specific yield *Sy*	0.15	0.2
Porosity [%]	43	19.5

Tested values

In the sensitivity analysis, tested parameters are recharge, dispersity, hydraulic conductivity and porosity of each unit, and salinity (***Table 4.4***). In Djursland, recharge is described to range between 50-100 mm yr^{-1}, these are the values tested. The effect of dispersity is tested so appropriated values chosen are 0 m and 50 m, inspired by the study of Meyer *et al*., (2019).

According to Højberg *et al*., (2010) hydraulic conductivity *K* of sand can vary between 2.00 10^{-6} to 2.00 10^{-4} m s^{-1}. The value 2.00 10^{-5} m s^{-1} is chosen to test *K* of the Quaternary unit. In the DK-model of Central Jutland, hydraulic conductivity is described to have a larger range 10^{-9} to 10^{-3} m s^{-1} for hydraulic conductivity of chalk (Højberg *et al.*, 2010). Hydraulic conductivity of limestone and chalk are very difficult to determine because of the degree of fractures is needed in terms of determine the conductivity. As pre-Quaternary sediment in Djursland has been subjected to glacial activity it must be assumed that the upper part of unit has a higher conductivity than the lower part (Vangkilde-Pedersen *et al.*, 2011; Rasmussen *et al.*, 2013). Bonnesen *et al*., (2009) has suggested the upper 30- 80 meter of the chalk in Denmark is very fractured because of the refreshening conditions. Two-layer structure of the pre-Quaternary sediment is tested. The upper 60 meters of the sediment has a higher *K* value of 7.13 10^{-4} m s^{-1}) and the lower layer of pre-Quaternary sediment keeps hydraulic conductivity as 7.13 10^{-5} m s^{-1}.

Porosity of sand is described to vary from 0.13 to 0.26, thus these are the values tested for porosity of the Quaternary unit (Meyer, Engesgaard and Sonnenborg, 2019). Porosity of chalk is described to vary from 0.33 to 0.53, thus these values are chosen to be tested for the pre-Quaternary unit. As the waters of Kattegat is impacted by inflow and outflow of saline and brackish water, salinity can vary depending on the wind patterns (Lund-Hansen *et al.*, 1994). Salinity of 18 TDS g L^{-1} and 32 TDS g L^{-1} are tested.

4.5.2. Simulating past, present and future conditions of Kolindsund

Based on the sensitivity analysis, a new model with appropriated parameter values will be constructed. It has been suggested that recharge could be lower in the past (Meyer *et al*., 2019). This is implemented in the new model in phase one. The new model will simulate the two first phases, including a third phase. The third phase simulates prediction scenarios of Kolindsund from 2020 to the end of the 21st century (2100). The purpose of the of last simulation phase, is to analyze the effects of future climate change according to scenario RCP4.5 and RCP8.5 with data from Klimaatlas, and to test the effect of drainage.

Two scenarios will be simulated with continuous drainage of Kolindsund with and without effects of sea level rise, and two scenarios will be simulated with no drainage of Kolindsund with and with effects of sea level rise. This is to see the respond the saltwater-freshwater system if the pumping is stopped today.

Information about the three phases, their length, time step etc. can be found in ***Table 4.5***.

Table 4.5. Information related to the three model phases.

Model phases	Time [date]	Duration [years]	Time length / Time steps	Boundary conditions	Comments
Phase 1: Past conditions	~4,000 B.P. to 1874	4000	1,460,000 days / 1000	Recharge rate: lower or constant Time-variant head of sea: 4 m to 0 m	Changing conditions from saline to fresher conditions
Phase 2: Pumping of Kolindsund	1874 to 2020	146	53,290 days / 268	Recharge rate: higher or constant Specified head of sea: 0 m	Adding drains and comparing with geophysical data
Phase 3: Future scenarios	2020 to 2100	80	29,200 days / 176	Time-variant head of sea: - 0 m to 0 m - 0 m to 0.27 m (RCP4.5) - 0 m to 0.49 m (RCP8.5)	Effect of rising sea level (climate change) in Denmark

5. Results

5.1. Ghyben-Herzberg theory: depth to saltwater-freshwater interface

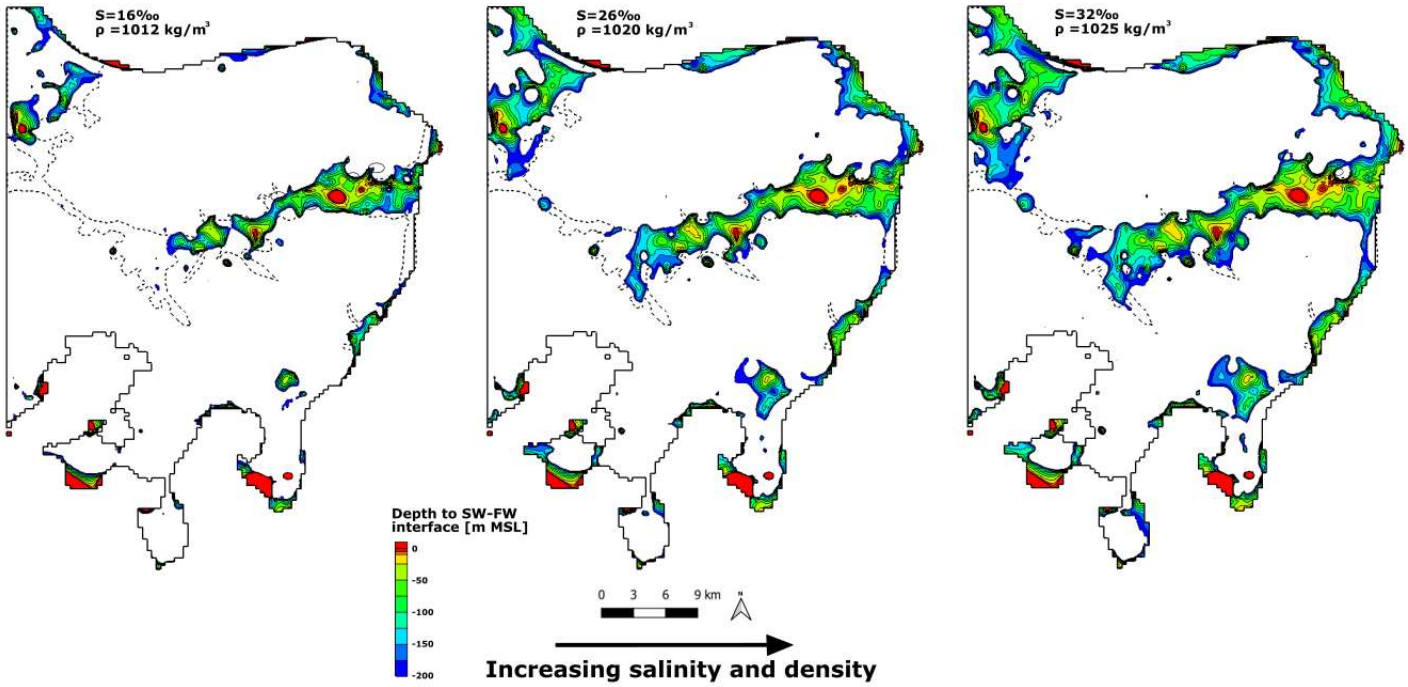

Figure 17. Surface map of the saltwater-freshwater interface in Djursland based on Ghyben-Herzberg approximation for three scenarios with different density value.

In the low (16 ‰) and intermediate (26 ‰) salinity scenarios, the aquifers of Djursland are affected by the upper less saline waters of Kattegat, whereas in the high salinity (32 ‰) scenario, the aquifers are impacted by saline bottom water of Kattegat (***Figure 17***). Saltwater-freshwater interface located in depths below -200 meters (MSL) is not illustrated on the maps, as geochemical data is not available at deeper depths. All scenarios show, the low-lying Kolindsund strait and the coastal areas especially along the northern and eastern coastline of Djursland, will be affected by seawater intrusion independent of the salinity scenario as the groundwater table within those areas is located close to sea level. When the density of the saline water body increases, the depth to the saltwater-freshwater interface decreases. In the strait, the interface (-200 m MSL) to dense water (32‰) moves three kilometers inland compared to a less dense scenario (16‰). The same occurs in the northern and eastern coasts of Djursland, where the front of Kattegat water is shifted further inland when the density increases, for same depths.

In Kolindsund (eastern part of strait), the depth to the interface does not exceed -100 m MSL, as the groundwater table within the area is close to sea level. Red areas in eastern Kolindsund and at the cost of southern Djursland indicate saltwater just below (< 5 m depth) the groundwater table. Head values below sea level were excluded (mostly in Kolindsund) when applied Ghyben-Herzberg theory (***Appendix A4).***

5.2. Geochemical analysis

5.2.1. Saline areas

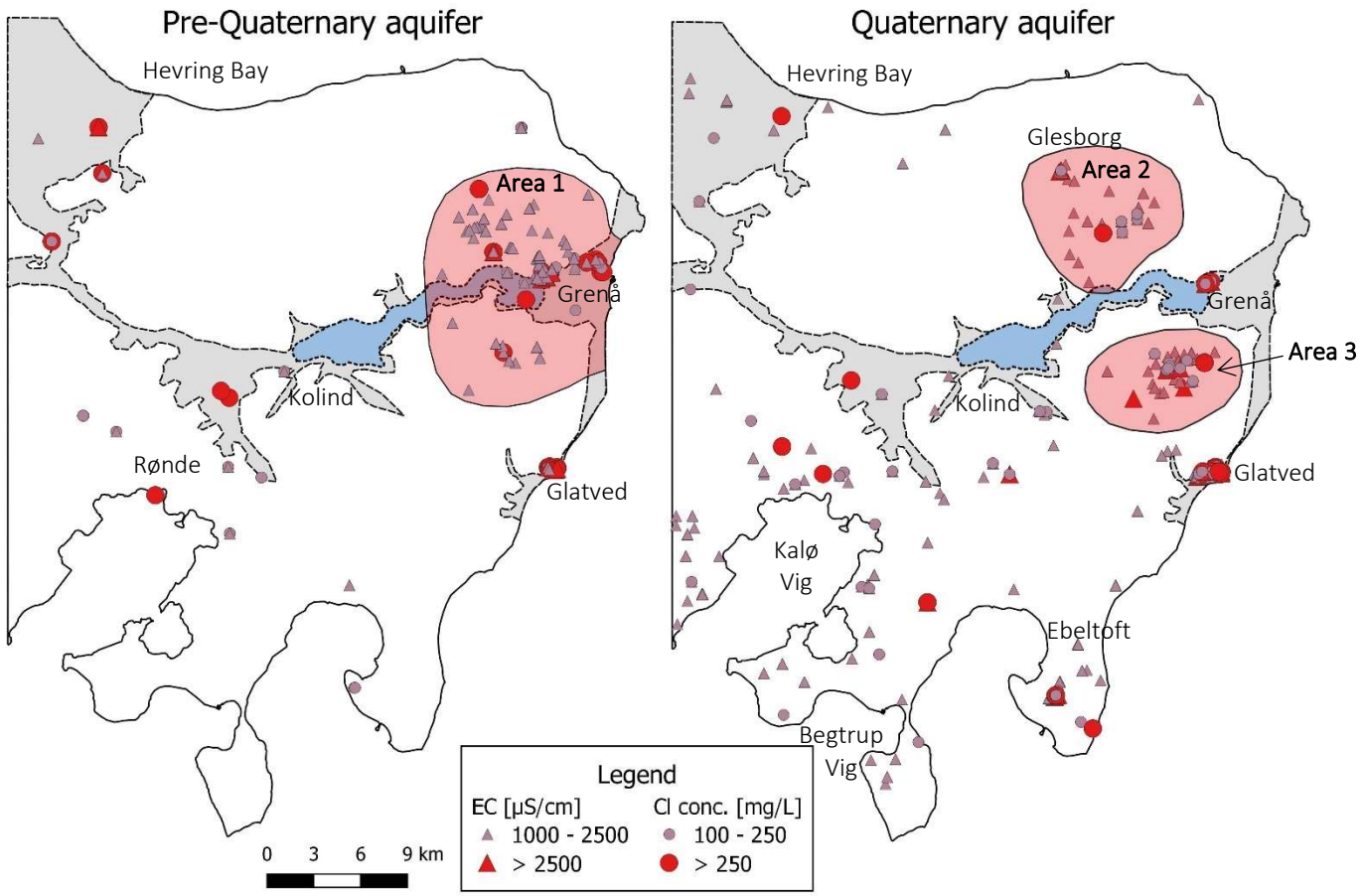

Figure 18. Spatial distribution of chloride (Cl) and electrical conductivity (EC) of pre-Quaternary (left) and Quaternary aquifer (right). Purple symbols represent transition water and red symbols represent saline water.

To create the map covering chloride concentration and electrical conductivity (***Figure 18***), all historical measurement (dataset 1) was applied together with maximum values (dataset 2), as there was a lack of measurements covering both Cl concentration and EC.

Water characterized as transition and saline water based on measurements of chloride and EC, show two distinctive patterns for each aquifer *(**Figure 18***). In the pre-Quaternary aquifer, most water samples reflecting EC and Cl exceeding freshwater characteristics, are mainly measured in the northeastern part of Djursland surrounding Grenå. South of Hevring Bay (NW Djursland), between Kolind and Rønde, and at the coast in Glatved (eastern Djursland) water samples reflecting transition to saline water type are measured too.

The spatial distribution of water representing transition to saline water is more distributed across Djursland in the Quaternary aquifer (***Figure 18***). In the southern- and northwestern part of Djursland, transition water generally predominates the areas based on EC measurements. In the south, a few samples representing saline water type based on chloride content, are measured but widely distributed.

For both aquifers, calcium, sodium, potassium, sulphate and chloride, and electrical conductivity show high concentrations at Glatved at the southeastern coast of Djursland.

Based on the spatial distribution of EC and Cl content for aquifer, three areas (Area 1, Area 2 and Area 3 ***Figure 18***) have been identified as salinized areas and a more comprehensive analysis of those areas is conducted.

Salinized area 1 (within pre-Quaternary aquifer)

Area 1 is located in the eastern Djursland and covers the eastern part of Kolindsund. The area contains water samples representing saline water (> 250 Cl mg L^{-1} and > 2,500 µS cm^{-1}) with chloride concentration samples exceeding 1,000 mg L^{-1} and electrical conductivity exceeding 3,000 µS cm^{-1} located within low topographical areas (***Figure 19-1***). As pre-Quaternary sediment sloping SW-NE (Vangkilde-Pedersen *et al.*, 2011), the pre-Quaternary surface within this area rises towards the coast NE. North of the Kolindsund strait, almost the entire pre-Quaternary surface exceed sea level whereas south of the Kolindsund strait, elevations decreases towards -25 m (MSL) southwestward (***Figure 19-2***).

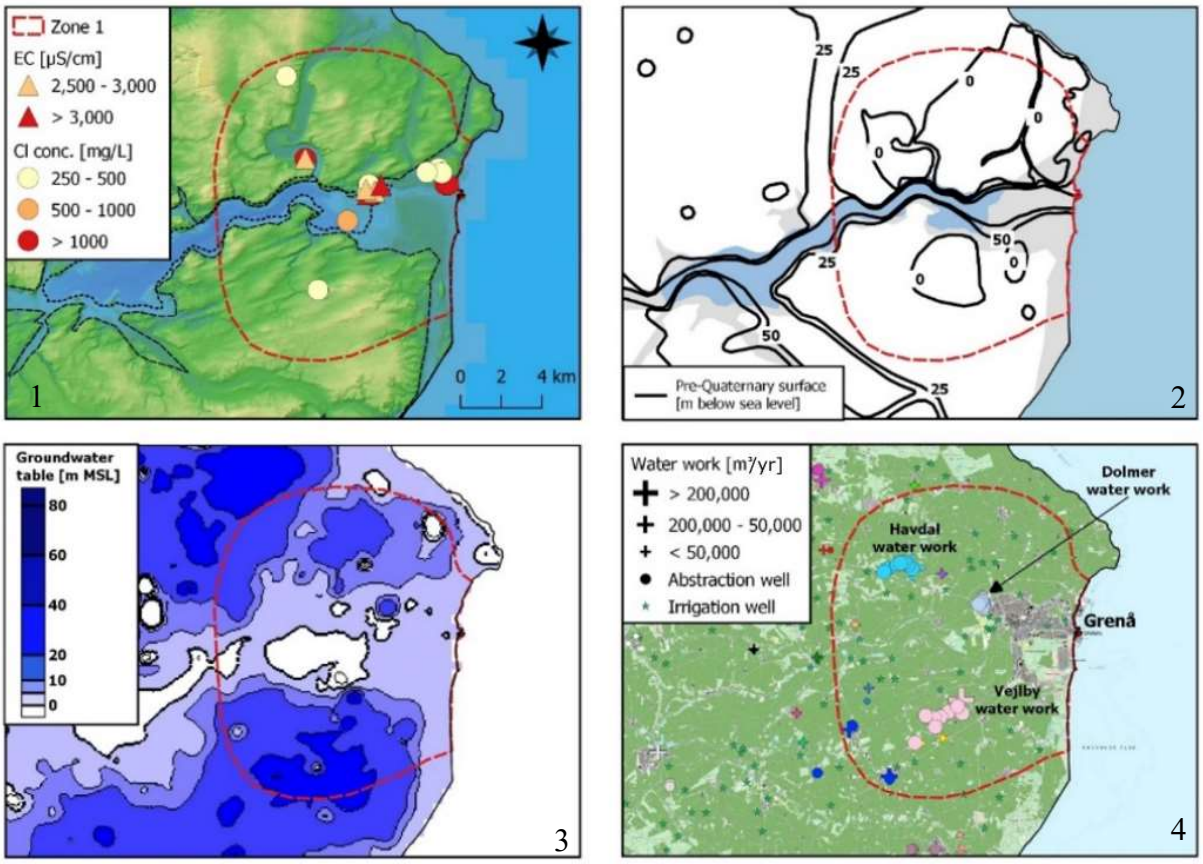

Figure 19. Identified salinized Area 1 within the pre-Quaternary aquifer 1) Topography and high EC and Cl measurements 2) Pre-Quaternary surface 3) Isopotential map of groundwater table 4) Water works and associated abstraction wells, including irrigation wells.

Isopotential contour lines show water flows from south and north towards the central part (**Figure *19-3***), where the water table are lower, but noticeable, water from the coast flows westward towards eastern Kolindsund. Groundwater table differences within the area are pronounced (> 25 m) (***Appendix A5***).

Cropland represents the largest extend but urban areas, forests and pastures are represented too (**Figure *19-4***). Of urban areas, Grenå represents the largest part. Three of the largest water works in Djursland,

Havdal water work, Vejlby water work and Dolmer water work (***Appendix A6***), are located within the area.

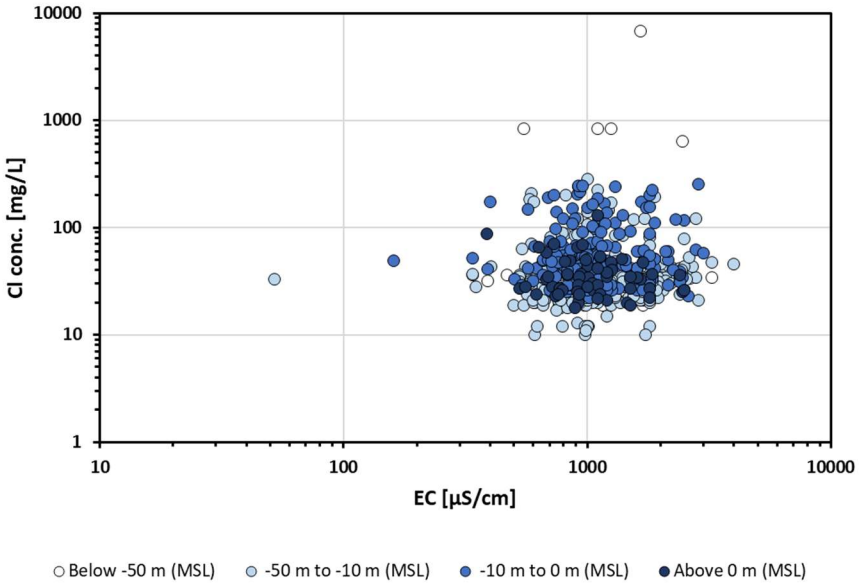

Figure 20. Chloride as function of electrical conductivity. Groundwater samples have been divided into depth intervals.

Groundwater samples with relatively high chloride concentration (>100 mg L^{-1}) and electrical conductivity value (> 1,000 µS cm^{-1}) are measured in depths below sea level (0 m) (***Figure 20***). Most groundwater samples irrespective of depth are characterized by high electrical conductivity (> 1,000 µS cm^{-1}) and lower chloride concentration (20 - 100 mg L^{-1}).

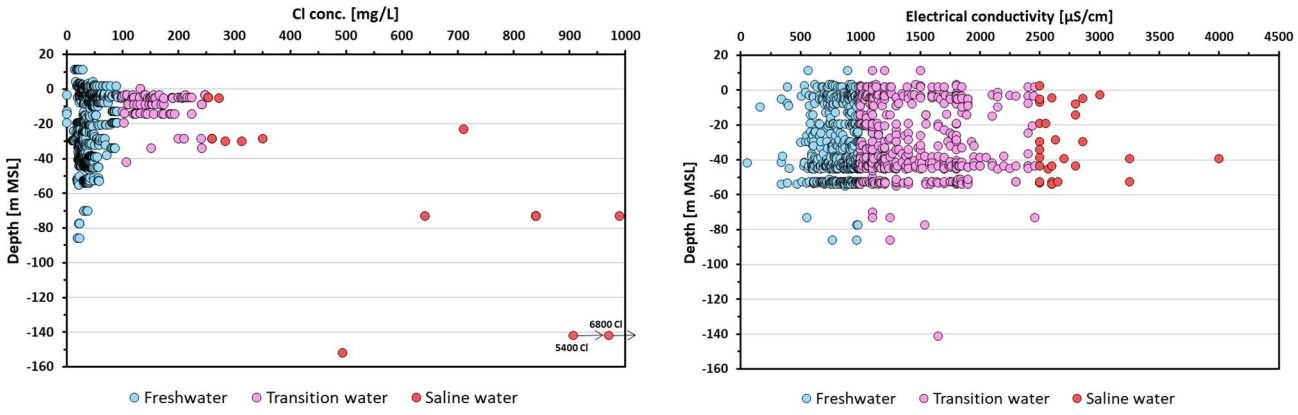

Figure 21. Chloride concentration and electrical conductivity (EC) plotted as function of depth for groundwater samples in Area 1.

Groundwater samples show increasing chloride concentration and electrical conductivity with depth (**Figure *21***). Just below sea level, the chloride content of groundwater samples exceeds Danish drinking-

water standards (>250 Cl mg L^{-1}) and below -20 m (MSL) chloride concentrations (>500 Cl mg L^{-1}) show saline water.

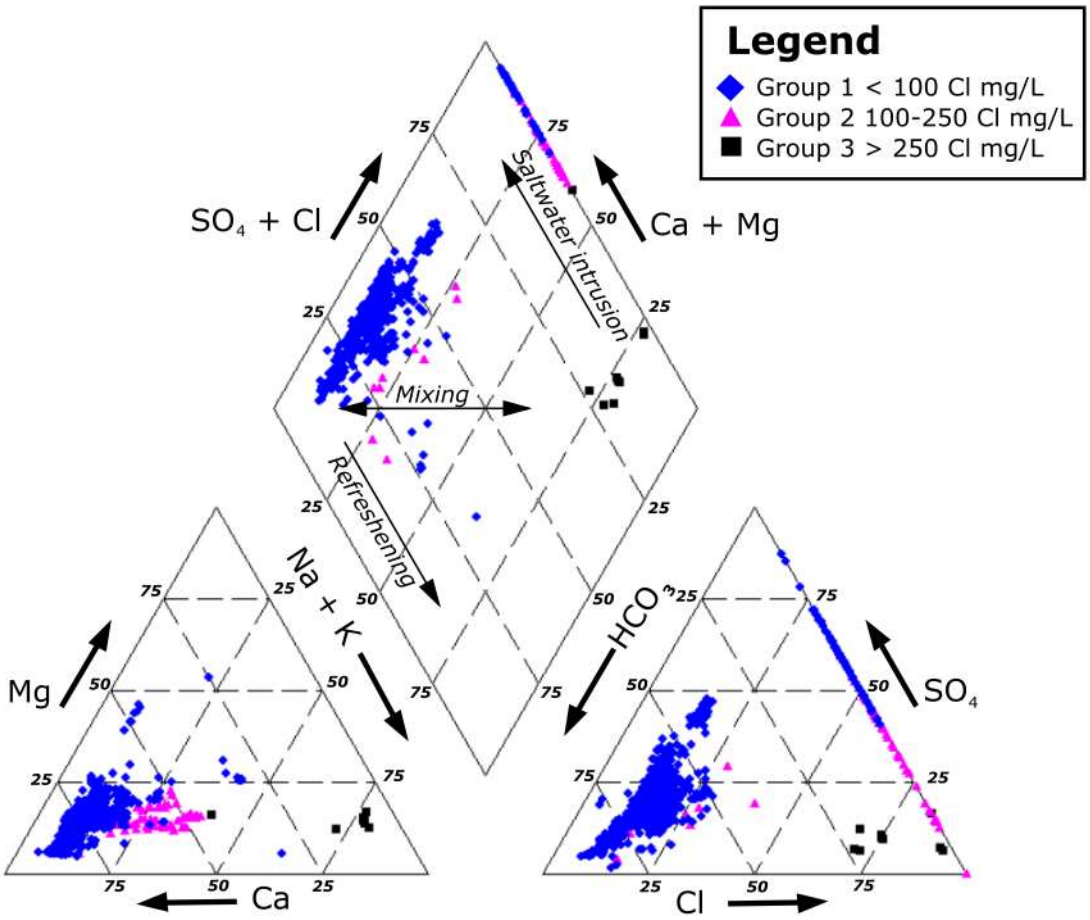

Figure 22. Piper plot of water samples from Area 1 categorized based on chloride concentration.

Groundwater samples of the area have been plotted in a Piper diagram to identify different water types (***Figure 22***). Two water types are identified in the piper plot for Area 1. Group 1 and 2 represent the first water type, and Group 3 represents the second water type. Group 3 (> 250 Cl mg L^{-1}) is enriched in magnesium, sodium, and chloride, and depleted in calcium and bicarbonate. These samples are characterized as Na-Cl water type as they approach seawater composition. Group 2 (100 - 250 Cl mg L^{-1}) shows a relatively lower content of calcium compared to Group 1 but similar range of bicarbonate. Group 2 is approaching the mixing line but still have more comparable composition to freshwater. Group 1 (< 100 Cl mg L^{-1}) is enriched in calcium, bicarbonate and sulphate and more depleted in chloride, sodium and magnesium. Group 1 and 2 are identified as Ca-HCO_3 water type and show similar

composition as freshwater. Samples located on the right border of the right triangle diagram and diamond shaped diagram have no measurements of bicarbonate content.

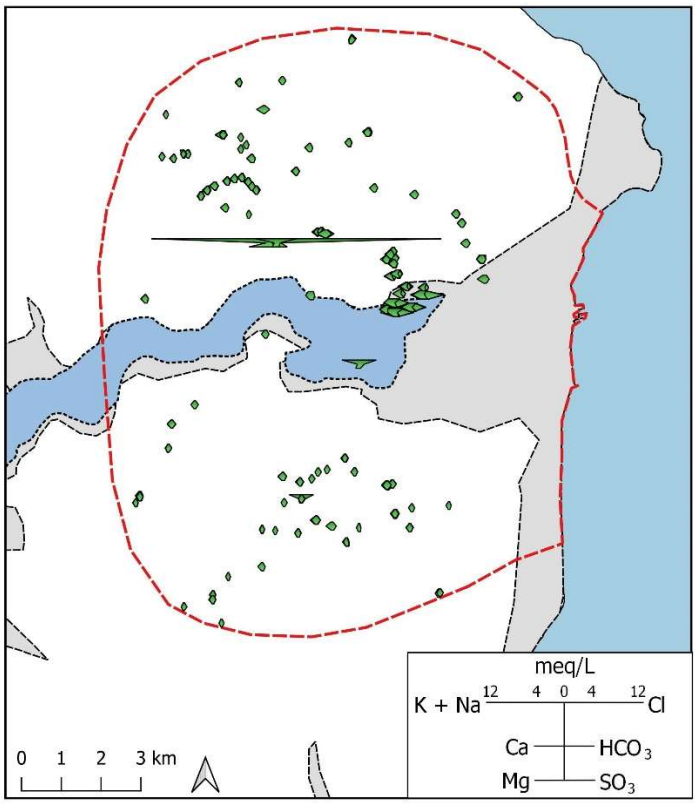

Figure 23. Groundwater composition plotted in Stiff diagrams for each sample in Area 1.

A few groundwater samples show excess of Na^+ and Cl^- including, and some have relative excess of Ca^{2+} comparing to HCO_3^- which imply saltwater intrusion. But most samples are characterized by high content of in Ca^{2+} and HCO_3^- reflecting groundwater composition based on their shapes.

Salinized area 2 (within Quaternary aquifer)

Area 2 is located north of Kolindsund and the strait. Most measurements in the area are characterized as transition water but some samples defined as saline water are observed in areas with elevated topography (***Figure 24-1***). The area is dominated by sandy depositions (aeolian sand, meltwater sandy deposits, and limey sandy till) but limey clayey till is present in the upper part of the area (***Figure 24-2***). The water table follows topography and from the central part of the area, water flows to each side (west and east) towards local streams, and south towards the Kolindsund strait (***Figure 24-3***). Water table fluctuations

in the area are generally smaller compared to Area 1 within the pre-Quaternary aquifer. In the western part of this area, water table can vary up to 25 meters (***Appendix A5***).

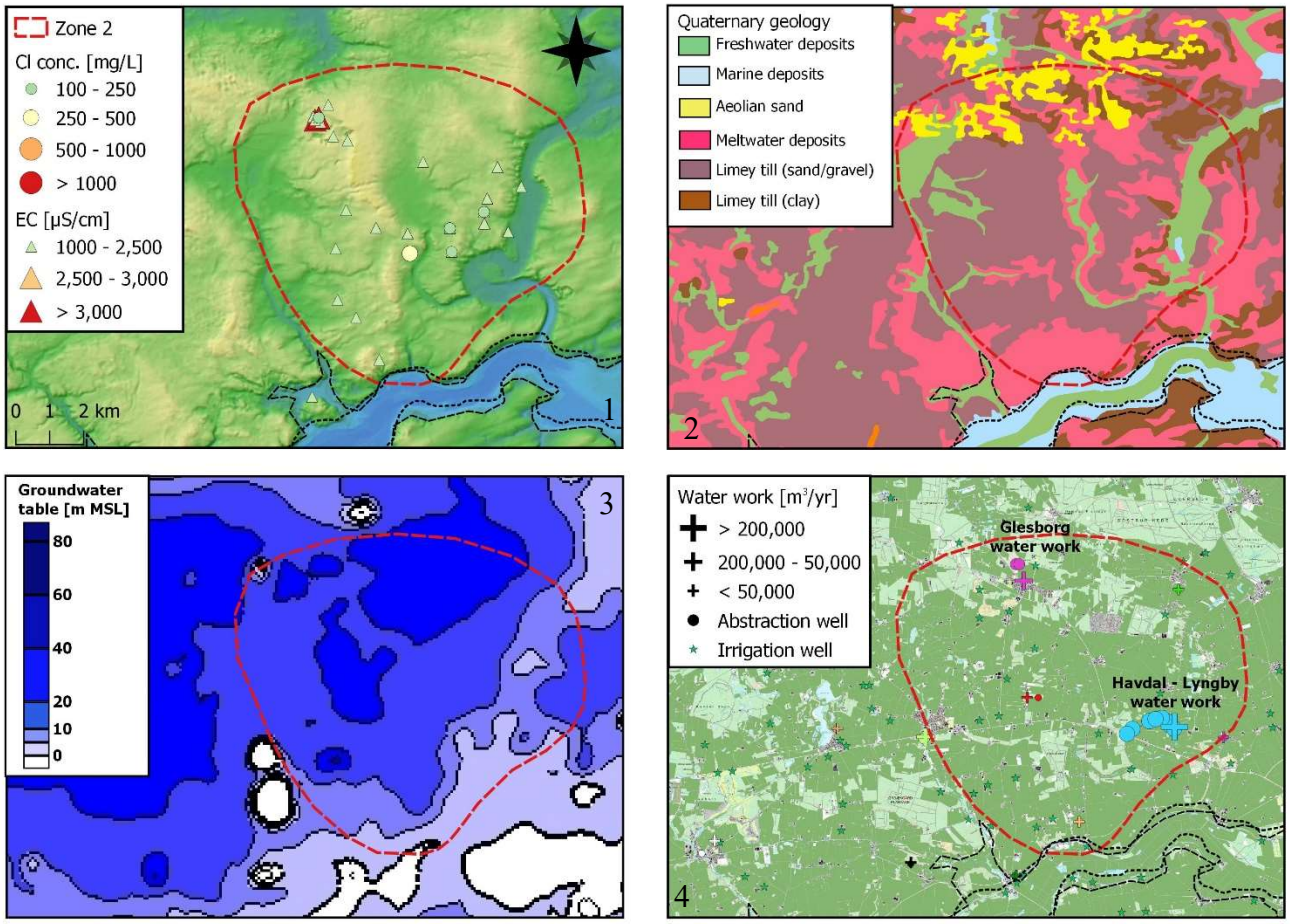

Figure 24. Identified salinized area 2 within the Quaternary aquifer. 1) Topography and high EC and Cl measurements. 2) Quaternary geology. 3) Isopotential map of groundwater table. 4) Water works and associated abstraction wells, including irrigation wells.

Of larger water works, Havdal and Glesborg water works are located in the area (***Figure 24-4***). Croplands predominate the area, including many irrigation wells. Urban areas are limited. Glesborg located in the north is the largest village in the area (***Figure 24-4***).

Water samples characterized by high chloride concentration (> 100 mg L^{-1}) and high electrical conductivity (> 1,000 µS cm^{-1}) are primarily measured at topographical elevations exceeding 10 m (MSL) (**Figure *25***). Most samples have a measured chloride concentration between 10 to 100 mg L^{-1} and conductivity above 1,000 µS cm^{-1} and are measured in all elevation intervals in the area.

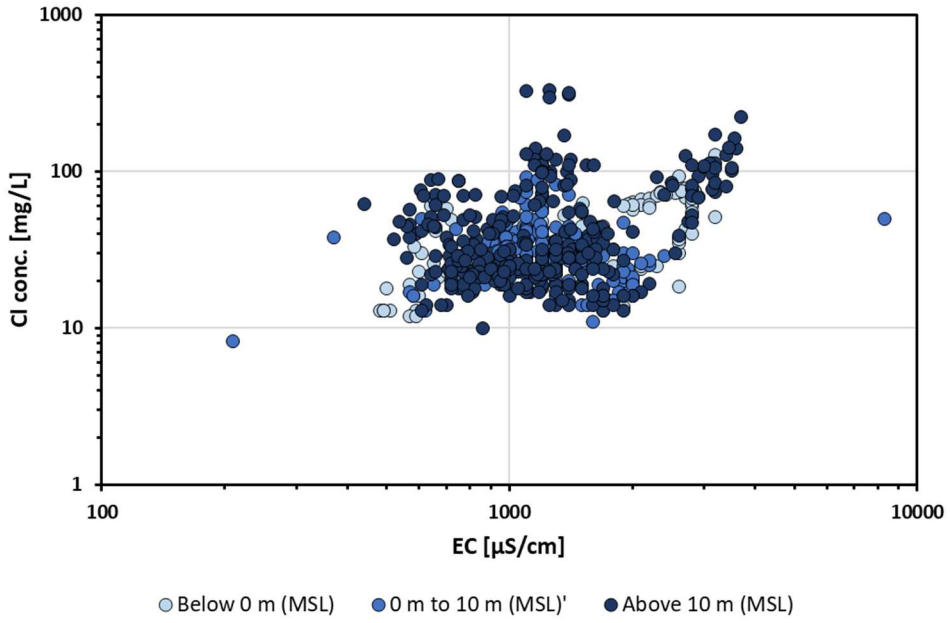

Figure 25. Electrical conductivity as function of chloride concentration of groundwater. Samples have been divided into depth intervals.

Electrical conductivity, and especially chloride concentration decreases with depth (***Figure 25***). Highest measured values of chloride (> 250 mg L^{-1}) have been measured at high elevations (~15 m MSL) (***Figure 26-left***) and for conductivity (***Figure 26-right***), water characterized as saline water are measured at the same depth as highest chloride measurements. It should be noted that, saline water samples observed by chloride measurements are all taken from one well, and for saline water samples based on electrical conductivity, the samples are taken from two wells, where one of the wells have two different depths.

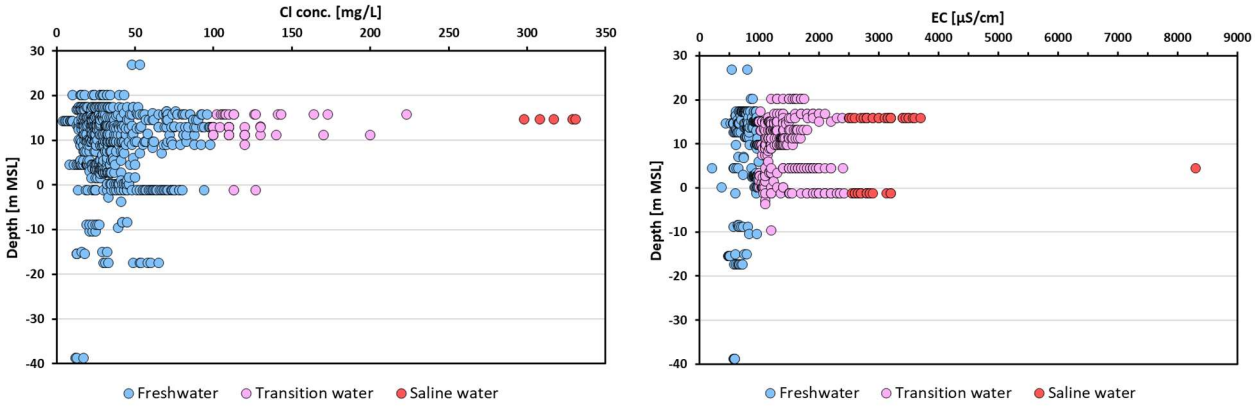

Figure 26. Chloride (Left) and electrical conductivity (Right) as function of depth for groundwater samples within area 2.

It was observed that, two wells (71.439 and 71.770) in the area show increased chloride levels in the upper layers compared to lower layers, and a temporal increasing chloride concentration. (***Figure 27***).

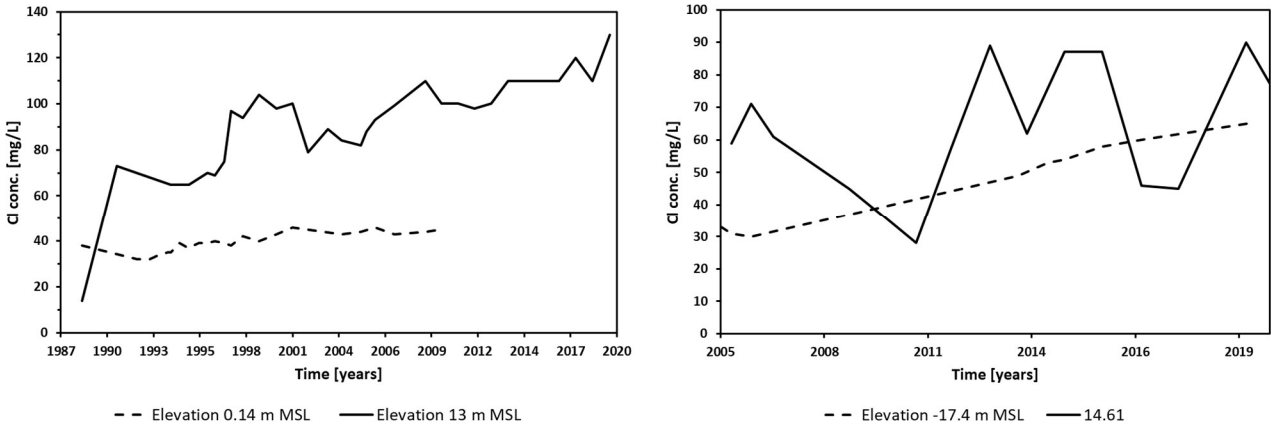

Figure 27. Temporal development of chloride content in well 71.439 (left) and well 71.770 (right).

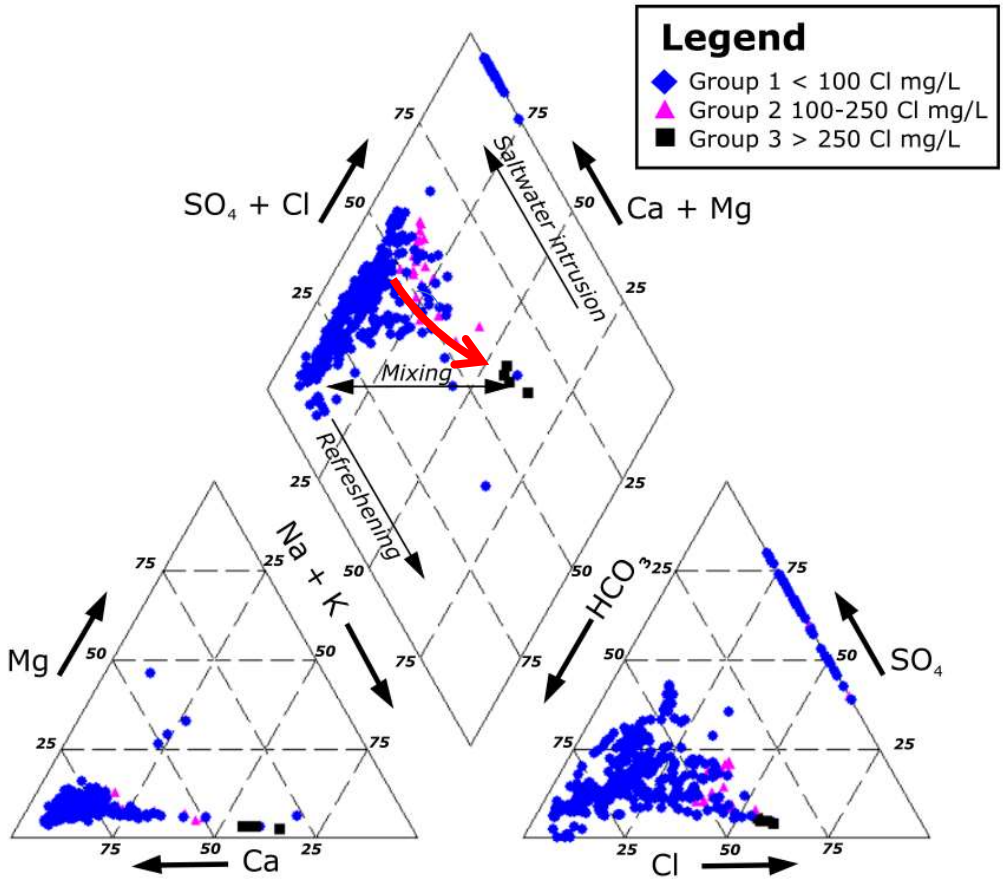

Figure 28. Piper diagram of plotted groundwater samples from Area 2. Red arrow indicates possible development of water.

Plotting groundwater samples in Piper diagram (***Figure 28***), show no distinctive water types, but a possible development from Group 1 towards Group 3. With higher levels of chloride, the sodium-calcium relationship changes from depletion of sodium in Group 1 towards relative enrichment in sodium and magnesium (Group 3). Group 3 characterized by high content in chloride (>250 mg L^{-1}) has experienced conservative mixing as the samples are located at the mixing line between seawater (right) and freshwater (left) composition. Samples within Group 1 (< 100 Cl mg L^{-1}) show characteristics as wider range bicarbonate and sulphate content within the group while samples with enrichment in sulphate and bicarbonate are defined as Ca-HCO_3 water type. A dominance of Ca-HCO_3 water types are illustrated in Stiff diagrams too (***Figure 29***), where some samples show a larger excess of calcium and bicarbonate content.

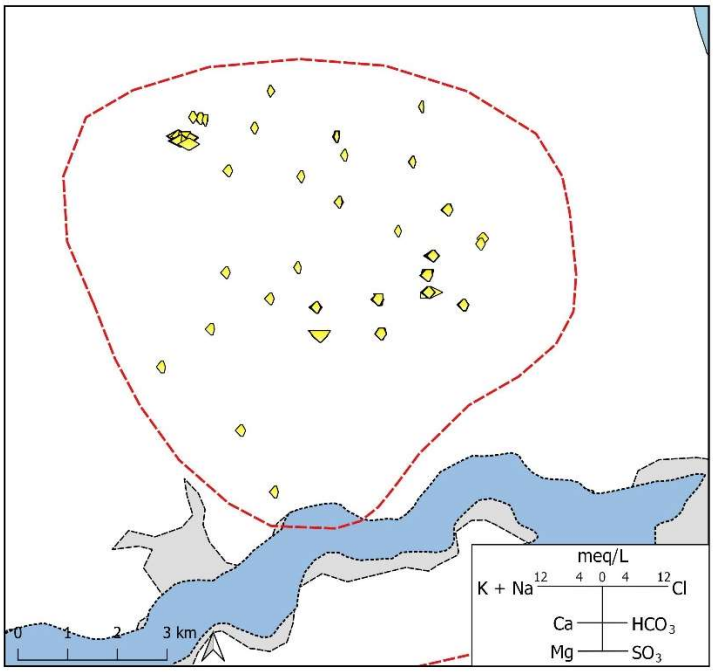

Figure 29. Groundwater composition of water samples in Area 2, illustrated in Stiff diagrams.

Salinized area 3 (within Quaternary aquifer)

Area 3 is located south of Kolindsund and the strait. It was discovered, some samples within the area were measured in 'contaminated wells', thus those samples were excluded in the further processing.

In this area, more samples are generally characterized by being conductive (> 2,500 µS cm^{-1}), but with intermediate levels (100-250 Cl mg L^{-1}) of chloride (***Figure 30-1***). Samples with higher electrical conductivity are measured in area with higher topographical elevations. The area is dominated by higher

elevations and decreases northward towards the low-lying strait. In the area, higher content of clay material is present within Quaternary sediment (***Figure 30-2***).

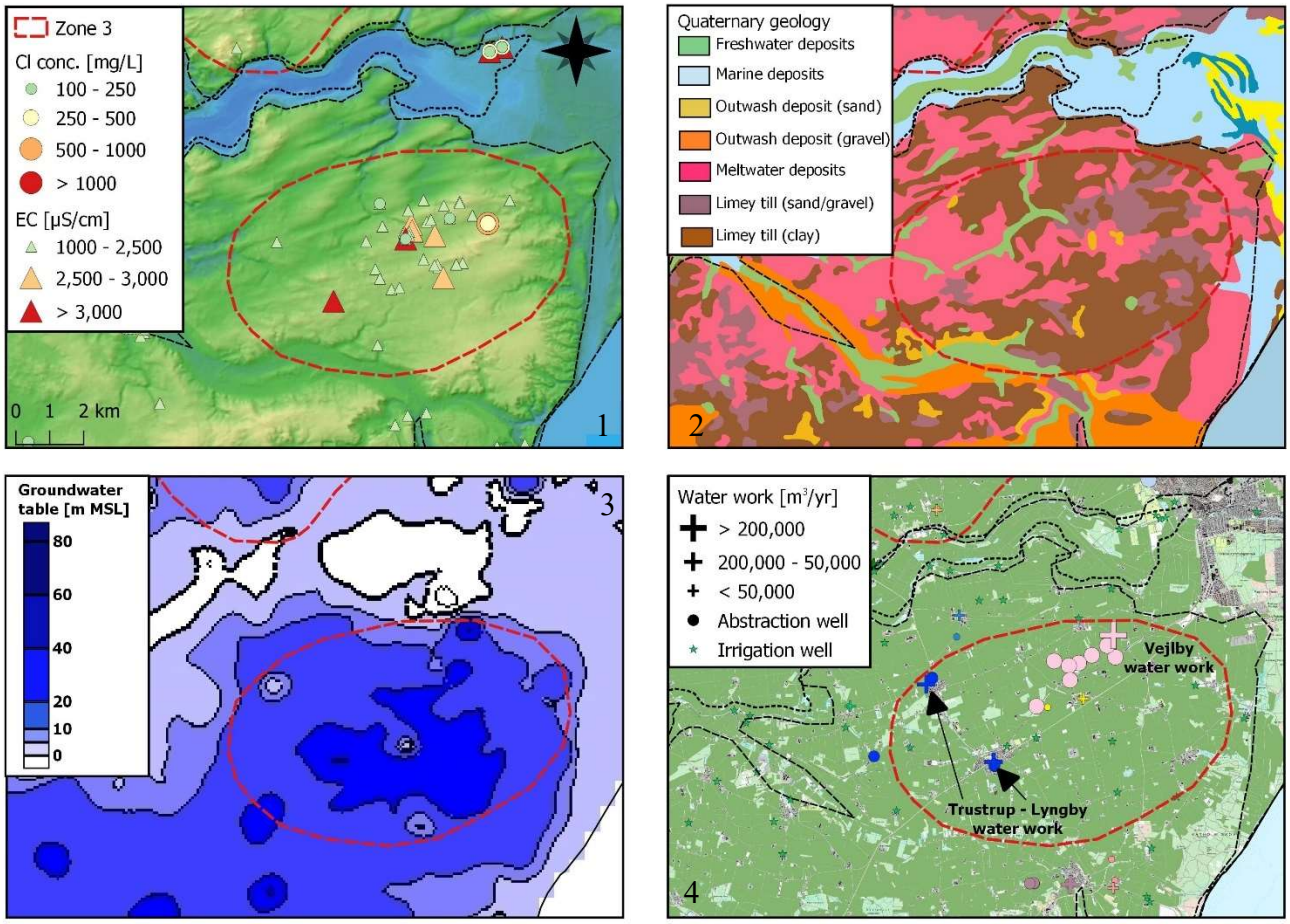

Figure 30. Salinized identified Area 3 within the Quaternary aquifer. 1) Topography and high Cl and EC measurements 2) Quaternary geology 3) Isopotential map of groundwater table 4) Water works and associated abstraction wells, including irrigation wells.

Isopotential contour lines depict groundwater flows in all directions from the center of the area where groundwater table is above 20 m (MSL) (***Figure 30-3***). This area is not affected by large variations (>25 m) in the groundwater table. The largest fluctuation of head varies between 5-10 m in the central to western part of the area (***Appendix A5***).

The land-use is dominated by croplands, and two smaller villages (Trustrup and Lyngby) in the western part of the area represent the largest part of urban area present (***Figure 30-4***). The villages have associated smaller water works (Trustrup-Lyngby water works), but a large water work (Vejlby water work) is

located in the northern part of the area, abstracting more than 200,000 m^3 of water annually. In addition, a few irrigation wells are present in the area.

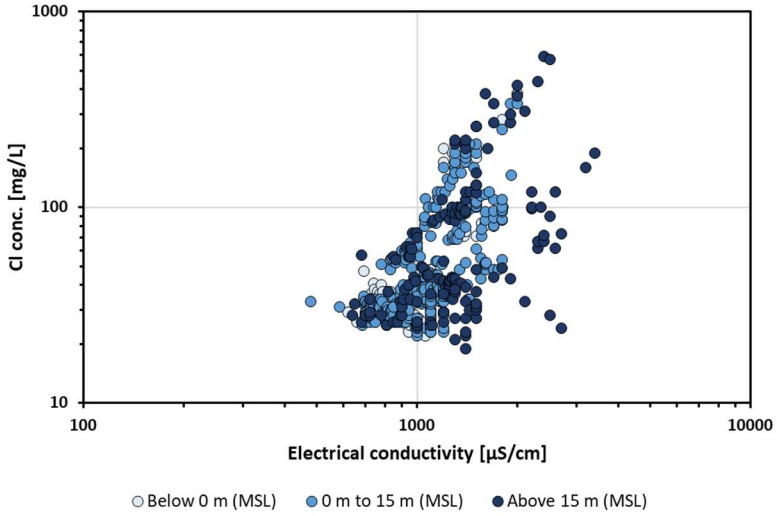

Figure 31. Electrical conductivity as function of chloride concentration for water samples. Samples represent different depth intervals.

For groundwater samples in the area, a positive correlation is observed between increasing chloride content and conductivity (***Figure 31***). Samples with chloride content above 200 mg L^{-1} are primarily measured in elevations above 15 m (MSL). Chloride content and conductivity decreases with decreasing depth (***Figure 31*** and ***Figure 32***). Groundwater samples characterized as saline water are measured within two wells in three different depths (~17 m, ~2 m, and ~0 m MSL) (***Figure 32***). Saline water (>2,500 µS cm^{-1}), based on electrical conductivity measurements, is only measured in elevations above 15 m (MSL).

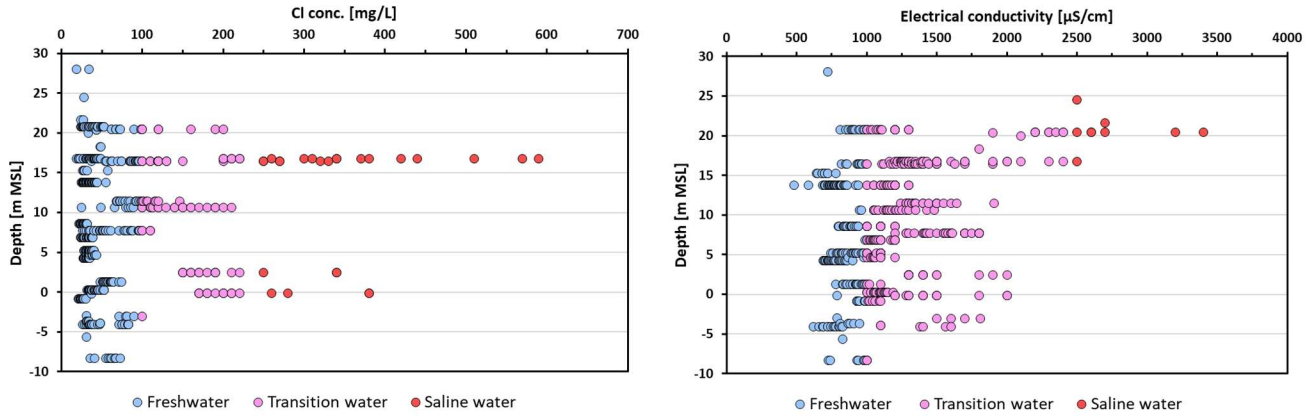

Figure 32. Chloride and electrical conductivity as function of depth for groundwater samples within area 3.

Two wells (71.482 and 71.484) located in the area (***Figure 33***), show a temporal increasing chloride concentration trend and higher levels of chloride concentration are measured within the upper layers of the Quaternary aquifer.

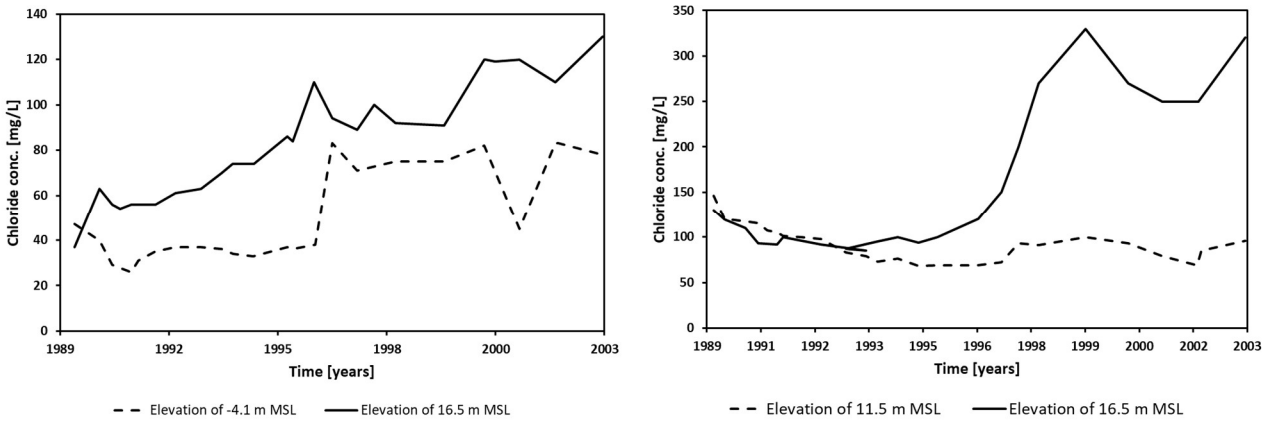

Figure 33. Temporal development of chloride concentration in well 71.482 (left) and well 71. 484 (right).

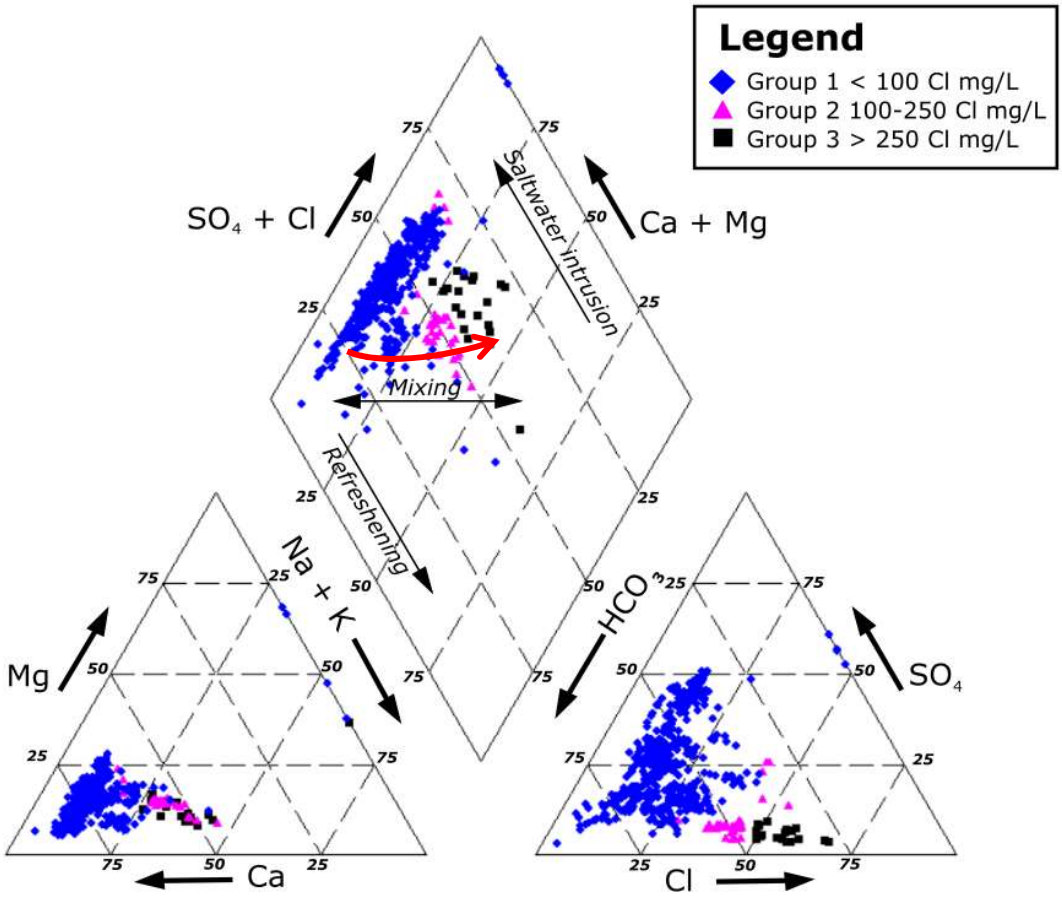

Figure 34. Piper diagram plotted with groundwater samples from Area 3. Red arrow shows possible development of water samples.

In the Piper diagram, water types for all groups have similar composition (***Figure 34***). In Group 2 and 3, samples have lower amount of calcium and higher amount of magnesium compared to group 1. Group 3 is more depleted in sulphate and enriched in chloride, relatively to Group 1 and 2. In the diamond shaped diagram, when chloride content increasing (from Group 1 to 3), the location of samples approach the right side of the diagram which suggest they have been subjected to conservative mixing. Samples within Group 1 with enrichment in calcium and bicarbonate and sulphate, can be defined as Ca-HCO_3 water type. This specific water type is observed in ***Figure 35*** where the composition of the samples has been plotted in Stiff diagrams.

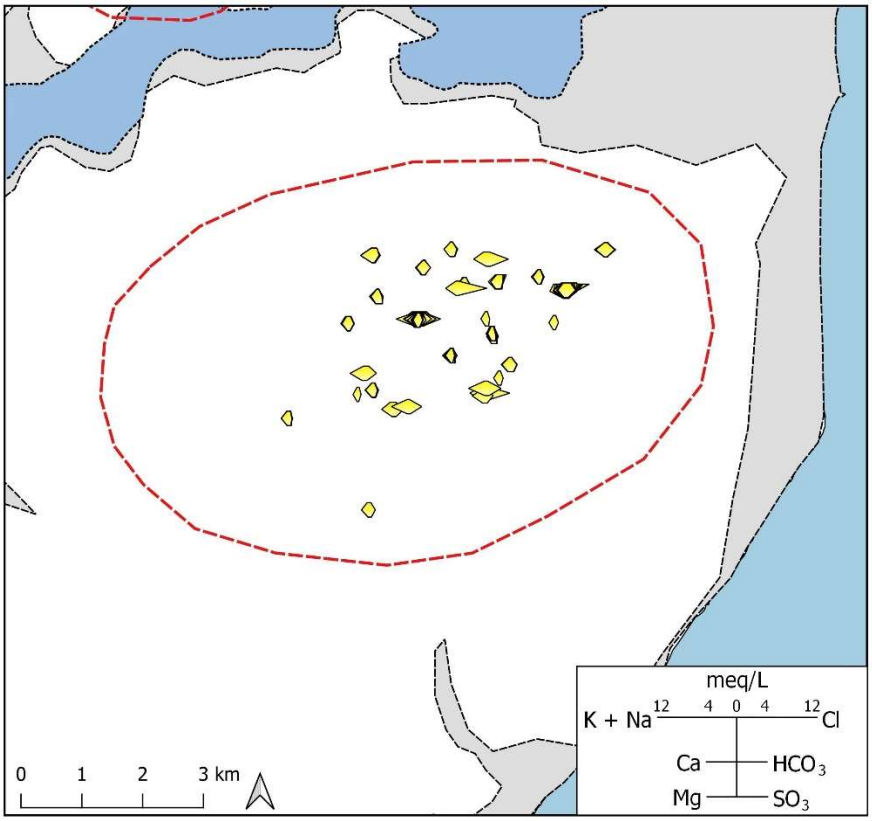

Figure 35. Composition of groundwater samples illustrated in Stiff diagrams in Area 3.

5.2.2. State of water

Base-Exchange Index

Salinization of the pre-Quaternary aquifer, seems to be restricted to the northeastern part of Djursland, north of Kolindsund based on negative BEX-values in a few groundwater samples within Area 1 (**Figure *36***).

In the Quaternary aquifer more samples reflect a salinization facies. These samples are distributed across Djursland but most are within, or near the low-lying strait, or within Area 2 and Area 3. In addition, samples with negative BEX-index are found in the southeastern part of Djursland and at the coast of Glatved on the east coast.

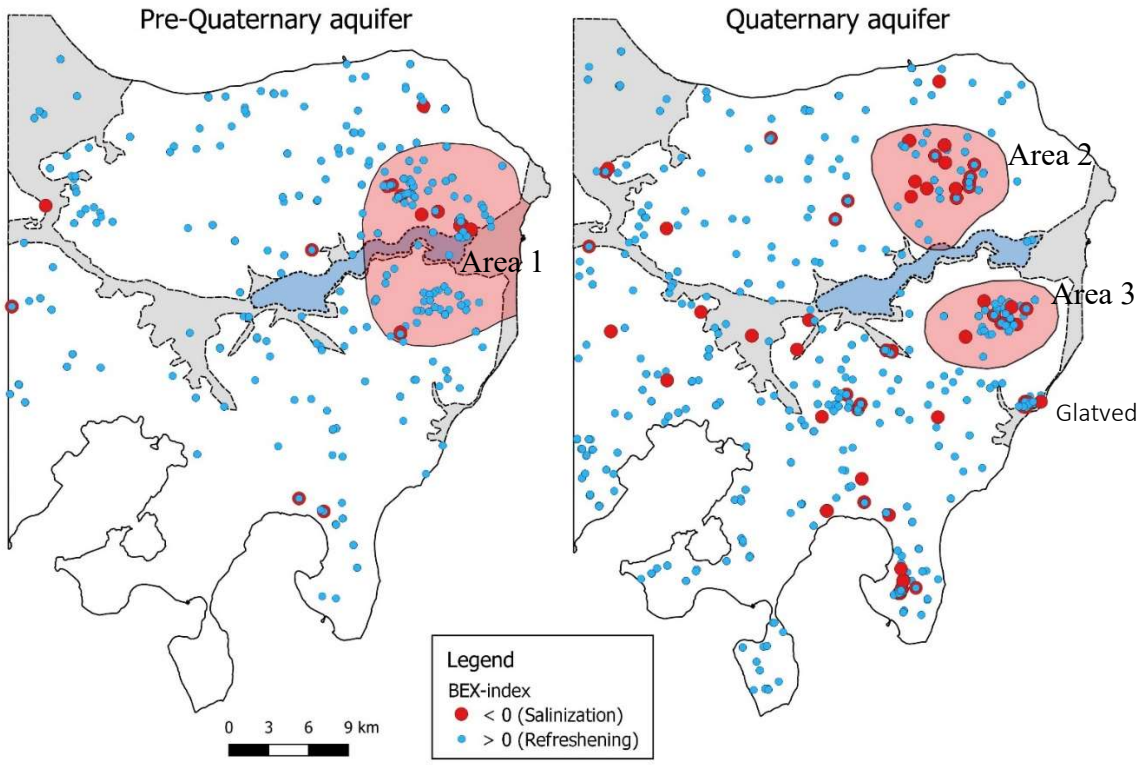

Figure 36. Spatial distribution of samples reflecting either salinized or refreshening state based on the Base-Exchange index.

Temporal development of chloride

Based on wells within the pre-Quaternary aquifer and Quaternary aquifers, with more than 10 chloride-measurements over time, the temporal development could be determined. Only increasing and decreasing trends of chloride development is shown (***Figure 37***).

Data was limited, as within the pre-Quaternary aquifer, only up to three chloride measurements were conducted through time in almost half the wells, and for the Quaternary aquifer, up to three chloride measurements were conducted through time in more than half of all wells (***Appendix A7***).

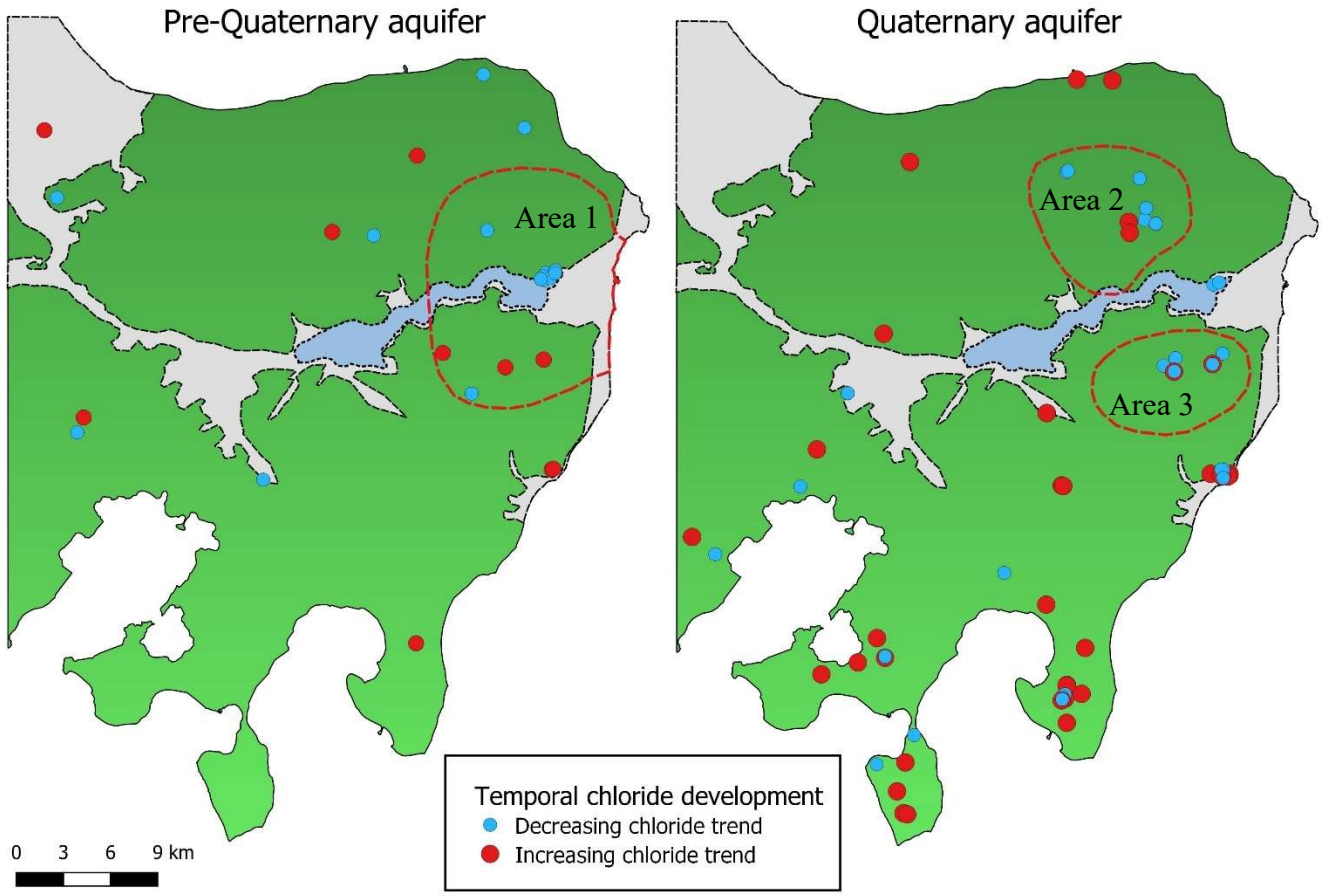

Figure 37. Temporal development of chloride content in wells with more than 10 temporal measurements.

The development in chloride concentration was examined, but no significant trend can be observed within the pre-Quaternary aquifer. In the Quaternary aquifer, an increasing trend is observed within the coastal areas of the southern part of Djursland. Temporal and spatial distribution of Cl-measurement conducted in Djursland is found in ***Appendix A8***.

5.2.3. Salinity sources

Molar ratio of sodium over chloride (Na/Cl)

Molar ratio of Na/Cl below 0.86 dominates the central to northeastern part of Djursland marked by the dotted line for the pre-Quaternary aquifer (***Figure 38-right***). Especially within Area 1, water samples below Na/Cl ratios (< 0.86) predominate. West of the dotted line, molar ratio above 0.86 predominates. Only in the northwestern part of Djursland, a few samples have low Na/Cl ratios (< 0.86).

The dotted line in the Quaternary aquifer (***Figure 38-left***) depict an area in the southwestern part of Djursland, where high Na/Cl ratios (>0.86) are most common. East of the dotted line, both low and high Na/Cl ratios samples have been measured and are evenly distributed. Within Area 2 and Area 3, most samples represent low Na/Cl ratios.

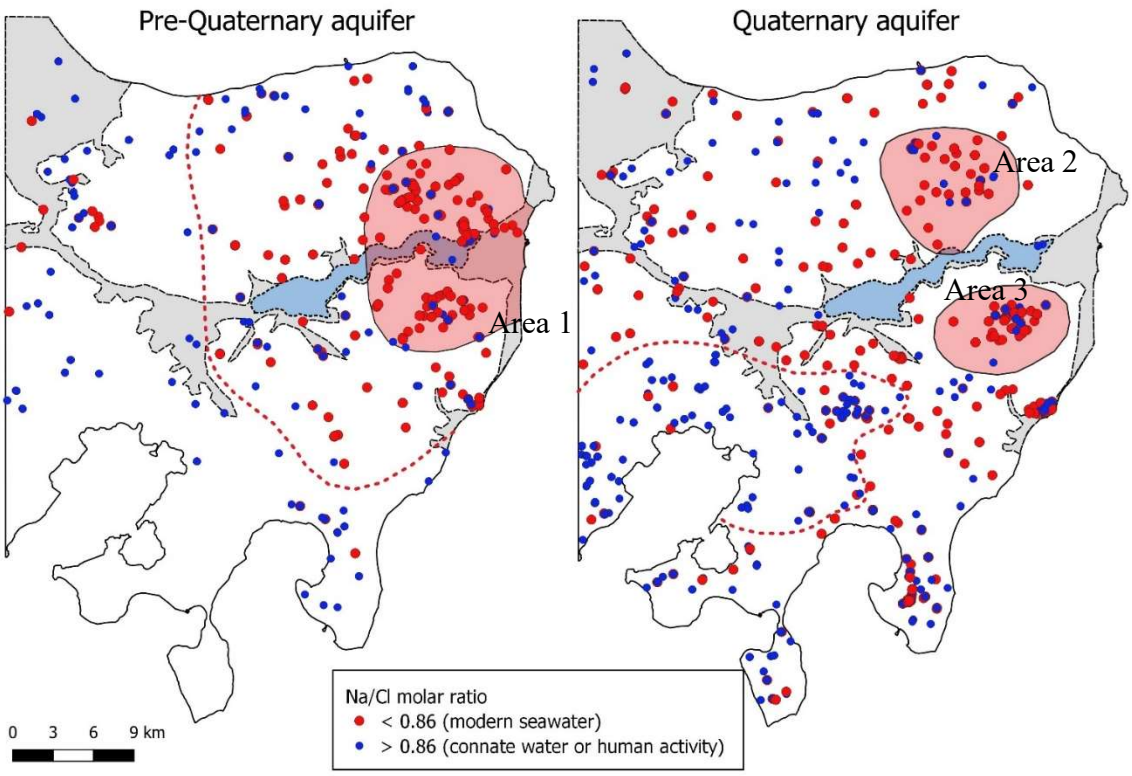

Figure 38. Spatial distribution of Na/Cl ratio to distinguish between modern seawater and connate water or water affected by human activity as salinity source. Dotted line distinguishs areas dominated by Na/Cl ratio above 0.86 and below 0.86.

Salinized areas

In Area 1 (in pre-Quaternary aquifer), the spread of Na/Cl molar ratio decreases with depth (***Figure 39***).

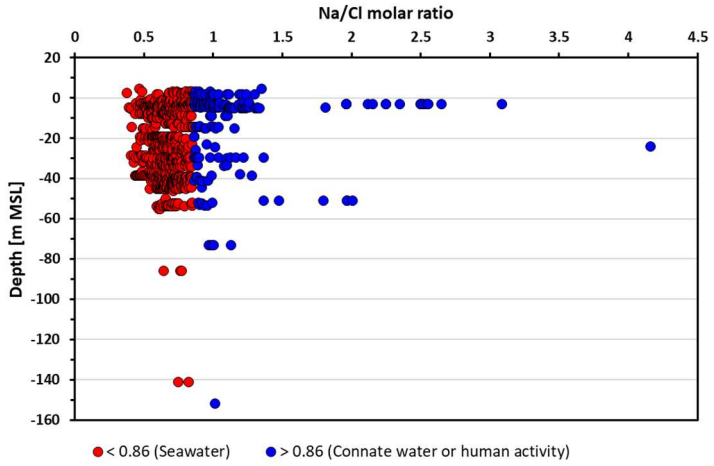

Figure 39. Molar ratio of Na/Cl for Area 1 within the pre-Quaternary aquifer.

In the Quaternary aquifer, groundwater samples within Area 1 and Area 2 (***Appendix A9***) show low and high ratios of Na/Cl, almost equally distributed with depth. It is hard to observe a trend.

Mass ratio of chloride over bromide (Cl/Br)

Chloride to bromide mass ratios were determined for groundwater samples in the pre-Quaternary and Quaternary aquifer (***Appendix A10***), but in most samples the concentration of bromide was too small to be accurate (< 0.2 Br mg L^{-1}, ***Appendix A11***). Secondly, in most of the samples chloride concentration was also too small (***Figure 40-right***), as it is method is recommended for chloride concentration exceeding 60-100 mg L^{-1}.

In the pre-Quaternary aquifer, Cl/Br ratios ranges either below 280, or between 300-400 (***Figure 40-left***). When the ratios are plotted against chloride concentrations, ratios in the range of 300-400 Cl/Br lie closer to the reference value of seawater ~280-297 Cl/Br. Ratios with chloride content below 60 mg L^{-1} have been assumed to be inaccurate.

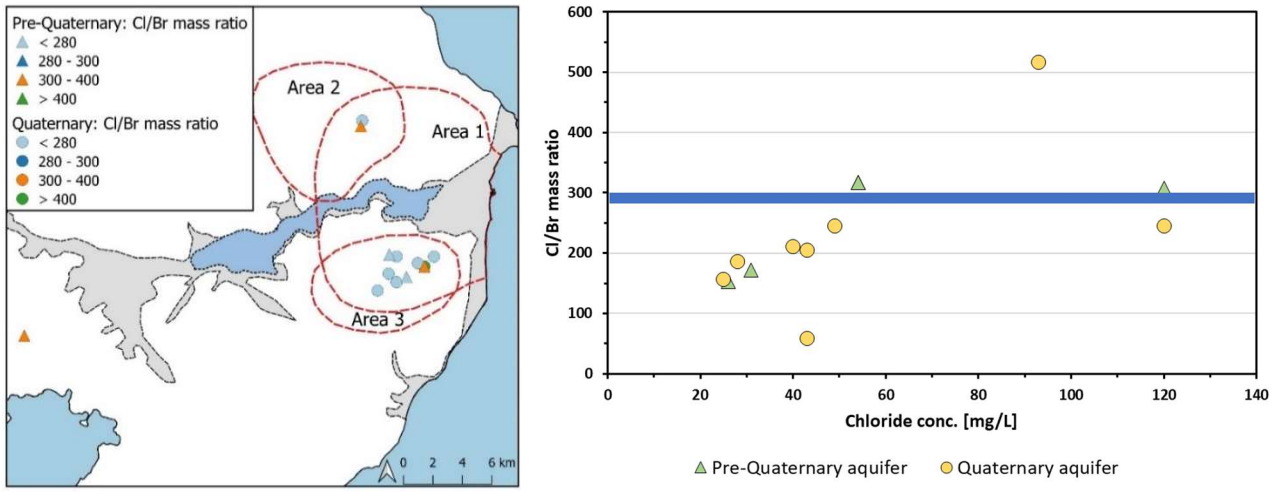

Figure 40. Cl/Br mass ratio measured from the pre-Quaternary and Quaternary aquifer.
Left: Spatial distribution of Cl/Br ratios. Right: Cl/Br ratio as function of chloride content. Blue line indicates Cl/Br ratio of seawater.

Most Cl/Br ratios from the Quaternary aquifer also show too low chloride concentrations (***Figure 40-right***). Only two measurements, one with ratio Cl/Br ratio of 244 and another with 517 Cl/Br ratio have reasonable chloride content. The lower ratio has same value as evaporated seawater or connate water, and the higher ratio reflect anthropogenic effects, as impact of domestic sewage effluents of de-icing salt.

Fluoride content

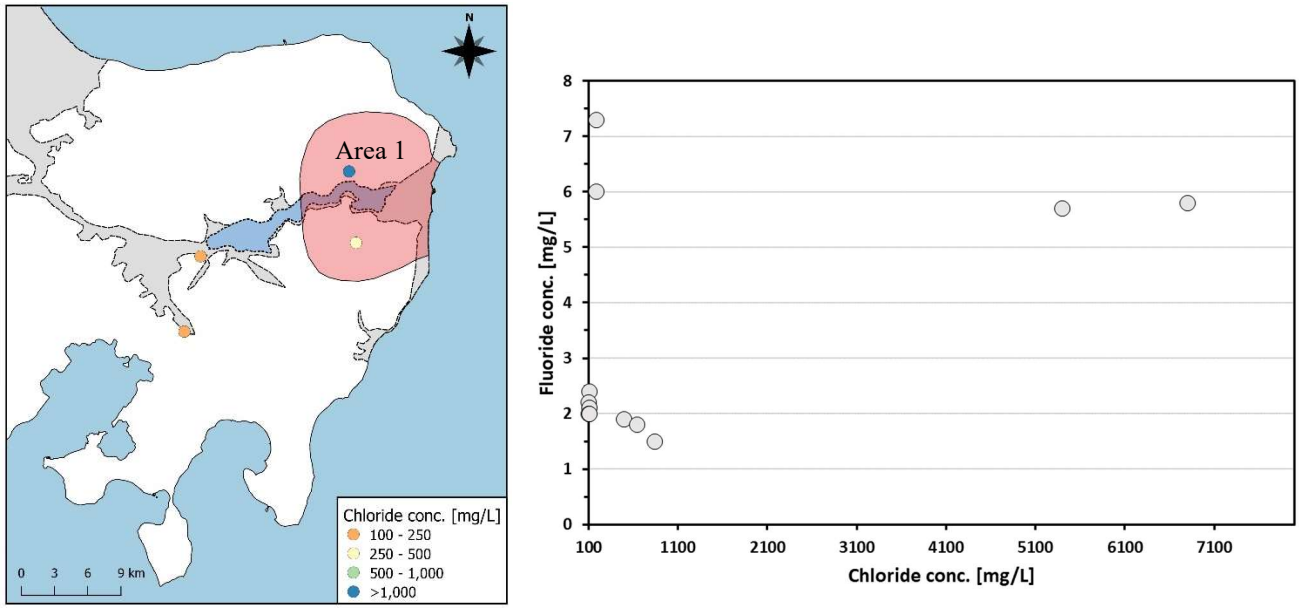

Figure 41. Left: Spatial distribution of samples with fluoride concentration (> 1.5 mg L^{-1}) **and** high chloride concentration in the pre-Quaternary aquifer.
Right: Samples plotted with high chloride (>100 mg L^{-1}) and fluoride content (> 1.5 mg L^{-1})

Four wells located near the Kolindsund strait (***Figure 41-left***), show high chloride content (>100 mg L^{-1}) and high fluoride content exceeding 1.5 mg L^{-1}. Within those wells, high chloride and fluoride measurements have been measured multiple times over time (***Figure 41-right***). There were more groundwater samples with high fluoride content (>1.5 mg L^{-1}), but where associated chloride measurement was lacking.

5.3. AEM method

AEM data covers the northern part of Djursland. As there is lack of geochemical data within the Kolindsund area, affecting the geochemical investigation in the previous section, the Kolindsund area has been chosen as target area of the geophysical investigation (***Figure 42***).

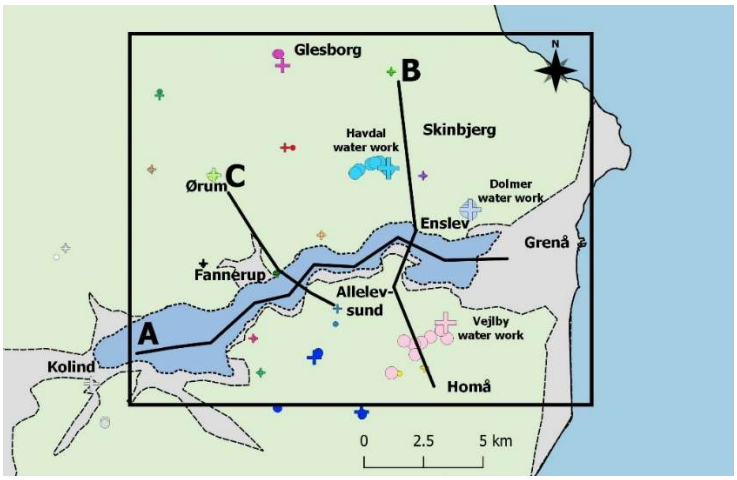

Figure 42. Geophysical investigation area in the NE of Djursland. Black triangle marks the scene extend of the geophysical investigation. A, B and C mark the longitudinal and transverse profiles in the area. Large water works within the area are depicted.

Horizontal depth profiles depict transition water (4 - 10 Ωm) to be identified at the terrain surface (-5 m MSL) in the eastern part of Kolindsund (***Figure 43***). At depth 50 m and 100 m below sea level transition water propagates northward and saline water (< 4 Ωm) are identified within the strait. This spreading of transition water is particularly in the eastern part, but with depth towards -150 m (MSL) the transition water spreads towards the central part of Kolindsund. In depth of -150 m (MSL) almost the entire area north of Kolindsund, show water characterized as transition water whereas south of Kolindsund, the resistivity identifies the groundwater as freshwater. Reaching depth of 190 m below sea level, in the western part of the horizontal section, an abrupt boundary between transition to saline water and

freshwater are observed. This is even more pronounced in the resistivity interpolation data found in ***Appendix A12***.

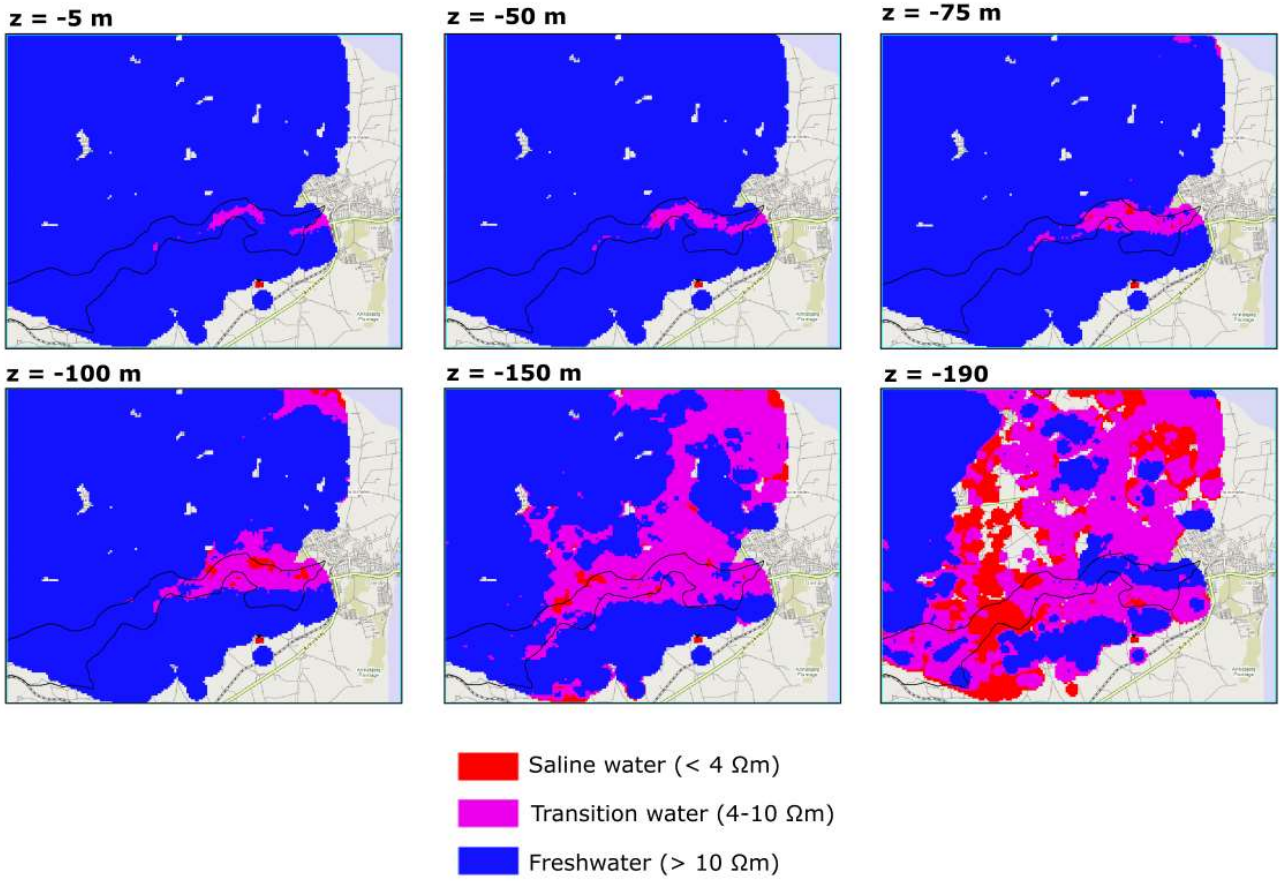

Figure 43. Horizontal sections of AEM data in the surrounding area of Kolinsund. Horizontal sections show depth measured in meter [m] in relation to mean sea level. Kolindsund is marked with black line.

Three profiles A, B and C (***Figure 44***) within the investigated area was extracted to depict the vertical development of freshwater-saltwater. Profile A shows a longitudinal profile of Kolindsund. Profile B and C show transverse profiles, one covering the eastern part of Kolindsund near Enslev and Dolmer water work (Profile B) and another covering the central part of Kolindsund (Profile C).

Profile A

In the eastern part of the profile (***Figure 44***), water representing transition water is close to terrain surface and near Enslev pumping station the transition water reaches the terrain surface. This is also the situation at the end of the profile near Grenå. Westward the interface between fresh and transition water decreases to depths between 180 m to 200 m below sea level but between Fannerup and Allelevsund, the interface

propagates upward as a plume. Water representing saline water is prominent in the western part of the profile (dotted lines), where the transition zone between fresh and saline water varies between 10-20 meters. In the eastern part of the profile, almost no areas show saline water. In addition, it should be noticed, below the thicker layer of transition water (> -160 m MSL) in the eastern part of the profile, resistivity increases and water is below defined as freshwater.

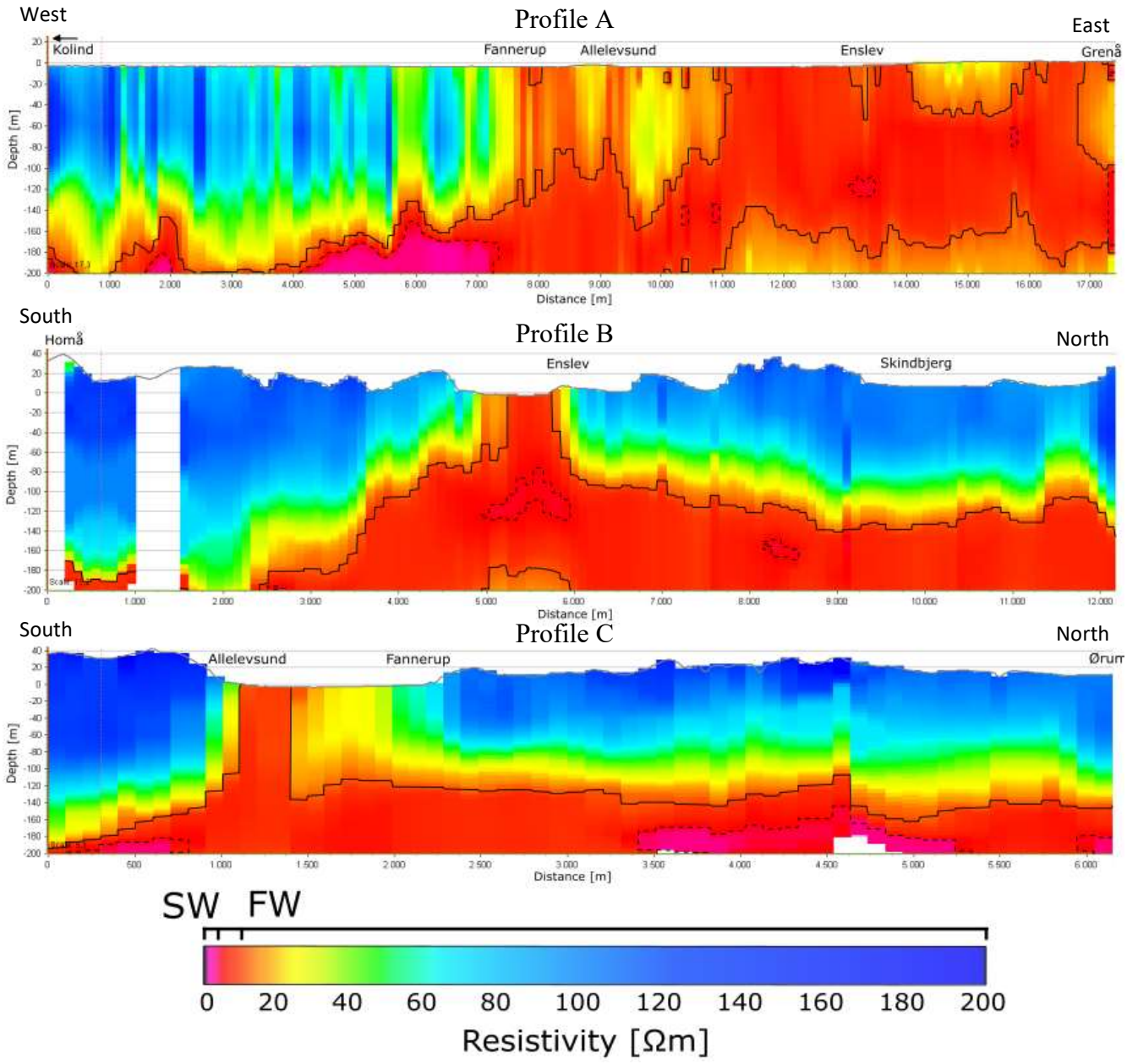

Figure 44. Cross-sections of profile A, B and C.
SW = saltwater defined by < 4 Ωm, and FW = freshwater defined by >10 Ωm. Within 4-10 Ωm transition water is defined. Solid line marks the interface between fresh- to transition water. Dotted line marks the transition between transition and saline water.

Profile B

In the transverse profile B (***Figure 44***) covering the outer part of NE Djursland, the interface of freshwater-transition water is only approaching terrain levels within the area of Kolindsund. Within this area approximately 100 meters below terrain surface, salt has accumulated from water flowing towards Kolindsund from the northern and southern sides, and this water is defined as saline water. The same trend is shown for transition water in the same area, where transition water is flowing towards Kolindsund from both sides, as below the transition water in the Kolindsund profile (Profile A), freshwater was identified. In this profile, there is a difference between the inclination of the transition-freshwater interface for the northern area and the southern area. Towards north the inclination is steep than southward. In the north, the interface between fresh and transition water is observed in depths of 100 m to 140 m below sea level while in the south, the interface is observed at depth of approximately -180 m (MSL).

Profile C

The second transverse profile (***Figure 44***) covers an area more inland. Near Allelevsund pumping station, in the southern end of Kolindsund, transition water reaches the terrain surface. In the northern end, resistivity increases slowing towards fresher conditions. The same trend as observed in profile B, shows the freshwater-transition water interface is located closer to surface north of Kolindsund than south. The interface to transition water can be found in depths of -140 m to -120 m (MSL) in the northern part of the profile. South of Kolindsund, the slope of the interface decreases towards -200 m (MSL). Both south and north of Kolindsund, thickness of transition water is thin and low resistivity indicating saline water, can be observed. In north saline water can be found in depths from -160 m (MSL) while in south saline water can be found from 180 m below sea level.

5.4. SEAWAT model of Kolindsund

5.4.1. Sensitivity analysis

The model simulates two phases from past to present conditions of Kolindsund, (Phase 1: 4,000 yrs. B.P. - 1874. Phase 2: 1874-2020). This was to analyze the effect of different parameters and to obtain similar salinity conditions as the geophysical skyTEM data show (Profile A, ***Figure 44***). Resistivity data show the transition zone is close to surface at east and decreasing to 180-200 m below sea level at west. This

structure of water layers will tried to be obtained. The influence of the parameters recharge, dispersity, hydraulic conductivity, porosity, and salinity were tested. The transition zone is defined as 1 - 20 TDS g L^{-1} as this is assumed to be appropriate values. All figures showing the location of the transition zone, is from the final timestep of the second phase (2020). All figures are oriented west-to-east.

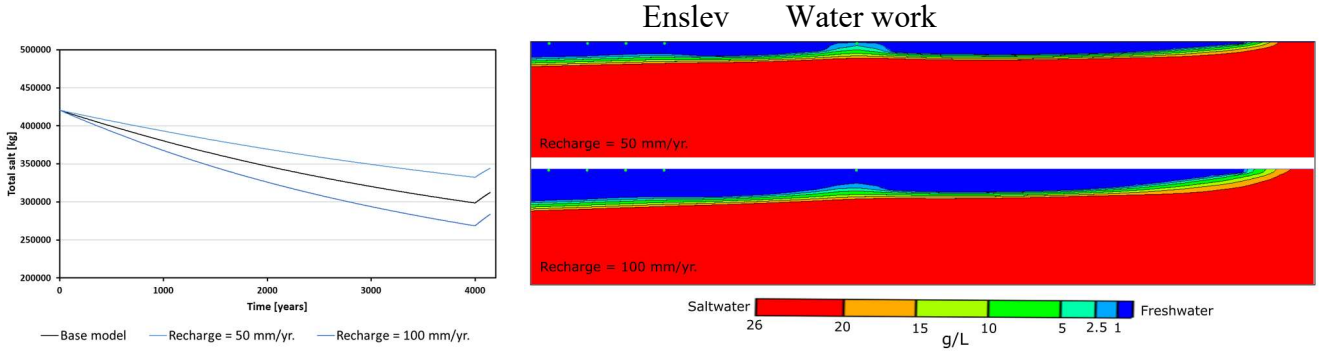

Figure 45. Effect of recharge. 1) Total salt content as function of time. 2) Location of transition zone.

Recharge has a large effect on the total salt content in the aquifer, as recharge supplies fresh groundwater to the system (*Error! Reference source not found.-**1***). The amount of freshwater recharging to the system, impacts the location of the transition zone. Increasing recharge, increases the thickness of the freshwater lens formed. In the low recharge scenario (50 mm yr^{-1}), the depth to the transition zone is approximately 210 m (MSL) whereas in the high recharge scenario (100 mm yr^{-1}) the transition zone depth is located at 410 m (MSL). When recharge is low, the transition zone approaches the terrain surface at the water work and in the high recharge scenario, the effect of upconing saline water is smaller.

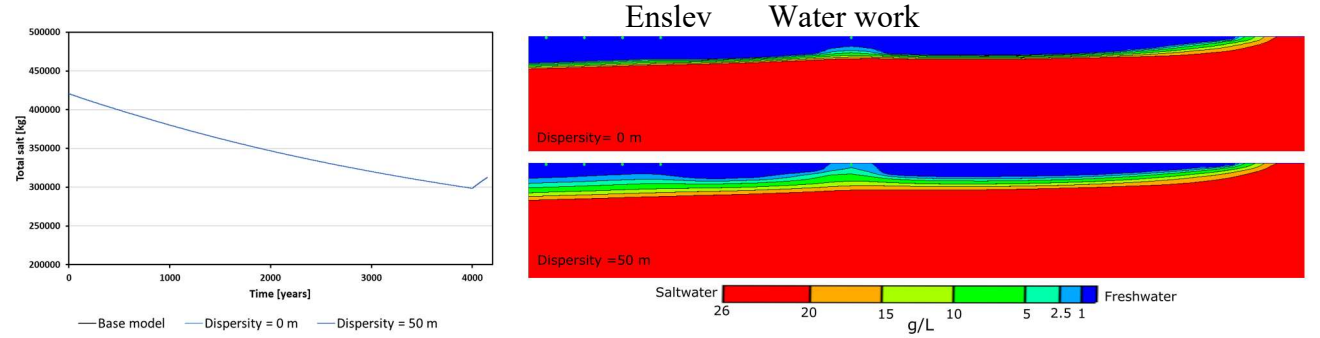

Figure 46. Effect of dispersity. 1) Total salt content as function of time. 2) Location of transition zone.

The total salt content in the aquifer, is not affected by changes in the longitudinal dispersity, but the distribution of salt content within the system is different (***Figure 46-2***). Increasing longitudinal dispersity has the biggest impact on the thickness of the transition zone, which influences saltwater intrusion at the water work.

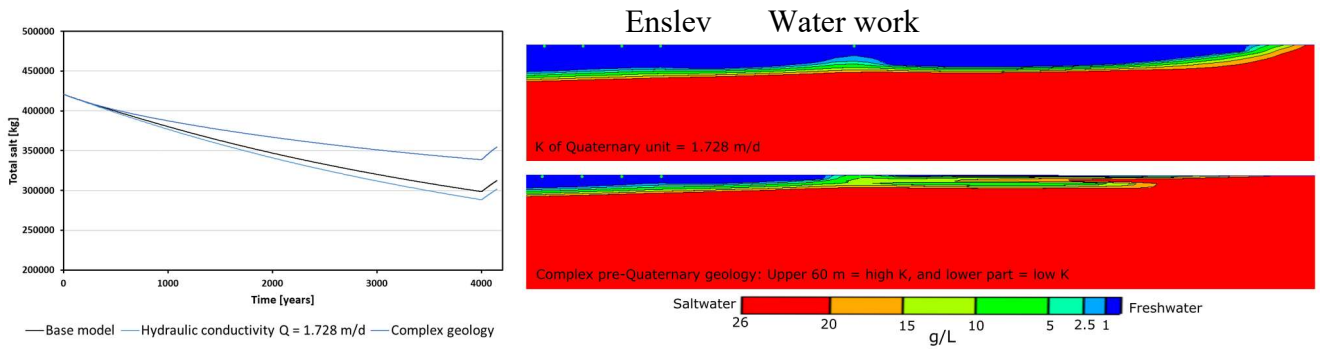

Figure 47. Effect of hydraulic parameters. Scenario 1) Total salt content as function of time. 2) Location of transition zone. Upper frame shows testing of lower hydraulic conductivity K = 1.728 m/day of Quaternary unit, and lower frame shows testing of complex geology of the pre-Quaternary unit: Upper 60 m: K = 61.6 m/day and the lower part: K = 6.16 m/day.

Testing hydraulic parameters (**Figure *47***) as lower hydraulic conductivity of the Quaternary unit, and a two-layered structure-model of the pre-Quaternary unit with different conductivities, show the complex geology of the pre-Quaternary unit has a larger effect on the total salt content within the aquifer. When initiating the pumps in the second phase, saltwater intrusion is intensified in the upper layers of the aquifer between the water work and the seaside to the east. Reducing the hydraulic conductivity of the Quaternary unit, has no significant effect on the total salt content in system, or the final location of the transition zone in the system.

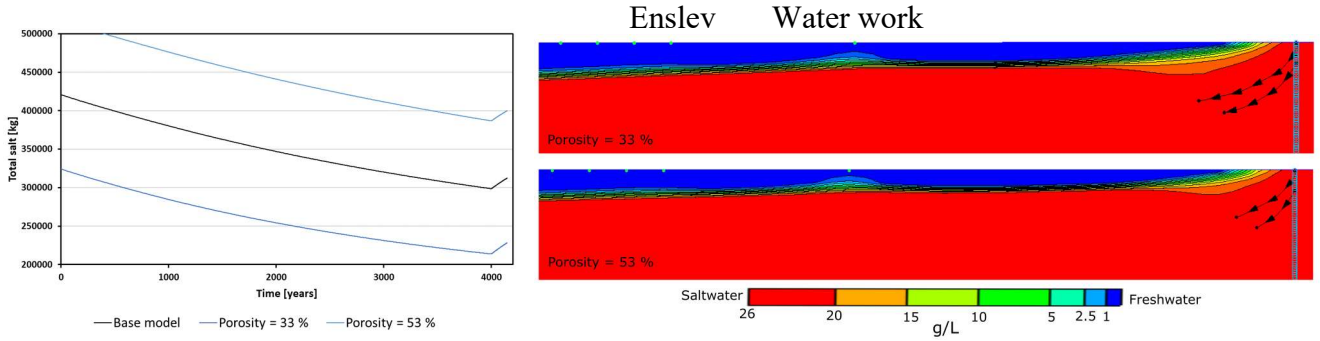

Figure 48. Effect of porosity in the pre-Quaternary unit. 1) Total salt content as function of time. 2) Location of transition zone. Travel arrows of the particles show every 300-meter step a particle has travelled.

Changing the porosity of pre-Quaternary sediment (***Figure 48***) changes the pore space between the sediment particles and therefore more or less saline water can be present within the aquifer. This changes the initial total salt concentration. When increasing the porosity, the transition zone is located about 120 meters higher than the transition zone in the low porosity scenario. Forward-tracking of particles within the second phase (1874-2020) shows seawater intrudes further inland in a less porous medium (33%) than in a more porous medium (53%).

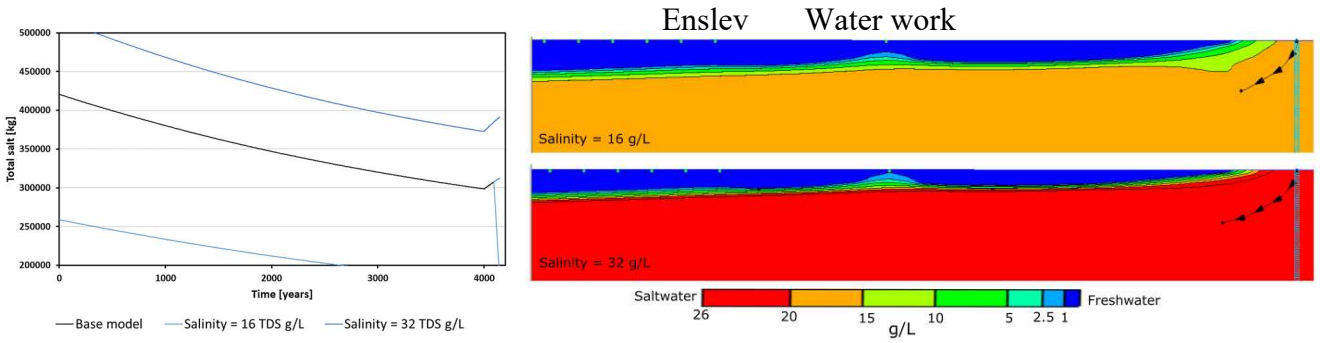

Figure 49. Effect of salinity. 1) Total salt content as function of time. 2) Location of transition zone. Particle forward-tracking in phase 2 (1874-2020). Arrows indicate every 300-meter step.

The effect of salinity impacts the total salt content the most (**Figure *49***). In the high salinity scenario, the transition zone is thinner than in the low salinity scenario. The location of the transition zone affects the final height of the plume in the second phase, when pumping is initiated. With increasing salinity, forward-tracking of particles show particles move ~300 meters further inland than in the low salinity scenario.

5.4.2. Past, present and future simulations of Kolindsund

Based on the sensitivity analysis, most of the values from the base model were implemented in the new model. Applied parameter values can be found in ***Appendix A13***.

Salt content within the aquifer through time (4,000 yrs. B.P to 2020 C.E.)

During phase 1, recharging freshwater to the aquifer decreases the total salt content by 0.0034 % per year (***Appendix A14***). When draining was initiated, the total salt content start increasing rapidly by 0.0168% per year towards the year 2020. If the excessive draining continues, the system will be supplied by further +0.0138% salt per year. If draining was stopped today, it will decrease the salt supply to the aquifer by -0.0066% per year (***Appendix A14***).

Present conditions of Kolindsund (2020)

Back-tracking of particles located in the upper layer at Enslev and the waterwork (during phase 2) (***Figure 50***) show a longer travel path for the particle located at the waterwork than for the particle at Enslev. Back-tracking shows the particles had origin in the past saline Stone Age water. Forward tracking of particles from the seaside show seawater intrudes less than 500 meters inland.

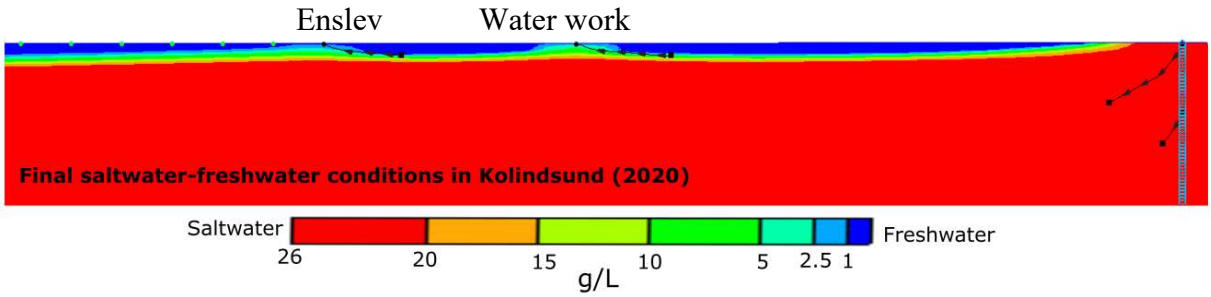

Figure 50. Eastern Kolindsund: timeframe of final timestep in phase 2 (2020). Back-tracking particles are added to cells near the waterwork and Enslev, and forward-tracking particles are added to the seaside (right column) in phase 2. Arrows indicate every 100-meter step.

Future conditions of Kolindsund (2020-2100)

During a future scenario with no drainage, within the first 3.5 years, the water table increases fast (5 meters) with landwards water flow (***Appendix A15***). As a result of groundwater flowing landward toward the low-lying Kolindsund, a watershed appears between the water work and the sea, where water flows in both directions. As the inland flow of water decreases, it increases the water flowing seawards. After ~14 years, almost no water flows landwards, except at the water work and the upper groundwater layers at Enslev. Water level in the western part of Kolindsund has now increased to 5 m MSL. After 18 to 22 years, above half of all cells are flooded and the groundwater table in the western part is reaching elevations of 12 meters (MSL). After 26 years, the system approaches an equilibrium state where changes of the water table are very small towards the end of the simulation.

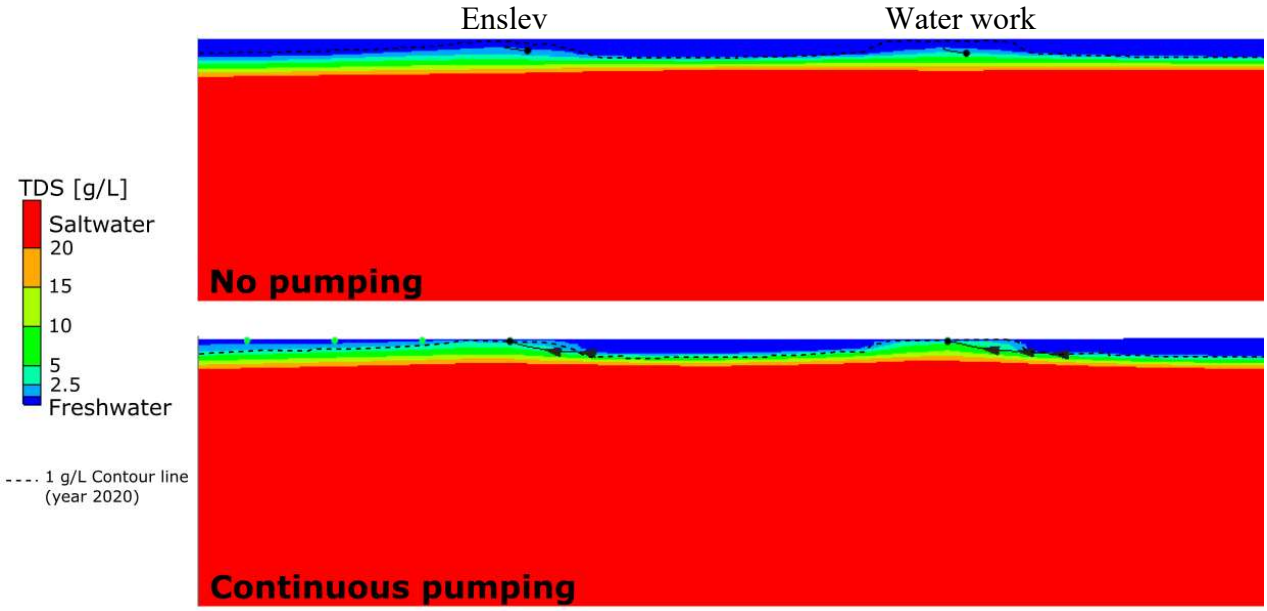

Figure 51. Final timeframe of saltwater-freshwater conditions in the eastern Kolindsund (2100). Backward-tracking of particles added to Enslev and at the water work. Arrows indicates every 200-meter step.

The future scenario with no drainage (***Figure 51***) shows the saline plumes at Enslev and the water work will decreased with time. Backward-tracking show salt particles have traveled approximately 150 meters in the past 80 years. In the case of continuous pumping, particles have traveled between 400-600 meter and water with salinity level above 5,000 TDS mg L^{-1} approaches the surface in Enslev and at the water work.

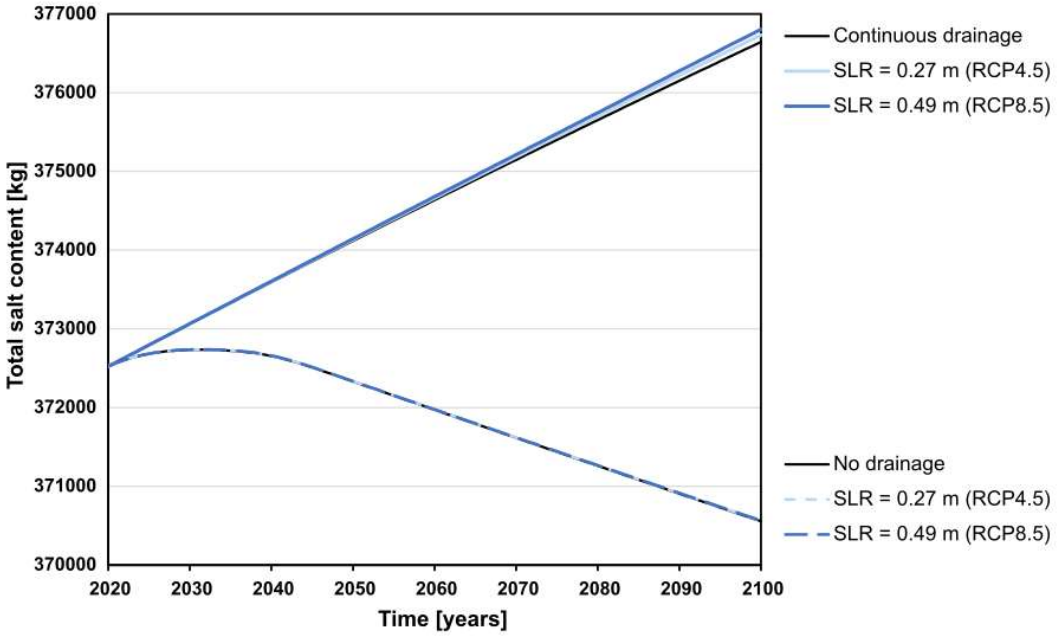

Figure 52. Effect of rising sea level due to climate change for the two scenarios: 1. With continuous drainage 2. With ended drainage.

For the aquifer in Kolindsund (***Figure 52***), sea level rises have only a smaller influence on the total salt content during the phase 3. In the future scenario with continuous drainage, the sea level rise in the most extreme climate scenario (RCP8.5) show the largest impact on the total salt content, whereas sea level rise (RCP8.5) in the future scenario with no drainage, show no impact on the total salt content. The largest effect on the total salt content within the system is the effect of draining the system.

5. Discussion

By using a multi-method approach based on data accessible from databases in Denmark, identification of saltwater intrusion in the case-study area, Djursland, will be evaluated. For the evaluation, three factors will be identified and discussed:

1. Areas at risk of saltwater intrusion in both aquifer types (pre-Quaternary and Quaternary aquifer)
2. Associated salinity sources leading to increased salinity levels observed
3. Key parameters important for saltwater intrusion

The second part of the discussion will be an evaluation of the use of data from public Danish databases including limitations, advantages and disadvantages. The final part of the discussion is an assessment of the multi-method approach, where it will be discussed, if it can be used to identify saltwater intrusion, and thus, can be applied in an arbitrary site in Denmark.

5.1. Impact of SWI on pre-Quaternary and Quaternary aquifers

5.1.1. Salinization in the pre-Quaternary aquifer of Djursland

In the pre-Quaternary aquifer, chloride concentration and electrical conductivity analysis were applied as proxies of salinity. Near Grenå, in the northeastern part of Djursland, deteriorated groundwater was discovered, with decreasing quality at increasing depth. At the inlet of Grenå towards Enslev in the eastern Kolindsund, 20 m below sea level, chloride concentrations exceeding 500 mg L^{-1} were measured. As chalk and limestone have been deposited in marine environments, residual water is present in deeper parts of these aquifer types (Vangkilde-Pedersen *et al.*, 2011). In the northeastern Kolindsund, the surface of the pre-Quaternary sediment is located very close to terrain, and in Enslev the limestone is exposed (Korkman, 1981). Previous studies of pre-Quaternary aquifers in Zealand have shown correlation between high measured chloride concentrations and pre-Quaternary aquifers located close to terrain, with the cause assigned to the effect of excessive pumping (Larsen and Berger, 2006). This suggest the effect of constant drainage of Kolindsund, exerts an impact on the saltwater-freshwater balance.

The numerical model supports the major effect of drainage. It was observed when drainage was initiated, incoming salt to the system increased by 0.0168 % per year, where before the pumping began the

incoming salt to the system decreased by 0.0034% per year. Inflow of discharge from the catchment zone of Kolindsund has not been accounted for in the model. In the study of Rasmussen *et al*., (2013) it was pointed out, head-controlled systems are sensitive to saltwater intrusion and especially the head-stage is sensitive, as it can intensify saltwater intrusion. As the pumping depth in Kolindsund has been lowered a few times since 1874, this could have an impact.

As groundwater table follows topography, hydraulic heads are lowest within the low-lying strait and Kolindsund. The three scenarios of Ghyben-Herzberg suggest, independently of chosen salinity value of the seawater, the strait and coasts along the eastern and northern Djursland are the most sensitive to saltwater intrusion. In the high salinity scenario (32 ‰), the area north of Kolindsund which covers the northern part of the salinized Area 1, is the second area to be impacted by saltwater intrusion, with increasing salinity. This could imply that saltwater affecting the pre-Quaternary aquifer has a higher density and salinity. Most groundwater exploitation in Denmark is derived from pre-Quaternary aquifers (GEUS, 1995; Nilsson and Gravesen, 2018), and in the eastern part of Djursland, three of the largest water works (largest supplier of drinking-water) are located, supplying Grenå, the largest town in Djursland (Miljøministeriet By- og Landskabsstyrelsen, 2009). Major head fluctuations were observed in this area, especially within the identified area (Area 1). This suggest the annual amount of water abstracted from pre-Quaternary groundwater resources in eastern Djursland, somewhat could be impacting the saltwater-freshwater balance as the saltwater-freshwater system is sensitive to head fluctuations. In addition, as croplands represent 66 % of land areas in Djursland (Miljøministeriet By- og Landskabsstyrelsen, 2009), water abstracted for agricultural irrigation is an important factor in the water balance.

Groundwater chemistry show two water types in the pre-Quaternary aquifer. One with similar composition as fresh groundwater characterized by lower concentration of chloride (>250 mg L^{-1}) and one with similar composition as Kattegat seawater, compared to water samples from Kattegat plotted in a Piper diagram (study from Læsø in northern Kattegat by Jørgensen, 2002). Similar seawater composition is supported by shapes of Stiff diagrams from Area 1. Group 2 in the Piper diagram with intermediate chloride concentration (100 mg L^{-1}) had water composition closer to group 1, which was why they were defined as the same water type. But the span between the two distinctive water types seems doubtful. To be plotted in a Piper diagram, a groundwater sample needs concentrations of calcium,

magnesium, sodium, potassium, bicarbonate, sulphate and chloride. For most samples, measurements have been conducted for chloride, sodium, and sulphate, as they are strictly important for the quality of drinking water (Miljø- og Fødevareministeriet, 2019). But there are only limited number of groundwater samples, where all ion concentrations have been measured at the same time.

Earlier theories have stated, that residual water originated from the Littorina Sea, is the source of salinity (Nielsen and Rauschenberger, 1982; Århus Amt, 1995; Thomsen *et al.*, 2005). Based on Na/Cl ratios, low ratios (< 0.86 Na/Cl) predominate the entire northeastern Djursland and indicates modern seawater as the salinity source. It has been observed that ratios very close the reference value (0.86 Na/Cl of seawater) are found in the deepest parts of the aquifer, and with decreasing depth, the ratios are more spread relatively to the reference value. Ratios above 0.86 Na/Cl, suggest intrusion of freshwater in a saline aquifer, where Na^+ is exchanged with Ca^{2+} from incoming freshwater (Bear *et al.*, 1999). As some groundwater samples have high ratios, this could indicate connate water also influences the aquifer. High fluoride and chloride content were measured in a few wells in the western Kolindsund, and they suggest, fossil stagnant water could contribute to salinization.

Groundwater modelling depict residual water as the source of salinity. From the modelling, it was observed from particle tracking, that seawater had only traveled short distances within the period from the pumping began 1874 to 2020. In addition, the groundwater modelling showed, that the effect of soil properties (hydraulic conductivity and porosity) are important for the effect of saltwater intrusion, as they can change the level of the transition zone, and the flow velocity of particles in the system. In Werner *et al*., (2013) the importance of hydraulic properties and heterogeneities in saltwater-freshwater systems have been emphasized. Profile A of Kolindsund, from AEM resistivity data, show a more complex aquifer system. Accumulated salt concentrations are observed within arbitrary areas, and in the upper layers of the eastern part, water was characterized as transition water, whereas the lower parts showed higher resistivity values indicating the presence of freshwater. In the study of Nilsson and Gravesen (2018), Grenå was pointed out as an area with karst systems. Depending on the extend of karsts, this could impact the heterogeneity of the aquifer matrix, the saltwater intrusion, and the spreading of saline water.

Geophysical horizontal profiles show the extend of saltwater intrusion in the northeastern Djursland. As expected, deteriorated water was identified closest to surface within the eastern Kolindsund, as this was

observed from studies in the 80's (Korkman, 1980; Nielsen and Rauschenberger, 1982). But below 100 m (MSL), it was observed how transition water was spreading northward and northwestward of Kolindsund. At depths of -190 m (MSL), resistivity data show a border between freshwater in the northwestern part of the profile and transition to saline water occupying the rest of the profile in the eastern part. Low ratios of Na/Cl (< 0.86) were only present in the northeastern part of Djursland, and the border to higher ratios (> 0.86), follows the border observed from geophysical resistivity data at depth -190 m (MSL).

This could suggest Kattegat saltwater intrusion in the pre-Quaternary aquifer in NE Djursland, and from the three scenarios with Ghyben-Herzberg, it suggests seawater with higher salinity is impacting the area. But very likely, connate water and fossil water contributes to the salinization too. The BEX-index showed groundwater samples with negative BEX-value (indicating salinization) are restricted to the NE Djursland. This also imply, that the aquifer is experiencing an ongoing saltwater intrusion. This is supported by observed increasing temporal trend of chloride content, even though wells with decreasing chloride trend are observed too. The numerical model shows how the effect of continuous drainage will add to the saltwater intrusion. But it was illustrated, the effect of future sea level changes, only have a minor effect on the saltwater intrusion compared to the exerted effects of a head-controlled system. In the study of Rasmussen *et al*., (2013) it was observed that changes in sea level must be significant before an effect are observed in a head-controlled system.

Based on geochemical, hydrological and geophysical results, it is very likely seawater and contributions from residual and fossil water that intrudes the pre-Quaternary aquifer northwestward.

5.1.2. Salinization in the Quaternary aquifer of Djursland

In the Quaternary aquifer, the spatial distribution of high chloride content and EC measurements vary compared to the pre-Quaternary aquifer. Two areas in the eastern Djursland, were identified as salinized areas based on EC and Cl measurements. Within those areas, it was observed that chloride concentration decreased with depth. This trend was observed within two single wells in each of the areas, including an increasing temporal trend of chloride. It should be pointed out, high chloride concentrations (< 1,000 mg L^{-1}) measured in the Quaternary aquifer are not as high as high chloride concentrations measured in the pre-Quaternary aquifer (>1,000 mg L^{-1}).

Water samples of the two identified areas (Area 2 and 3) plotted in the Piper diagram, show a different location of samples with high chloride concentration (>250 Cl mg L^{-1}) compared to the same type of samples (>250 Cl mg L^{-1}) within the pre-Quaternary aquifer. This could suggest saltwater impacting the aquifer originates from another source, especially as high chloride concentrations were measured closest to the surface. A study from Fyn, observed the same trend of high chloride content in the upper layers and decreasing content with depth. It was suggested road de-icing salt was the salinity source (Fyens Amt, 2001).

Based on Na/Cl ratios of groundwater samples from within the areas, both ratios above and below the reference value 0.86 Na/Cl are present. This suggest the salinity sources; domestic waste water (anthropogenic effects) and/or connate water - old seawater trapped in the sediment for ratios above 0.86 Na/Cl, or modern seawater for low ratios (<0.86 Na/Cl) (Bear *et al.*, 1999). As seawater and connate water would be expected to intrude from below, and the high concentrations of chloride was observed in the upper parts, this could imply domestic wastewater as the source of salinity. Ratios of Cl/Br were very restricted as concentrations of both ions were too small for this method, but one sample from the Quaternary aquifer showed a Cl/Br ratio above 500, which reflects impact of domestic sewage effluents or de-icing. This could support the idea of anthropogenic effects are the salinity source.

From skyTEM data, profile B covers both areas (Area 2 and 3) and showed, the depth to the transition water and saline water within these areas, were ~ -120 m (MSL) for Area 2 and approximately -180 m (MSL) for Area 3. It is, therefore, unlikely that upwelling seawater (connate or modern) is impacting the areas. In a report by Århus Amt (1995), these areas are described to be very vulnerable to nitrate leaching, as the aquifers are mainly composed of sandy sediment. This will thus, make them vulnerable to other anthropogenic effects infiltrating to the aquifer. As cropland is the most extended land-use in Djursland, and fertilization contains chloride, this could be a suggested source of salinity. But a more comprehensive geochemical analysis will be recommended. New measurements of chloride and bromide could be useful, as they can be good indicators of different types of sources, but samples need to have appropriate concentrations of both ions.

To sum up, saltwater intrusion has been identified in the pre-Quaternary aquifer, and to a lesser degree in the Quaternary aquifer. Kattegat seawater, in combination with connate and stagnant fossil water could be the source of the salinity observed in the pre-Quaternary aquifer, and anthropogenic effects infiltrating

from the terrain surface is very likely the source of salinity for the Quaternary aquifer. Key parameters identified from the numerical modelling, is the effect of recharge as it can impact the location of the transition zone, and hydraulic soil parameters (hydraulic conductivity and porosity), as the geology of the system seems more complex.

5.2. Using data from Danish databases: limitations, dis- and advantages

Available hydrological, geochemical, geophysical and future climate data from Danish databases, Jupiter, GERDA, and Klimaatlas have been used within the multi-method approach to identify and evaluate saltwater intrusion in Djursland.

Jupiter database comprises the majority of necessary geochemistry data applicable for saltwater intrusion studies. This include both major and minor ions, and electrical conductivity (GEUS, 2021). But it was discovered that information about numbers of measurements for each well and the actual number of measurements reported to the database did not match. For some wells, some measurements were missing. This was especially a disadvantage for chloride concentration and EC measurements, as they were used as primary indicators to identify salinized areas. To compensate for the lack of data, a combination of maximum measured values and all historical measurements from the database for both parameters were applied.

For many wells, a disadvantage from the use of geochemical data, is that only a single measurement of chloride concentration is available, which limits the understanding of the temporal development of salinization within the system.

For the few bromide measurements reported to the database, almost all measurements were worthless in the studies of saltwater intrusion. To use bromide measurements within Cl/Br ratio, Br concentrations is recommended to be above 0.2 mg L^{-1} otherwise, the data can be unreliable and inaccurate (FAO, 1997).

The largest advantage by using geochemical data from Jupiter database is the availability of data of all the main chemical components, as concentrations of main components are the most important element in saltwater intrusion studies (FAO, 1997; Bear *et al.*, 1999).

Within Kolindsund, almost no geochemical measurements have been conducted. Only one measurement in the western part and a few measurements in the eastern part exist. But as GEUS administer different databases, data from the geophysical database GERDA was applied instead.

Numerical modelling within this study, has only been used as a tool to understand different mechanisms and important factors in relation to saltwater intrusion. Therefore, no validation of extracted data from databases has been done, and the construction of the model could more or less, has been done without any data from databases. But as it is a tool, to understand the mechanisms and the saltwater-freshwater system, data from the area, was needed to calibrate the model.

For the modelling part, estimated climate data from the Klimaatlas database was used. The database contains information about sea level rise, precipitation, evaporation and storm patterns (DMI, 2021a). This information can be most useful in saltwater intrusion studies, as changes can enhance or reduce the risk of saltwater intrusion in an area (Werner *et al.*, 2013; Oppenheimer *et al.*, 2019)

5.3. Overall evaluation of combined method to identify SWI

The second objective was to investigate if this multi-method approach can provide sufficient information to evaluate the impact/risk of saltwater intrusion, and if so, would it be an appliable method to use in an arbitrary area in Denmark.

Based on the examination of the geochemical, geophysical, analytical and numerical results it is verified that a saltwater intrusion is impacting the study area in the pre-Quaternary aquifer. Three areas were identified as salinized areas based on geochemical data. An evaluation of geochemical, geophysical and numerical modelling results helped to identify salinity source for the three areas within the two types of aquifers. Numerical modelling was a tool applied to understand the effect of different parameters and was used to predict future development of saltwater intrusion in Kolindsund with the effect of climate change and drainage. It was discovered that drainage and abstraction of water exerts significant impact on the saltwater-freshwater system. In addition, heterogeneities of an aquifer can have a large effect on saltwater intrusion. Even though data was lacking within some areas, a large amount of data was available.

Overall, saltwater intrusion could be identified based on this multi-method approach with data from Danish databases. The results from the different methods supported each other within the evaluation identifying saltwater intrusion. Jupiter and GERDA are comprehensive databases and contains more data, than applied in this study, that could be relevant for saltwater intrusion studies (eg. ERT and log).

For future application of this multi-method approach to investigate saltwater intrusion, following recommendations should be noted:

- Account for ion balance as this can impact the geochemical results
- Bromide concentrations is recommended to be above 0.2 mg L^{-1} and chloride concentrations should be above 60-100 mg L^{-1}
- Be aware of wells characterized as 'Miljøpåvirket' - contaminated, as they can bias the overall results.

6. Conclusion

In coastal aquifers, there is a natural balance between salty seawater and fresh groundwater, but excessive exploitation of groundwater resources disturbs the saltwater-freshwater system and as a result, it can lead to saltwater intrusion. The impact of future sea level rise as a consequence of climate change, can move the saltwater-freshwater transition zone landwards. Especially low-lying coastal areas are the most vulnerable to this. Denmark is a flat country with a large coastline. In Djursland, eastern Jutland, a drainage system was established in the 1870's in Kolindsund as part of reclaiming the area. Kolindsund is located within a low-lying strait crossing Djursland from east to west that once was flooded by past seawater in the early Holocene epoch due to high sea level as a consequence of the end of the last ice age.

The aim of the study is to identify saltwater intrusion based on public accessible data from Danish databases by using a multi-method approach. Djursland was chosen for a case-study as the area contains low-lying and coastal areas and the excessive pumping of the Kolindsund. All factors that have been ascribed to induce saltwater intrusion.

Earlier theories about Djursland and Kolindsund have stated, the area is salinized by residual seawater once flooded the strait, but empirical data has been missing to support this theory. In this paper, geochemical, hydrological and geophysical data provides evidence that a saltwater intrusion is intruding the pre-Quaternary aquifer in the northeastern part of Djursland. The depth of the transition zone is more shallow north of Kolindsund than south of which could be reflected of the complex geology of the area. Water impacting the pre-Quaternary aquifer probably has its origin in the Kattegat seawater, but stagnant fossil water and residual water is very likely contributing too. The Quaternary aquifer is influenced by contamination from the terrain surface which is reflected in the Quaternary sediment as it is mainly composed of sand. As croplands are the most extended in Djursland, the source of observed increasing chloride could be fertilization but further investigations are needed to verify this.

Based on a combination of four methods to enlighten saltwater intrusion in Djursland, it has been validated that the use of public databases in Denmark could identify saltwater intrusion in Djursland. Therefore, this multi-method could be applied to an arbitrary site in Denmark if sufficient data is

available in the different databases (geological, geochemical, and geophysical) for the area. But caution must be taken when applying the data and additional sampling of geochemical or geophysical data could be beneficial if data for an area is limited or inadequate to support identification of salinity sources. In addition, numerical modelling can be useful to understand the response of the saltwater-freshwater system to different parameters.

References

Alcalá, F. J. and Custodio, E. (2008) 'Using the Cl/Br ratio as a tracer to identify the origin of salinity in aquifers in Spain and Portugal', *Journal of Hydrology*, 359(1–2), pp. 189–207. doi: 10.1016/j.jhydrol.2008.06.028.

Anders, R. *et al.* (2013) 'A Geochemical Approach to Determine Sources and Movement of Saline Groundwater in a Coastal Aquifer', *Groundwater*, pp. 1–13. doi: 10.1111/gwat.12108.

Appelo, C. A. J. and Postma, D. (2005) '6.1. Cation exchange at the salt/fresh water interface', in *Geochemistry, groundwater and pollution*. 2nd edn. CRC Press, pp. 242–247.

AQUAVEO (2017) *GMS:Natural Neighbor - XMS Wiki*. Available at: https://www.xmswiki.com/wiki/GMS:Natural_Neighbor (Accessed: 5 June 2021).

Bachtouli, S. and Comte, J. C. (2019) 'Regional-Scale Analysis of the Effect of Managed Aquifer Recharge on Saltwater Intrusion in Irrigated Coastal Aquifers: Long-Term Groundwater Observations and Model Simulations in NE Tunisia', *Journal of Coastal Research*, 35(1), pp. 91–109. doi: 10.2112/JCOASTRES-D-17-00174.1.

Barlow, P. M. (2003) 'Ground Water in Freshwater-Saltwater Environments of the Atlantic Coast', *USGS*, pp. 1-113.

Bear, J. *et al.* (1999) *Seawater Intrusion in Coastal Aquifers - Concepts, Methods and Practices*. Kluwer Academic Publishers, pp. 1-625.

Cai, J., Taute, T. and Schneider, M. (2015) 'Recommendations of Controlling Saltwater Intrusion in an Inland Aquifer for Drinking-Water Supply at a Certain Waterworks Site in Berlin (Germany)', *Water Resources Management*, 29(7), pp. 2221–2232. doi: 10.1007/s11269-015-0937-7.

Carol, E. S. and Kruse, E. E. (2012) 'Hydrochemical characterization of the water resources in the coastal environments of the outer Río de la Plata estuary, Argentina', *Journal of South American Earth Sciences*. Elsevier Ltd, 37, pp. 113–121. doi: 10.1016/j.jsames.2012.02.009.

Clark, P. U. *et al.* (2009) 'The Last Glacial Maximum', *Science*, 325(5941), pp. 710–714. doi: 10.1126/science.1172873.

Cohen, K. M. . *et al.* (2020) *International Chronostratigraphic Chart v2020/01*. Available at: https://stratigraphy.org/icschart/ChronostratChart2020-01.pdf (Accessed: 14 September 2020).

Custodio, E. (2005) 'Coastal aquifers as important natural hydrogeological structures', *Groundwater and Human Development*. doi: 10.1201/9781439833599.ch3.

Danmarks-Statistik (2019) *Danmarks Statistik 2019*.

Davis, S. N., Whittemore, D. O. and Fabryka-Martin, J. (1998) 'Uses of chloride/bromide ratios in studies of potable water', *Ground Water*, 36(2), pp. 338–350. doi: 10.1111/j.1745-6584.1998.tb01099.x.

Dinesen, B. (1961) 'Salt Mineralvand fra Danmarks dybere Undergrund', *Danmarks Geologiske Undersøgelser IV. række. No. 6*. C. A. Reitzels Forlag (Jørgen Sandal), 4.

DMI (2021a) *Introduktion til Klimaatlas*. Available at: https://www.dmi.dk/index.php?id=1118&L= (Accessed: 12 May 2021).

DMI (2021b) *Vejrarkiv*. Available at: https://www.dmi.dk/vejrarkiv/ (Accessed: 30 April 2021).

Dokou, Z. and Karatzas, G. P. (2012) 'Saltwater intrusion estimation in a karstified coastal system using density-dependent modelling and comparison with sharp-interface approach', *Hydrological Sciences Journal*, 57(5), pp. 985–999. doi: 10.1080/02626667.2012.690070.

Essink, G. H. P. (2001) *Salt Water Intrusion in a Three-dimensional Groundwater System in The Netherlands: A Numerical Study*, *Transport in Porous Media*.

FAO (1997) *Seawater intrusion in coastal aquifers: Guidelines for study, monitoring and control*, *Water Reports*. Rome: Food and Argiculture Organization of the United Nations.

Fitts, C. R. (2013) *Groundwater Science*. 2nd edn. Academic Press.

Fyens Amt (2001) *Grundvand 2000*.

GeoScene3D (no date) *Inverse Distance Weighted [GeoScene3D]*. Available at: https://wiki.geoscene3d.com/doku.php?id=geoscene3d:application:interpolation:interpolation_algorithms:inverse_distance_weighted (Accessed: 6 June 2021).

GEUS (1995) *Grundvandsovervågning 1995 GEUS.*

GEUS (2021) De National Geologiske Undersøgelser for Danmark og Grønland. https://www.geus.dk/

Gottschalk, I. *et al.* (2020) 'Using an airborne electromagnetic method to map saltwater intrusion in the northern Salinas Valley, California', *Geophysics*, 85(4), pp. B119–B131. doi: 10.1190/geo2019-0272.1.

Guo, W. and Langevin, C. D. (2002) *User ' s Guide to SEAWAT : A Computer Program For Simulation of Ground-Water Flow*. U.S. Geological Survey Techniques of Water-Resources Investigations.

Han, D. *et al.* (2011) 'Geochemical and isotopic evidence for palaeo-seawater intrusion into the south coast aquifer of Laizhou Bay, China', *Applied Geochemistry*. Elsevier Ltd, 26(5), pp. 863–883. doi: 10.1016/j.apgeochem.2011.02.007.

Hansen, J. W. *et al.* (2012) 'Fysiske og kemiske forhold', *Fagligt notat fra DCE - Nationalt Center for Miljø og Energi*, pp. 1–63. Available at: http://dce.ai.dk.

Hansen, K. (2011) 'Lokalt kom ingen til at »skumme fløde« på Kolindsund', *Det tabte land*, pp. 1–12.

Hendriks, M. . (2010) 'Fresh and saline: Ghijben-Herzberg', in *Introduction to Physical Hydrology*. New York: Oxford University Press Inc., pp. 104–106.

Højberg, A. L. *et al.* (2010) 'DK-model2009. Modelopstilling og kalibrering for Midtjylland'. Available at: http://vandmodel.dk/xpdf/dk-model2009_midtjylland.pdf.

Høyer, A. S. *et al.* (2011) 'Combined interpretation of SkyTEM and high-resolution seismic data', *Physics and Chemistry of the Earth*, 36(16), pp. 1386–1397. doi: 10.1016/j.pce.2011.01.001.

IPCC (2014) 'Synthesis Report. Contribution of Working Groups I, II and III to the Fifth Assessment Report of the Intergovernmental Panel on Climate Change', *Climate Change 2014*. Edited by . Core Writing Team, R. K. Pachauri, and L. A. Meyer, (2), p. 151. doi: 10.1016/S0022-0248(00)00575-3.

Jørgensen, F. *et al.* (2012) 'Transboundary geophysical mapping of geological elements and salinity distribution critical for the assessment of future sea water intrusion in response to sea level rise', *Hydrology and Earth System Sciences*, 16(7), pp. 1845–1862. doi: 10.5194/hess-16-1845-2012.

Jørgensen, L. F. and Stockmarr, J. (2009) 'Groundwater monitoring in Denmark: Characteristics, perspectives and comparison with other countries', *Hydrogeology Journal*, 17(4), pp. 827–842. doi: 10.1007/s10040-008-0398-7.

Jørgensen, N. O. (2002) 'Origin of shallow saline groundwater on the Island of Læsø, Denmark', *Chemical Geology*, 184(3–4), pp. 359–370. doi: 10.1016/S0009-2541(01)00392-8.

Klimaatlas (2020) *Klimaatlas*. https://www.dmi.dk/klimaatlas/ (Accessed: 13 May 2021).

Klitten, K., Larsen, F. and Sonnenborg, T. O. (2006) *Saltvandsgrænsen i kalkmagasinerne i Nordøstsjælland, hovedrapport*.

Kolindsundnatur.dk (no date) *Historien om Kolindsunds tilblivelse*. Available at: https://www.kolindsundnatur.dk/fakta/historie (Accessed: 31 August 2020).

Korkman, T. (1979) 'Grundvandstilstrømning til Kolindsund', p. 1-19.

Korkman, T. (1980) *En hydrologisk-hydrokemisk undersøgelse af det kunstigt afvandede Kolindsund*.

Korkman, T. (1981) 'Beskrivelse af kilder og væld i Kolindsund'. Århus Amtskommune, pp. 1–33.

Kristiansen, S. M. (2012) 'Salt Grundvand - Vandet under det ferske grundvand', *Geoviden - Geologi og Geografi*, 2, pp. 10–13.

Kristiansen, S. M., Hansen, B. and Christensen, F. D. (2009) *Vurdering af danske grundvandsmagasiners sårbarhed overfor vejsalt*.

Krøyer, H. and Jensen, J. M. (2013) *Kolindsund Dannelse, anvendelse og fremtid*. Grenå.

Langevin, C. D. *et al.* (2007) 'SEAWAT Version 4: A Computer Program for Simulation of Multi-Species Solute and Heat Transport', *U.S. Geological Survey Techniques and Methods Book 6*, p. 39.

Larsen, F. and Berger, K. (2006) *Saltvandsgrænsen i kalkmagasinerne i Nordøstsjælland, delrapport 5*.

Larsen, G. and Sand-Jensen, K. (2017) 'Geologien', in *Naturen i Danmark*. Gyldendal, pp. 1–552.

Lund-Hansen, L. C. *et al.* (1994) *Basisbog i fysisk-biologisk Oceanografi*. København: G.E.C Gads Forlag.

Lyles, J. R. (2000) 'Is seawater intrusion affecting ground water on Lopez Island, Washington?', *U.S. Geological Survey*, USGS Fact, p. 9.

Mabrouk, M. B. *et al.* (2013) 'A review of seawater intrusion in the Nile Delta groundwater system – the basis for assessing impacts due to climate changes and water resources development', *Hydrology and Earth System Sciences*, 10, pp. 10873–10911.

Masson-Delmotte, V. *et al.* (2018) 'Summary for Policymakers. Global Warming of 1.5°C. An IPCC Special Report on the impacts of global warming of 1.5 ºC above pre-industrial levels.', *IPCC*, p. 32 pp. doi: 10.1017/CBO9781107415324.

Meyer, R., Engesgaard, P. and Sonnenborg, T. O. (2019) 'Origin and Dynamics of Saltwater Intrusion in a Regional Aquifer: Combining 3-D Saltwater Modeling With Geophysical and Geochemical Data', *Water Resources Research*, 55(3), pp. 1792–1813. doi: 10.1029/2018WR023624.

Mielby, S. and Sandersen, P. (2005) 'Indsatskortlægning i Nyborg-området - om samspillet mellem geologiske stor-skala strukturer og forekomsten af salt grundvand', pp. 1–5.

Miljøstyrelsen (no date) *Drikkevand*. Available at: https://mst.dk/natur-vand/vand-i-hverdagen/drikkevand/ (Accessed: 12 May 2021).

Miljøministeriet By- og Landskabsstyrelsen (2009) 'Miljøvurdering af vandplan 1.6 Djursland', *Vandplaner (2009-2015)*. Available at: https://mst.dk/media/122334/16_djursland_bilag5_miljoevurdering_20100930.pdf.

Miljø- og Fødevareministeriet (2019) *Drikkevandsbekendtgørelsen*, *BEK nr. 1070*. Available at: https://www.retsinformation.dk/eli/lta/2019/1070 (Accessed: 12 May 2021).

Najib, S. *et al.* (2017) 'Contribution of hydrochemical and geoelectrical approaches to investigate salinization process and seawater intrusion in the coastal aquifers of Chaouia, Morocco', *Journal of Contaminant Hydrology*, pp. 24–36. doi: 10.1016/j.jconhyd.2017.01.003.

Nielsen and Rauschenberger (1982) *Udnyttelse af Kolindssunds kilder*.

Nilsson, B. and Gravesen, P. (2018) 'Karst Geology and Regional Hydrogeology in Denmark', pp. 289–298. doi: 10.1007/978-3-319-51070-5_34.

Oppenheimer, M. *et al.* (2019) 'Sea Level Rise and Implications for Low-Lying Islands, Coasts and Communities', *IPCC Special Report on the Ocean and Cryosphere in a Changing Climate*. Edited by H.-O. Pörtner et al., pp. 321–445. doi: 10.1126/science.aam6284.

Pedersen, S. A. S. (2017) *Norddjurs Kommunes landskaber*, *Trap Danmark*. Available at: https://trap.lex.dk/Norddjurs_Kommunes_landskaber (Accessed: 31 August 2020).

Pedersen, S. A. S. and Petersen, K. S. (2000) *Djurslands Geologi*. Danmark og Grønlands Geologiske Undersøgelser (GEUS).

Prince Edward Island Department of Environment, Labour and Justice. (2011) 'Saltwater Intrusion and Climate Change A primer for local and provicial decision-makers', in Linzey, D. (ed.) *Atlantic Climate Adaptation Solutions Association*, p. 26. Available at: www.atlanticadaptation.ca.

Rasmussen, P. *et al.* (2013) 'Assessing impacts of climate change, sea level rise, and drainage canals on saltwater intrusion to coastal aquifer', *Hydrology and Earth System Sciences*, 17(1), pp. 421–443.

doi: 10.5194/hess-17-421-2013.

Safi, A. *et al.* (2018) 'Synergy of climate change and local pressures on saltwater intrusion in coastal urban areas: effective adaptation for policy planning', *Water International*. Routledge, 43(2), pp. 145–164. doi: 10.1080/02508060.2018.1434957.

Schwartz, F. and Zhang, H. (2003) *Fundamentals of Groundwater*. John Wiley & Sons, Ltd.

Sørensen, K. (2012) 'Salt i Danmarks undergrund', *Geoviden - Geologi og Geografi*, 2, pp. 4–9.

Sørensen, K. I. and Auken, E. (2004) 'SkyTEM - a new high-resolution helicopter transient electromagnetic system', *Exploration Geophysics*, 35(3), pp. 194–202. doi: 10.1071/EG04194.

Stuyfzand, P. J. (2008) 'Base exchange indices as indicators of salinization or refreshening of (coastal) aquifers', *20th salt water intrusion meet.*, pp. 262–265.

Task Force for Klimatilpasning (2012) 'Kortlægning af klimaforandringer - muligheder og barrierer for handling'. Available at: http://www.klimatilpasning.dk/media/600814/121212_kortl_gning_af_klimaforandringer_final.pdf.

Theilgaard, J. (2017a) *Norddjurs Kommunes klima | lex.dk – Trap Danmark*. Available at: https://trap.lex.dk/Norddjurs_Kommunes_klima (Accessed: 28 April 2021).

Theilgaard, J. (2017b) *Syddjurs Kommunes klima i Trap Danmark*. Available at: https://trap.lex.dk/Syddjurs_Kommunes_klima (Accessed: 28 April 2021).

Thomsen, R. *et al.* (2005) *Grundvandsplan 2005*. Århus Amt.

Thorn, P. (2011) 'Groundwater salinity in Greve, Denmark: Determining the source from historical data', *Hydrogeology Journal*, 19(2), pp. 445–461. doi: 10.1007/s10040-010-0680-3.

Unesco (1981) 'Background papers and supporting data on the International Equation of State of Seawater 1980'. United Nations Educational Scientific and Cultural Organization, p. 192.

Vangkilde-Pedersen, T. *et al.* (2011) 'Kortlægning af kalkmagasiner', *GEUS. Geo Vejledning*, 8, p. 108. Available at: www.geus.dk (Accessed: 31 August 2020).

Vengosh, A. and Rosenthal, E. (1994) 'Saline groundwater in Israel: its bearing on the water crisis in the country', *Journal of Hydrology*, 156, pp. 389–430.

Vijay, R. and Mohapatra, P. K. (2016) 'Hydrodynamic assessment of coastal aquifer against saltwater intrusion for city water supply of puri, India', *Environmental Earth Sciences*. Springer Verlag, 75(7). doi: 10.1007/s12665-016-5357-3.

Werner, A. D. *et al.* (2013) 'Seawater intrusion processes, investigation and management: Recent advances and future challenges', *Advances in Water Resources*. Elsevier Ltd, 51, pp. 3–26. doi: 10.1016/j.advwatres.2012.03.004.

Wright, J. and Colling, A. (1995) 'Chapter 3 - Salinity in the oceans', in *Seawater: Its Composition, Properties and Behaviour*. 2nd edn, pp. 29–38.

Århus Amt (1995) *Statusrapport 1994 - Grundvandsovervågning i Århus Amt*.

Århus Amts (2000) *NATUR OG MILJØ I NORD-OG MIDTDJURSLAND 2000 (del 1)*. Århus Amts. Available at: www.aaa.dk/nm. (Accessed: 31 August 2020).

Appendix

Ion	Total number of measurements /	Number of latest measured	Concentration range
Chloride	10,288	1,259	0.045 - 33,620 mg/L
Sulfur	9,391	1,231	0.1 - 2,430 mg/L
Sodium	8,318	1,207	1 - 16,700 mg/L
Calcium	6,601	1,191	5 - 1,700 mg/L
Magnesium	6,441	1,159	0.28 - 384 mg/L
Potassium	6,169	1,091	0.23 - 870 mg/L
Bicarbonate	5,151	1,131	2.8 - 8,780 mg/L
Fluoride	3,892	1,059	0.03 - 8.5 mg/L
EC	6,601	1,183	5 - 1,700 mS/m
Bromide	-	71	30 - 730 µg/L

A1. Information about geochemical data.

Project name	Identity	Date
SkyTEM test Djurs Vest	dk.mim.aar.grundvand-djursvesttestkortlaegning-skytem.1dv.SCI_19L_v1_I1_6	14-01-2011
-	dk.mim.aar.grundvand-syddjurs-tem.1dv.TEM_Djurs01	-
Djurs Oest SkyTEM	dk.mst.grundvand-DjursOest-skytem.1dv.SCI_5L_V2_I01_6	09-08-2017
Djurs Vest SkyTEM	dk.nst.grundvand-DjursVest-skytem.1dv.SCI_19L_V3_I01_8	22-10-2013
Djurs Vest SkyTEM	dk.nst.grundvand-DjursVest-skytem.1dv.SCI_6L_V2_I03_7	22-10-2013
Djurs Vest SkyTEM	dk.nst.grundvand-DjursV-TEM.1dv.DjursV09	22-10-2013

A2. Information about geophysical data.

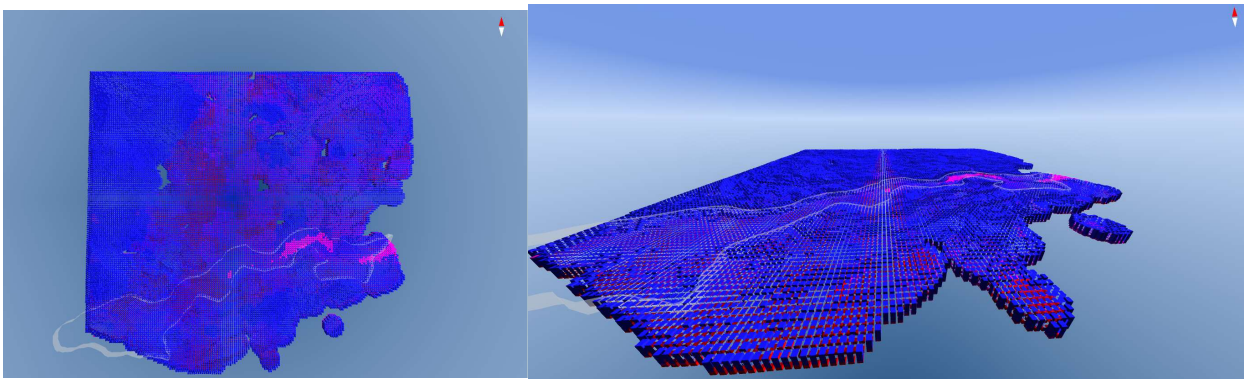

A3. 3D-voxel model, used to categorize three water types; freshwater, transition water, and saline water.

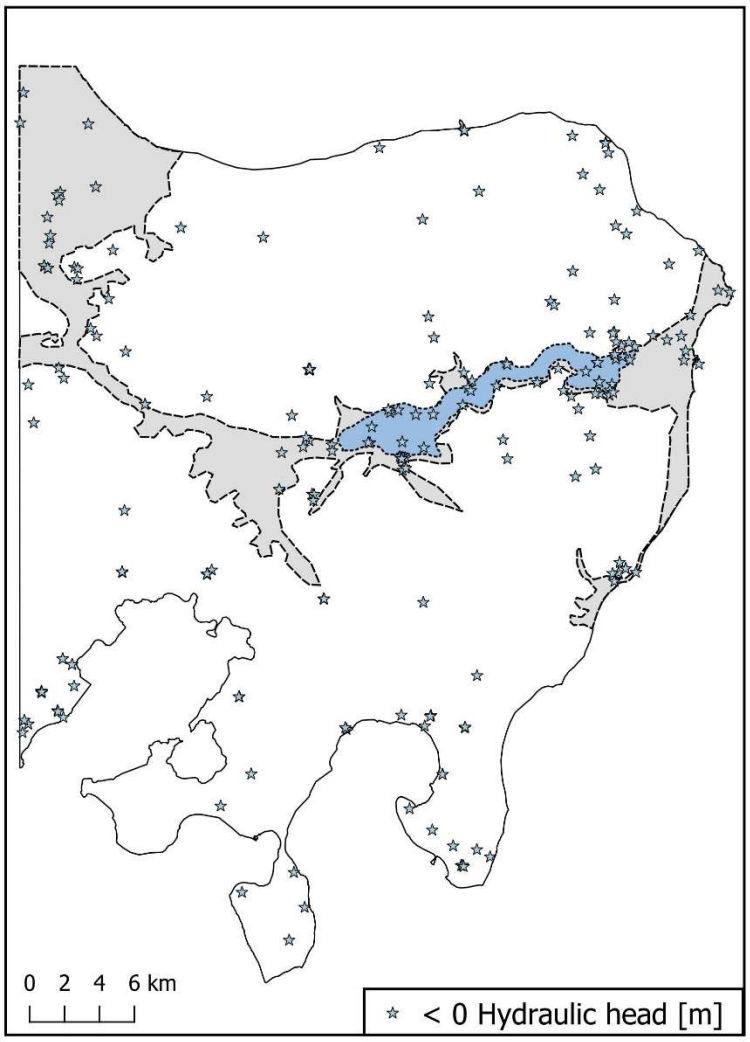

A4. Head measurements below sea level.

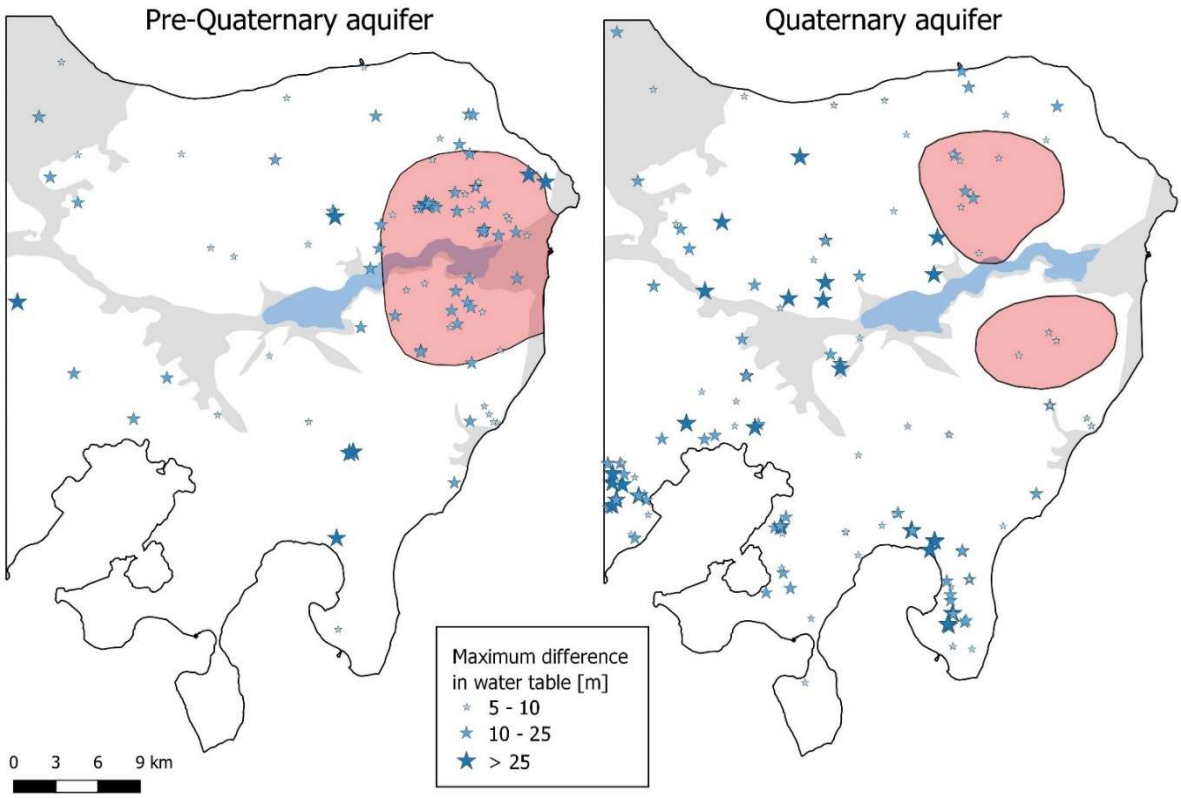

A5. Difference of measured maximum head and minimum head values. (Groundwater fluctuations).

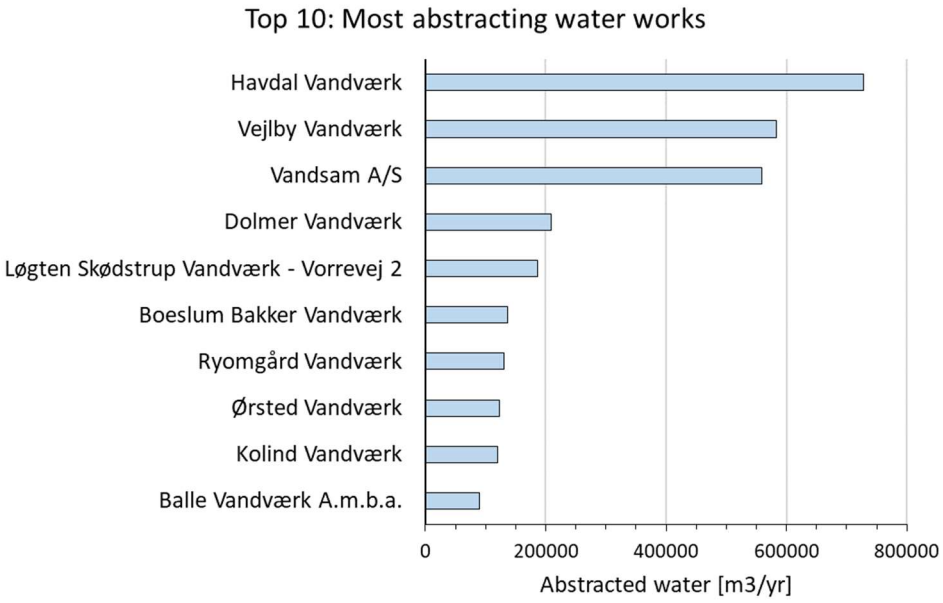

A6. Largest water works in Djursland.

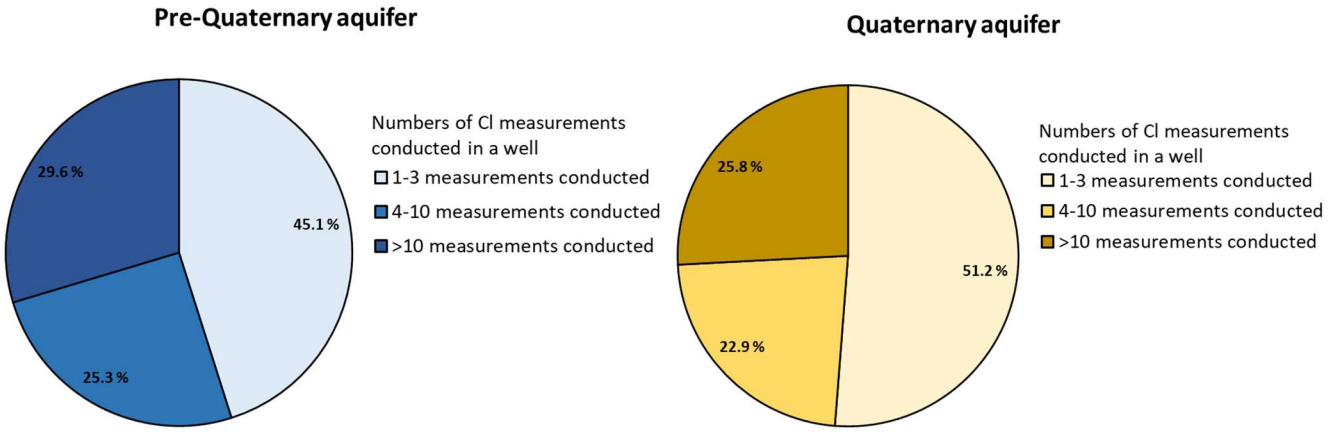

A7. Statistics of measured Cl-measurements for the pre-Quaternary and the Quaternary aquifers.

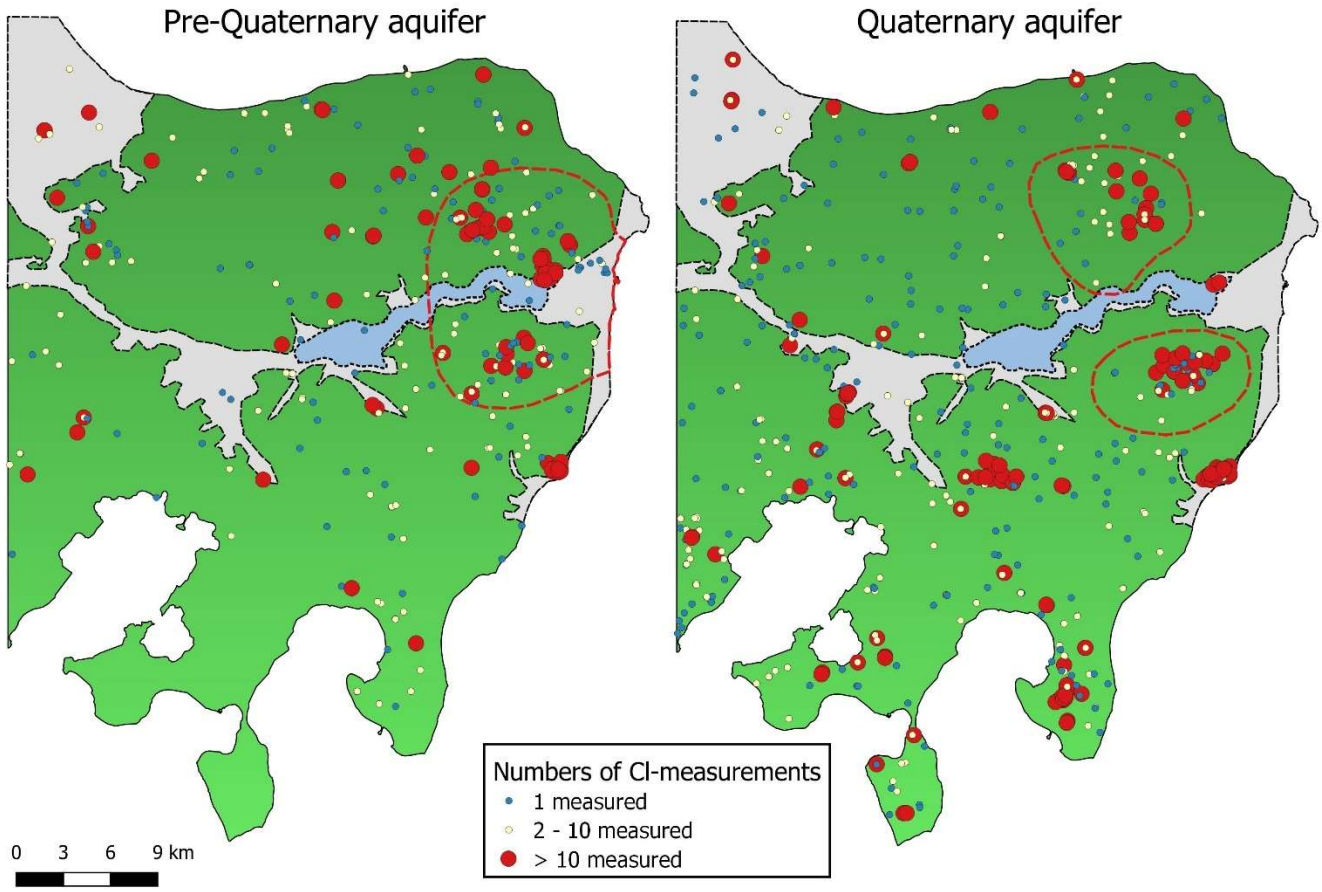

A8. Spatial distribution of historical measured measurements.

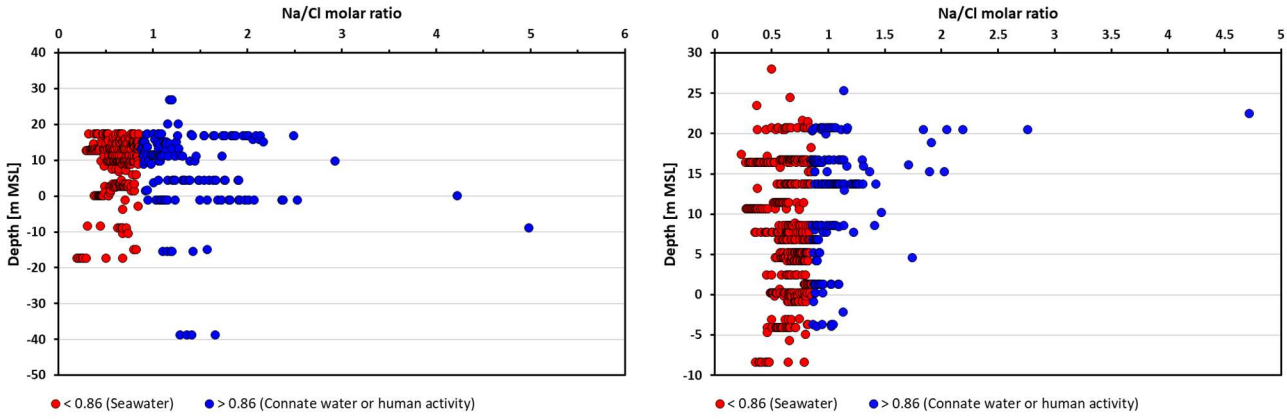

A9. Na/Cl molar ratio as function of depth. Left: Area 2. Right: Area 3.

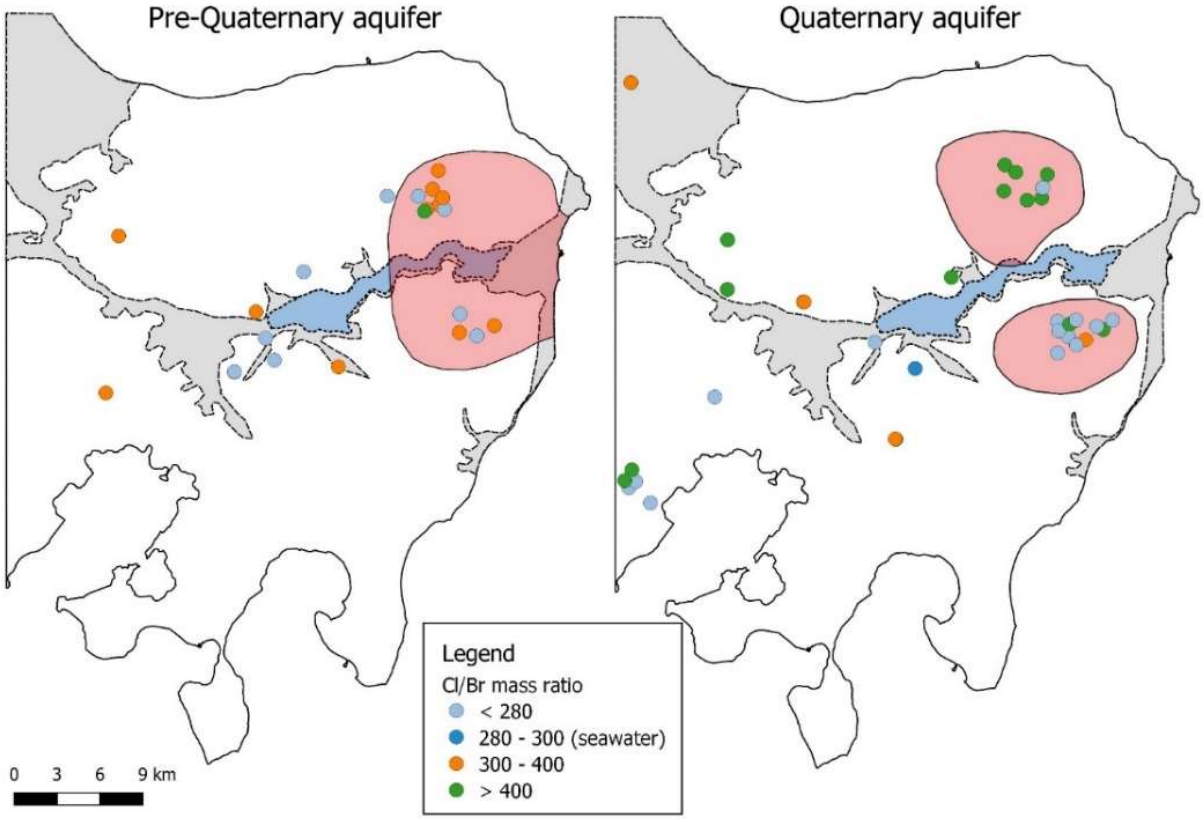

A10. All Cl/Br mass ratios within the pre-Quaternary aquifer (Left) and Quaternary aquifer (Right).

Well No.	Date	Aquifer sediment	Br [mg/L]	Cl (mg/L)	Cl/Br mass ratio
70. 949	01-05-2014	Pre-Quaternary	0.08	25	312.5
71. 333	08-08-1994	Pre-Quaternary	0.11	36	327.3
71. 338	13-05-1998	Pre-Quaternary	0.14	35	250.0

71. 394	11-07-2000	Pre-Quaternary	0.17	26	152.9
71. 439	06-05-1998	Pre-Quaternary	0.06	13	216.7
71. 442	03-12-1998	Pre-Quaternary	0.092	25	271.7
71. 482	20-06-2000	Pre-Quaternary	0.11	40	363.6
71. 484	22-09-1997	Pre-Quaternary	0.17	54	317.6
71. 567	05-05-1998	Pre-Quaternary	0.13	33	253.8
80. 332	23-06-1999	Pre-Quaternary	0.05	18	360.0
80. 335	23-06-1999	Pre-Quaternary	0.07	18	257.1
80. 853	26-05-2014	Pre-Quaternary	0.39	120	307.7
70. 390	23-06-1999	Pre-Quaternary	0.1	26	260.0
71. 483	10-07-2000	Pre-Quaternary	0.18	31	172.2
71. 522	14-04-1998	Pre-Quaternary	0.089	33	370.8
80. 384	22-11-1999	Pre-Quaternary	0.0802	19	236.9
70. 380	22-11-1999	Pre-Quaternary	0.0852	21.5	252.3
71. 295	13-05-1998	Pre-Quaternary	0.13	44	338.5
71. 296	13-05-1998	Pre-Quaternary	0.08	43	537.5
71. 532	05-05-1998	Pre-Quaternary	0.17	54	317.6
71. 630	18-03-2002	Pre-Quaternary	0.086	29	337.2
80. 236	23-06-1999	Pre-Quaternary	0.05	17	340.0
70. 192	23-06-1999	Pre-Quaternary	0.06	20	333.3
59. 461	02-04-2014	Quaternary	0.11	28	254.5
71. 439	06-05-1998	Quaternary	0.06	42	700.0
71. 483	10-07-2000	Quaternary	0.1	33	330.0
71. 522	14-04-1998	Quaternary	0.051	22	431.4
59. 461	02-04-2014	Quaternary	0.08	30	375.0
70. 267	23-06-1999	Quaternary	0.06	19	316.7
70. 343	23-06-1999	Quaternary	0.07	32	457.1
70. 392	23-06-1999	Quaternary	0.08	25	312.5
70. 442	22-11-1999	Quaternary	0.104	21.4	205.8
70. 949	01-05-2014	Quaternary	0.076	37	486.8
70. 949	02-05-2014	Quaternary	0.085	45	529.4
71. 466	13-11-1991	Quaternary	0.054	24	444.4
71. 468	12-11-1991	Quaternary	0.06	51	850.0
71. 482	20-06-2000	Quaternary	0.49	120	244.9
71. 484	09-09-1997	Quaternary	0.18	93	516.7
79. 440	21-02-2001	Quaternary	0.078	17.8	228.2
79. 770	29-01-2001	Quaternary	0.066	15	227.3
71. 511	05-05-1998	Quaternary	0.12	49	408.3
79. 1242	29-01-2001	Quaternary	0.042	23	547.6
70. 106	23-06-1999	Quaternary	0.08	39	487.5
70. 402	23-06-1999	Quaternary	0.07	29	414.3
71. 470	27-06-2000	Quaternary	0.14	29	207.1
71. 472	21-06-2000	Quaternary	0.1	28	280.0
71. 473	21-06-2000	Quaternary	0.073	33	452.1

71. 474	15-09-1997	Quaternary	0.16	25	156.3
71. 476	16-09-1997	Quaternary	0.2	49	245.0
71. 478	20-06-2000	Quaternary	0.19	40	210.5
71. 480	28-06-2000	Quaternary	0.21	43	204.8
71. 568	23-04-2001	Quaternary	0.066	34	515.2
71. 569	11-05-1998	Quaternary	0.09	31	344.4
71. 569	11-05-1998	Quaternary	0.15	28	186.7
79. 478	19-02-2001	Quaternary	0.1	14.4	144.0
79. 1204	29-01-2001	Quaternary	0.053	48.1	907.5
80. 104	23-06-1999	Quaternary	0.03	14	466.7
80. 105	23-06-1999	Quaternary	0.04	14	350.0
80. 394	23-06-1999	Quaternary	0.09	26	288.9
80. 854	26-05-2014	Quaternary	0.12	33	275.0
81. 177	27-06-2000	Quaternary	0.73	43	58.9

A11. Tabel showing all measurements of Cl and Br, and their associated ratio.

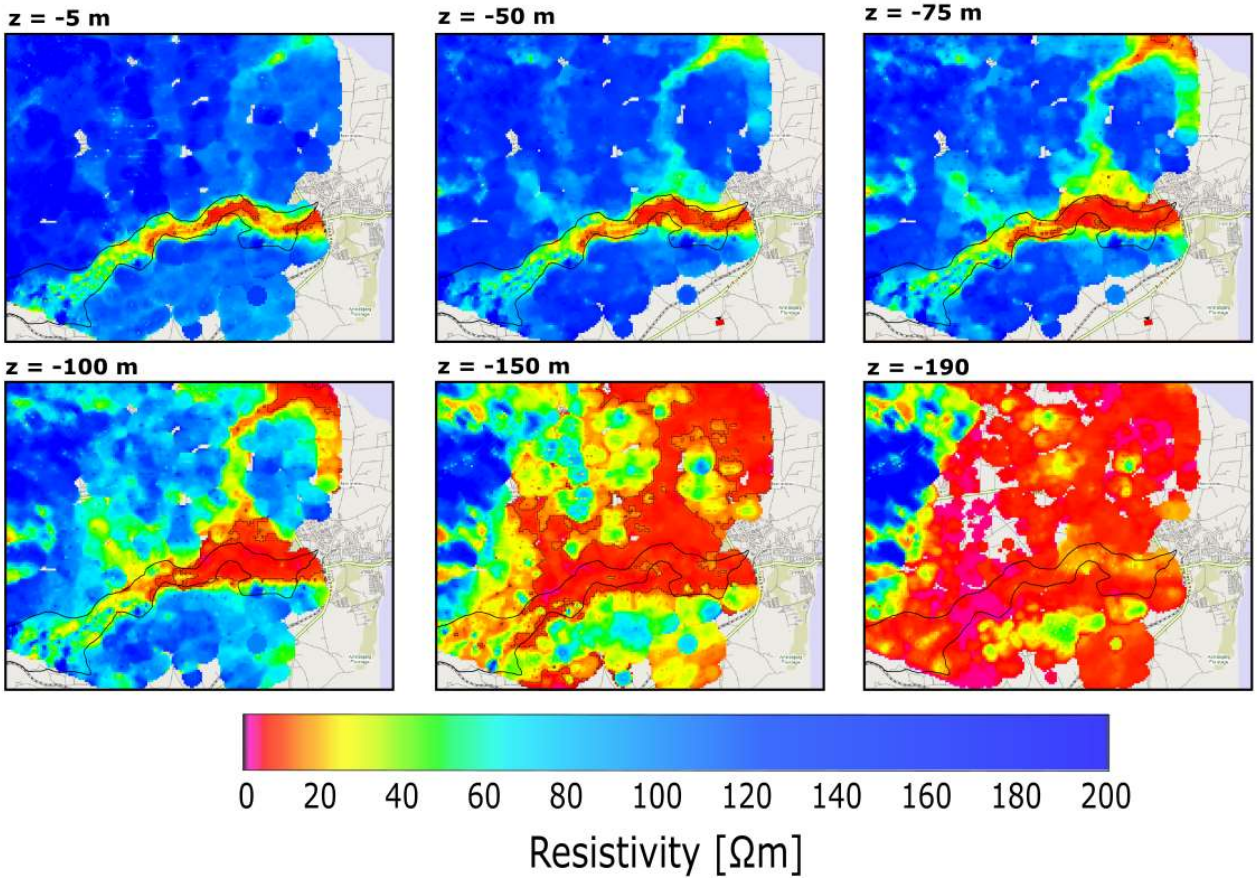

A12. Interpolated resistivity data.

Constant parameters	Pre-Quaternary unit	Quaternary unit
Specific storage *Ss* [m^{-1}]	1.0 10^{-5}	5.0 10^{-5}
Specific yield *Sy*	0.15	0.2
Porosity [%]	43	19.5
Hydraulic conductivity K [m s^{-1}]	7.13 10^{-5}	2.00 10^{-4}
Parameters	**Value**	
Longitudinal dispersity [m]	8	
Recharge [mm yr^{-1}]	Phase 1: 30 Phase 2-3: 75	
Salinity [g L^{-1}]	26	

A13. Applied values for the final model.

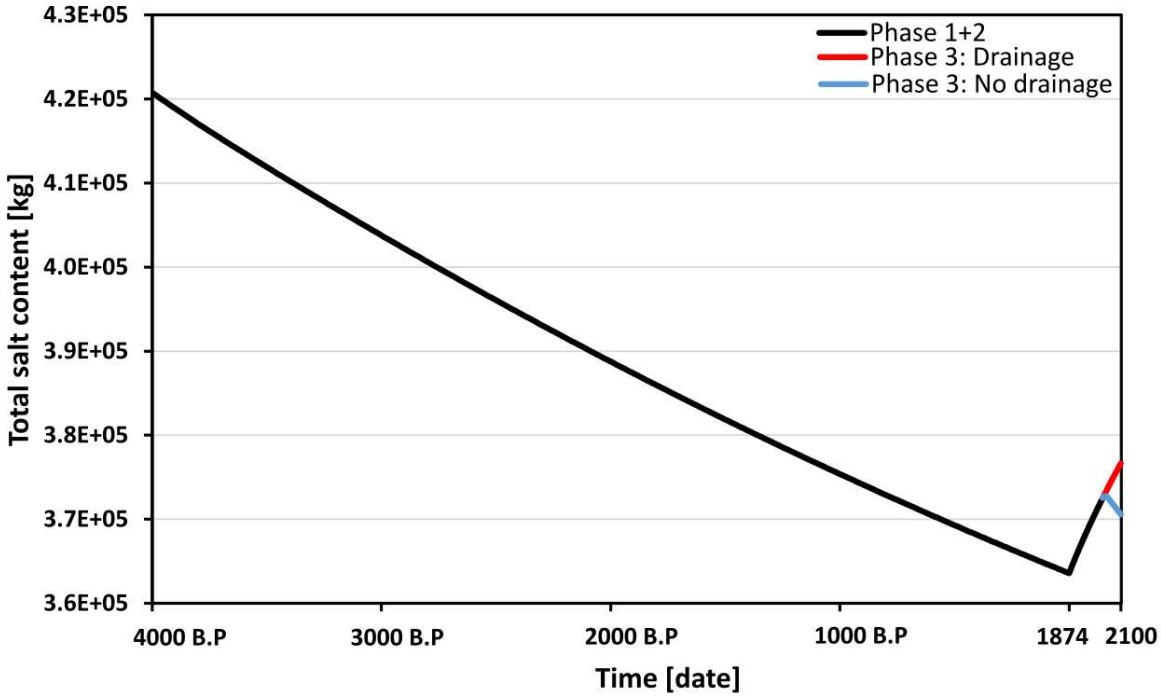

A14. Total salt content though the entire simulation (Phase 1, 2 and 3).

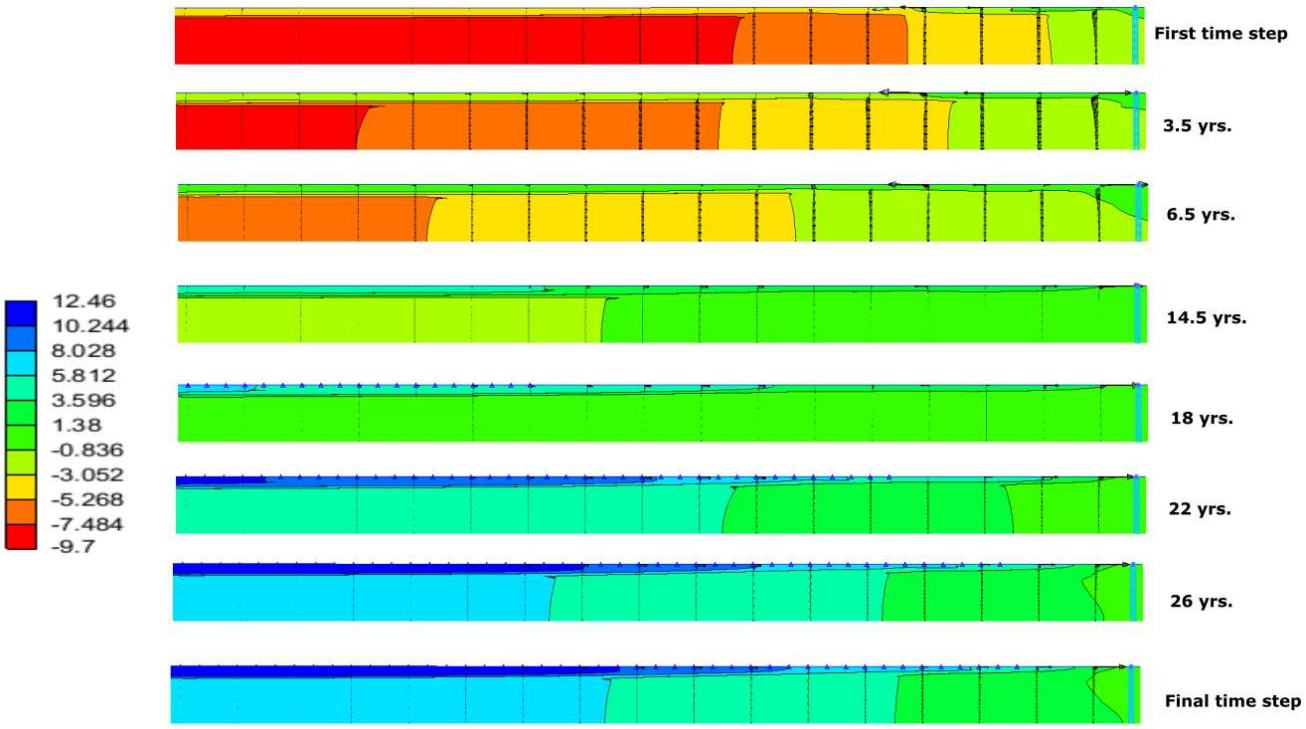

A15. Groundwater head changes through phase 3: Period 2020-2100.